INTERNATIONAL SCIENTIFIC JOURNAL

GEOGRAPHICA PANNONICA

Impact factor: 1.2 | CiteScore: 2.8

Volume 28, Issue 3 (September 2024)

UNIVERSITY OF NOVI SAD, FACULTY OF SCIENCES

DEPARTMENT OF GEOGRAPHY, TOURISM AND HOTEL MANAGEMENT

UNIVERSITY OF NOVI SAD | FACULTY OF SCIENCES
DEPARTMENT OF GEOGRAPHY, TOURISM & HOTEL MANAGEMENT

INTERNATIONAL SCIENTIFIC JOURNAL

GEOGRAPHICA PANNONICA

Impact factor: 1.2 | CiteScore: 2.8 Volume 28, Issue 3, September 2024

ISSN 0354-8724 (hard copy) | ISSN 1820-7138 (online) | UDC 05:91(497.1)=20

ISSN 0354-8724 (hard copy) | ISSN 1820-7138 (online) | UDC 05:91(497.1)=20

INTERNATIONAL SCIENTIFIC JOURNAL

GEOGRAPHICA PANNONICA

UNIVERSITY OF NOVI SAD | FACULTY OF SCIENCES | DEPARTMENT OF GEOGRAPHY, TOURISM & HOTEL MANAGEMENT

EDITORIAL OFFICE

Faculty of Sciences
Department of Geography, Tourism and Hotel Management
Trg Dositeja Obradovića 3, 21000 Novi Sad, Serbia
tel. +381 21 450-105
fax +381 21 459-696
Official site: www.dgt.uns.ac.rs

CONTACTS

Lazar Lazić, PhD, full professor
Department of Geography, Tourism and Hotel Management, Serbia, lazar.lazic@dgt.uns.ac.rs

Dragan Milošević, teaching assistant
Department of Geography, Tourism and Hotel Management, Serbia, dragan.milosevic@dgt.uns.ac.rs

Official mail of the Journal
gpscijournal@dgt.uns.ac.rs

Internet portal
www.dgt.uns.ac.rs/pannonica.html

Instructions to authors
www.dgt.uns.ac.rs/pannonica/instructions.htm

Contents

INTERNATIONAL SCIENTIFIC JOURNAL
GEOGRAPHICA PANNONICA
Volume 28, Issue 3, 158–168 (September 2024)
Journal homepage: http://www.dgt.uns.ac.rs/en/homepage/pannonica/

The Spatial and Temporal Behaviour of Particulate Matter and Submicron Particles in the Molise Region

Ivan Notardonato[A*], Luigi Pierno[B], Claudia Cafaro[C], Paolo Ceci[C], Pasquale Avino[A]

[A] *Department of Agriculture, Environmental and Food Science, University of Molise, Via F. De Sanctis, Campobasso 86100, Italy; ORCID IN: 0009-0006-4793-5286; ORCID PA: 0000-0003-4030-7624*

[B] *ARPA Molise, via U. Petrella 1, Campobasso 86100, Italy*

[C] *Institute of Atmospheric Pollution Research, Division of Rome, c/o Ministry of Environmental Security, via Cristoforo Colombo 44, Rome, 00147, Italy; ORCID CC: 0000-0001-7761-0489; ORCID PC: 0000-0003-2078-0887*

KEYWORDS

particulate matter
ultrafine particles
pollution
traffic
heating systems

ABSTRACT

Environmental pollution and its impact on human health has become a topic of great concern. In recent years, the scientific community has significantly increased its attention towards the protection of human health and an increasing number of analytical determinations are being carried out on food and environmental matrices to guarantee their quality. Within these determinations, the monitoring of air quality, both in indoor and outdoor environments, is of particular scientific interest. In particular, the presence of micrometric particles, atmospheric particulate matter (PM) and ultrafine particulate matter (UFP) has become a marker of air quality in recent years. The study of these substances is particularly important since the diameter of the particles is inversely proportional to their ability to penetrate the respiratory system. In places of greatest attendance and areas with high vehicular traffic, units are installed for continuously monitoring the air quality. This paper aims to bring a snapshot of the concentrations of these particles in Molise, a small region in Italy. The results obtained present rather limited PM_{10}, PM_4, $PM_{2.5}$, PM_1 and UFP ranges, especially as regards Campobasso, the regional capital.

Introduction

The terms "fine dust" or "atmospheric particulate matter" (*i.e.*, PM) refer to a series of particles suspended in the air that humans breathe daily. PM_{10} is characterised by a diameter of less than 10 μm. Its presence in the air is due to natural events or anthropic activities. PM_{10} is considered an indicator of air quality (Vahlsing & Smith, 2012; Costa et al., 2014) as well as of the entire ecosystem (Wright et al., 2018). It is well-known that atmospheric particulate persists in the air for a long time. Such persistence determines that PM could be transported over long distances (Arfin et al., 2023). Studies showed that PM had an impact on human health, particularly disorders of the respiratory system (Johannson et al., 2015; Avino et al., 2013; Marini et al., 2015; Dondi et al., 2023; Madureira et al., 2020). Organic and inorganic pollutants could adhere to the surface of fine dust, facilitating their penetration into the human body (Dongarrà et al., 2010; Turpin et al., 2000). PM_{10} is also called the thoracic fraction. It can reach the throat and trachea, located in the first part of the respiratory system. The smallest particles, characterized by a suspension

* Corresponding author: Ivan Notardonato, e-mail: ivan.notardonato@unimol.it

doi: 10.5937/gp28-49008

Received: January 31, 2024 | Revised: June 27, 2024 | Accepted: August 19, 2024

with a particle size class < 4 μm (*i.e.* PM_4), represent the respirable fraction. Due to the effect of respiratory motions, they can reach even deeper until they reach the alveolar area, the non-ciliated part of the lung. $PM_{2.5}$ is a numerical classification given to fine particulate matter based on the average size of its particles. The term $PM_{2.5}$ encompasses all particles with dimensions equal to or smaller than 2.5 μm, where 1 μm. These tiny particles can penetrate deep into the lungs and even enter the bloodstream. $PM_{2.5}$ particles can reach the alveoli in the lungs, potentially causing serious health issues (Feng et al., 2016). Studies have shown that exposure to elevated levels of $PM_{2.5}$ is associated with an increased risk of cancer (Xing et al., 2016). Exposure to $PM_{2.5}$ has been linked to mutations in genes Egfr and Kras associated with lung cancer (Han et al., 2023; Hill et al., 2023). PM_1 consists of particles with an aerodynamic diameter of less than 1 μm. PM_1 is incredibly small and can remain suspended in the atmosphere for extended periods. PM_1 particles can penetrate deep into the lungs, potentially causing harm. PM_1 particles can originate from both natural and anthropogenic sources. Organizations like the World Health Organization (WHO) and the European Union have studied and regulated $PM_{2.5}$ and PM_{10} particles for air quality, but PM_1 remains less explored. In summary, PM represents fine particulate matter with potentially serious health implications, and efforts to reduce exposure are crucial for public health. Minimizing exposure to fine particulate matter is essential for maintaining good respiratory health. Furthermore, the air is characterized also by the presence of ultrafine particles (*i.e.*, UFP), with a diameter between 10 and 100 nm. Such small diameters can penetrate the deeper ways of the respiratory system (Donaldson et al., 2001). Their size is comparable to those of human blood cells or alveolar macrophages, which could be able to internalise UFP. UFPs remain suspended in the air for hours or days, meaning that their deposition can occur far from the point of emission (Avino & Manigrasso, 2017). It is well-known that UFPs mainly arise from vehicle emissions, as well as fuels used for heating systems (Stabile et al., 2018; Jiang et al., 2019). Furthermore, industrial processes (i.e., oil industry, waste incineration and plant treatments) contributed the most to UFPs emissions in the air (Fernández-Camacho et al., 2012; Buonanno et al., 2011; Buonanno & Morawska, 2015; Borrow et al., 2018; Wang et al., 2018; Soggiu et al., 2020). Furthermore, due to their high persistence in the air before deposition, UFPs generally tend to clot/accumulate, leading to an increase in their size (Famiyet et al., 2023; Manigrasso et al., 2020). Generally, deposition of particles > 1 μm occurs by sedimentation, whereas for those smaller than 100 nm, the deposition occurs following chaotic diffusion motions of the particles, dependent on the diffusion coefficient (Famiyeh et al., 2023; Manigrasso et al., 2020). It has been reported that PM_{10} and UFPs become the main causes of diseases, affecting both the respiratory system (*e.g.*, lungs) and the cardiovascular and nervous systems (Du et al., 2016; Heusinkveld et al., 2016; Li et al., 2003; Lodovici & Bigagli, 2011). Recently, traces of ultrafine metal particles were detected in the human brain (Maher et al., 2016). The International Agency for Research on Cancer (IARC) classified PM_{10} as carcinogenic to humans (Word Health Organization, 2010). Therefore, European Member States proposed establishing appropriate guidelines to increase the protection level of their citizens (Settimo et al., 2023).

Generally, most of the population spends most of the hours of the day (up to 90%) indoors (Kelly & Fussell, 2019), so it becomes a necessity for every person to go out into the open air and take short or long walks. Monitoring air quality becomes of fundamental importance for the health of the population (Manigrasso et al., 2017; Notardonato et al., 2019). The present paper aims to carry out a characterization of the distribution of thoracic and respirable fractions and UFP on the exposure of a person during a recreational walk-in in different areas of the Molise region.

Materials and Methods

Sampling Sites

The sampling campaign was carried out in five sites in the Molise region, Italy, about 150 km away from Rome in a southeast direction (Figure 1). The territory is predominantly hilly and there are municipalities and small towns with a population of less than 50000. The surface area of 4461 km^2 and the density of 64.81 inhabitants per km^{-2} describe the predominance of a naturalistic landscape. The sites were chosen for their differences in terms of pollution levels and they can be considered representative of Italian cities characterized by a low population density. Particular attention was paid to the regional capital, Campobasso (41°33'39.6"N 14°40'06.24"E), a city of approximately 49700 inhabitants, with a surface area of 56.11 km^2, 701 m above sea level, with a density of 838.1 inhabitants km^{-2}. Furthermore, an area of environmental whiteness has been identified, the protected natural oasis of "Montedimezzo" (41°45'28.08"N 14°12'46.44"E, approximately 6.4 km^2, between 920 and 1284 m above sea level). The oasis is one of the first natural areas, among the eight Italian ones, to be registered as a "Biosphere Reserve" for the conservation and protection of the environment. The municipality of Agnone (41°48'37.44"N 14°22'42.6"E, approximately 4600 inhabitants, 96.85 km^2, 830 m above sea level, density of 48.17 inhabitants km^{-2}) is the municipality closer to the environmental white which has a sufficient population to con-

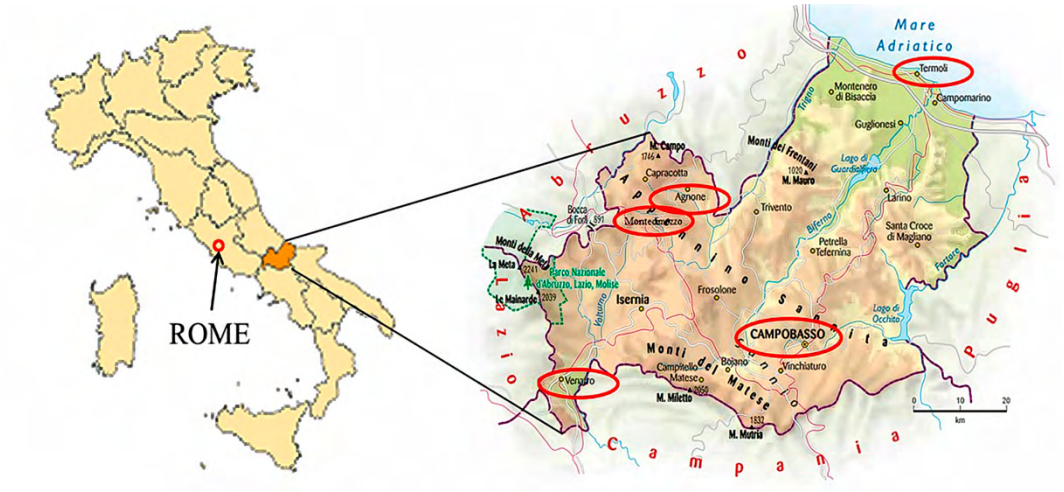

Figure 1. Geographical location of the Molise region and sampling sites

sider the significant anthropic activity. Samplings were also carried out in two municipalities that represent the access routes to the region. The municipality of Venafro (41°28'57"N 14°02'51"E, approximately 10800 inhabitants, surface area of 46.45 km^2, 222 m above sea level, density 232.85 inhabitants km^{-2}), is characterized by high heavy traffic, both cars, buses and trucks. There are two industries, a cement plant and an incinerator. The municipality of Termoli (42°00'10"N 14°59'41"E, approximately 32000 inhabitants, 55.64 km^2, 15 m above sea level, density 576.8 inhabitants km^{-2}) is characterized by the presence of a small port size and a motorway stretch that connects the south with the north of Italy. There are two medium-sized industries relating to the automotive and chemical-pharmaceutical sectors. Where possible, three different areas were identified for each sampling location. Specifically, city centre, residential and green areas were selected. To evaluate the impact of climatic conditions, a sampling campaign was conducted both during the summer and winter seasons. Each sampling activity was repeated twice within the same day at the site of Campobasso, Termoli e Venafro: in the morning between 9.30 and 11.30 AM and in the afternoon between 3.30 and 6.30 PM. In the sites of Montedimezzo and Agnone, areas with zero and low population density respectively, sampling was carried out only once per season as anthropic activity was considered null or almost null. All sampling lasted between 30 and 90 minutes.

Instrumentation

All measurements were performed with certified and appropriately calibrated portable electronic instruments from TSI Instruments (Shoreview, MN, USA). Specifically, the PM was studied under different size fractions using the DustTrak™ II Aerosol Monitor 8532, this is a handheld battery-operated, data-logging, single-channel, light-scattering laser photometer. The DustTrak™ II provides real-time aerosol mass readings using a sheath air system. This system isolates the aerosol in the optics chamber, ensuring cleaner optics for improved reliability and low maintenance. It's useful for assessing workplace air quality. It is ideal for monitoring indoor environments. The DustTrak™ II can measure aerosol concentrations corresponding to PM_1, $PM_{2.5}$, PM_4, or PM_{10} size fractions. It covers an aerosol concentration range from 0.001 to 150 mg m^{-3}. The handheld unit is lightweight and portable, making it easy to carry. The DustTrak™ II Aerosol Monitor 8532 is a versatile tool suitable for various environments, from clean office settings to harsh industrial workplaces and outdoor applications. Its real-time monitoring capabilities make it valuable for assessing aerosol contaminants such as dust, smoke, fumes, and mists. To count the number of nanoparticles (# m^{-3}) with dimensions between 10 and 365 nm, a NanoScan SMPS 3910 was used, which adopts a particle sizing technology with scanning mobility. Nanoparticles were counted in real-time at 60 s time resolutions in thirteen different size channels (11.5 nm, 15.4 nm, 20.5 nm, 27.4 nm, 36.5 nm, 48.7 nm, 64.9 nm, 86.6 nm, 115.5 nm, 154.0 nm, 205.4 nm, 273.8 nm and 365.2 nm), of these all the lower fractions smaller than 115.5 nm were examined. The SMPS NanoScan is ideal for applications requiring portability such as on-the-road measurements, field studies or workplace surveys. The internal Condensation Particle Counter (CPC) uses isopropyl alcohol as a working fluid, making the NanoScan suitable for use in various sensitive environments. The focus fell on ultrafine particles, *i.e.*, on size channels from 11.5 nm to 115.5 nm. A backpack was equipped with a portable DustTrack system, while the Nanoscan was carried by hand. The NanoScan SMPS 3910 is a revolutionary nanoparticle sizer. It opens the door to routine nanoparticle size measurements and delivers a Scanning Mobility Particle Sizer (SMPS™) spectrometer in a portable package and it is an excellent choice for researchers, students, and industrial workers alike.

Results and discussion

The results obtained are detailed and described below.

Natural oasis of Montedimezzo

Results of PM_1, $PM_{2.5}$, PM_4 and PM_{10} are reported in Table 1.

The ultrafine particles present very low values, in the winter period lower than 409 # m^{-3} and in the summer period lower than 750 # m^{-3} and prove to be in line with the concentrations of atmospheric particulates.

Table 1. Average concentrations of PM_1, $PM_{2.5}$, PM_4 and PM_{10} the (µg m^{-3}) related to the summer and winter periods; standard deviation (SD); minimum (min) and maximum (max) value; 60, 80, 95 percentiles of Montedimezzo. (*sum.* = summer; *win.* = winter)

	Concentration (µg m^{-3})							
	PM_1		$PM_{2.5}$		PM_4		PM_{10}	
	sum.	*win.*	*sum.*	*win.*	*sum.*	*win.*	*sum.*	*win.*
mean	8.7	4.9	11.2	5.4	12.5	5.5	15.8	6.0
SD	0.3	7.5	0.5	7.5	0.8	7.5	2.1	7.5
min	7.9	0.9	9.9	1.3	10.9	1.4	13.2	1.5
max	9.3	28.9	12.6	29.5	14.5	29.6	22.4	30.1
60 %	8.7	2.5	11.3	3.1	12.5	3.4	15.6	4.1
80%	8.8	4.5	11.5	5.2	13.1	5.3	17.7	6.5
95%	9.0	25.4	12.2	26.0	14.1	26.2	19.5	26.3

From Table 1 emerged that PM concentrations (µg m^{-3}) in the summer period have higher values than in the winter period. In the summer period, the delta between the minimum value and the maximum value is very narrow, both values approach the average value. In the winter period, however, the minimum and maximum values present a greater delta, which often deviates from the average value. Furthermore, the table shows the values of the eightieth percentile (80%) are in almost all cases close to the average. Such a difference could be due to the increase in recreational anthropogenic activities.

Agnone

Results obtained during the sampling campaign in Agnone are summarised in Table 2.

The average concentrations of atmospheric particulate matter are different between the summer period and the winter period. Concentrations during the winter period tend to almost triple compared to the summer period. Considering the altitude of the municipality, this increase is attributable to the use of heating systems such as methane boilers or wood-burning fireplaces, present in almost all homes in the municipality. The combustion processes influence the winter values. The minimum and maximum

Table 2. Average concentrations of PM_1, $PM_{2.5}$, PM_4 and PM_{10} the (µg m^{-3} relating to the summer and winter periods; standard deviation (SD); minimum (min) and maximum (max) value determined; 60, 80, 95 percentiles. (*sum.* = summer; *win.* = winter)

	Concentration (µg m^{-3})							
	PM_1		$PM_{2.5}$		PM_4		PM_{10}	
	sum.	*win.*	*sum.*	*win.*	*sum.*	*win.*	*sum.*	*win.*
mean	6.5	18.6	9.3	20.1	11.8	20.6	22.4	32.0
SD	0.5	13.4	2.9	13.8	7.5	13.9	58.2	14.2
min	5.7	6.8	7.7	7.9	8.2	8.0	9.1	8.3
max	8.0	75.6	21.5	78.1	44.7	78.6	291.8	79.4
60 %	6.5	16.0	8.6	17.4	9.5	18.3	12.6	20.8
80%	6.7	21.3	9.1	22.6	10.8	23.1	18.4	25.2
95%	7.6	46.8	15.5	49.1	26.5	49.5	153.8	52.2

values present a greater delta compared to the average value in the winter period. Also, in this determination, the values at the eightieth percentile are close to the averages in almost all determinations.

Campobasso

Campobasso city was monitored in different meteorological situations, to have a representativeness of the pollution level of the area.

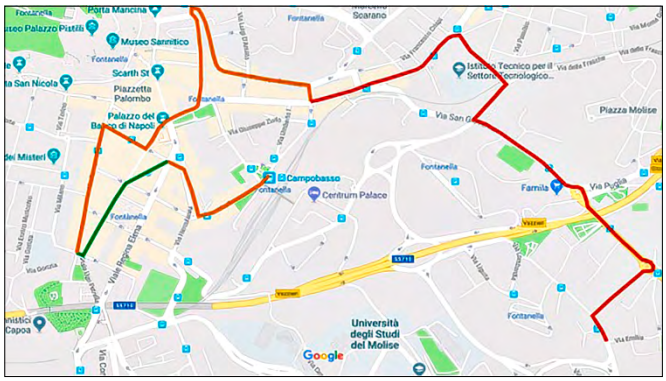

Figure 2. Route in Campobasso city: the red line indicates residential area with high traffic intensity, the orange line indicates residential area with medium traffic intensity, whilst the green line represents pedestrian area

The entire route (Figure 2), touched different areas of the city, appropriately selected based on population density, vehicular traffic and green areas. The route highlighted in red shows a peripheral road, characterized by a high population density, and heavy vehicular traffic of cars and coaches which also operate routes outside the city. In the area, there is a bus terminal located a short distance from the road examined. The route highlighted in orange indicates a road in the city centre, characterized mainly by light vehicular traffic and city buses. Finally, the route represented by the green line represents the pedestrian area closed to traffic where there is a green park used by the majority of the population for walking. The housing units are similar to those of the orange route but the park is very large, full of trees and varied vegetation. These three situations identify and characterize different practicable routes within the town centre. They simulate a different exposure to atmospheric particulates and ultrafine particles to which the pedestrian is subjected.

Table 3 shows the average results of the PMs, with the SD, MIN, MAX, 60, 80, and 95 percentiles. The average values during the summer period are between 7.2 and 11.1 ppm, while the winter values were between 8.8 and 26.8 ppm. Significant differences between the maximum values are noted. The maximum values determined during the afternoons of the summer period (401.0 - 521.0 $\mu g\ m^{-3}$) are far higher than the respective average values (8.8 - 11.1 $\mu g\ m^{-3}$). However, by comparing the maximum values with the relative values at 95% (23 – 28 $\mu g\ m^{-3}$), it can be noted that the maximums represent instantaneous values of little significance. Furthermore, especially in the summer sampling, the average composition of the aerosol is predominantly PM_1 (around 66.0% in the morning and 79.3% in the afternoon).

The correspondences between percentiles and averages are also different. During the summer period, considering the standard deviation, the average values are comparable to those of 95%. While in the winter period, the correspondence is 80%. In the winter period, the average values of the various particulate fractions become comparable between morning and afternoon. The data show an increase in particulate values in the winter period compared to the summer period. This could be due to an anthropic action linked to the use of heating systems. Campobasso is characterized by a fairly harsh climate during the winter period. Consequently, the use of combustion boilers leads to doubling the values of both the respirable fraction and PM_{10} compared to the values found during the summer period.

Table 3. Average concentrations of the different sizes of atmospheric particulate matter ($\mu g\ m^{-3}$) relating to the summer and winter periods; standard deviation (SD); minimum (min) and maximum (max) value determined; 60, 80, 95 percentiles. (*mor.* = morning; *aft.* = afternoon)

	Concentration mean ($\mu g\ m^{-3}$)															
	Summer								Winter							
	PM_1		$PM_{2.5}$		PM_4		PM_{10}		PM_1		$PM_{2.5}$		PM_4		PM_{10}	
	mor.	*aft.*	*mor.*	*aft.*	*mor.*	*aft.*	*mor.*	*aft.*	*mor.*	*aft.*	*mor.*	*aft.*	*mor.*	*aft.*	*mor.*	*aft.*
mean	6.8	8.8	7.2	9.1	8.2	9.7	10.3	11.1	8.8	9.6	15.2	13.9	17.9	17.0	21.9	26.8
SD	1.9	13.5	2.0	13.5	2.7	13.9	5.9	17.1	8.1	4.3	9.5	6.2	10.2	8.5	11.0	17.5
min	5.0	1.0	5.0	1.0	6.0	1.0	6.0	1.0	2.4	4.6	5.3	7.4	6.6	8.6	8.4	11.1
max	17.0	401.0	19.0	403.0	25.0	410.0	46.0	521.0	48.5	22.3	57.4	37.9	60.7	52.9	62.7	99.8
60 %	7.0	7.0	7.0	7.0	8.0	8.0	10.0	9.0	8.4	10.0	16.5	13.8	19.4	16.3	23.2	23.2
80%	7.0	10.0	7.2	10.0	9.0	11.0	11.0	14.0	10.1	11.6	18.2	16.7	22.2	20.9	27.0	34.0
95%	8.1	23.0	9.1	24.0	12.0	24.0	17.0	28.0	23.9	18.1	31.6	26.0	35.9	32.2	41.4	54.7

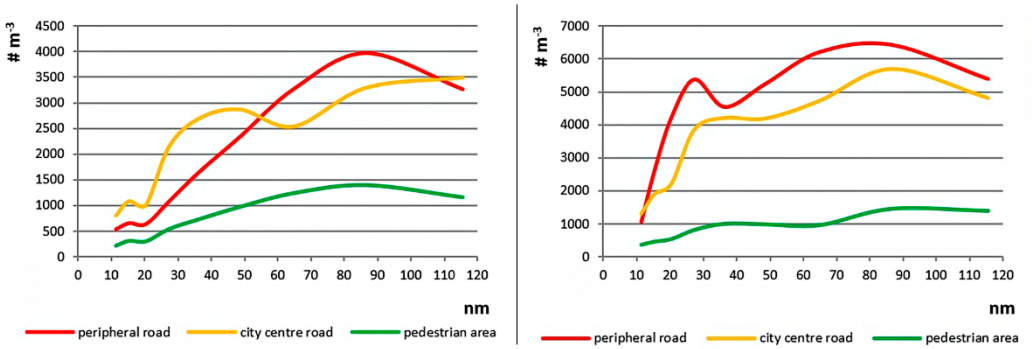

Figure 3. Comparison between the average distribution of ultrafine particles (# m^{-3}) VS the diameter of the particles (nm) between the summer and winter periods in the three types of routes

The comparison between the composition of UFPs between the summer and winter periods confirms a change in air quality (Figure 3). The number of UFPs per cubic meter (# m^{-3}) of air also tends to increase in the analyzed routes. Specifically, in the red and orange routes, the number of UFPs tends to grow in the winter period compared to the summer period, with values respectively lower than 6500 # m^{-3} and 4000 # m^{-3}. Such a trend was not observed in the green one, where the UFPs are comparable in the two periods.

Venafro

Routes carried out during the sampling campaign in Venafro are represented in Figure 4.

A route was identified that covered almost the entire country. An alasting of approximately 30 minutes was considered: two different areas can be identified on the selected stretch. The route highlighted in red develops along the "SS6" and the "SS85", the two main roads that connect Venafro with the motorways and the industrial area, characterized by a high density of heavy vehicular traffic. The route highlighted in orange is in the centre with medium traffic density, essentially local traffic.

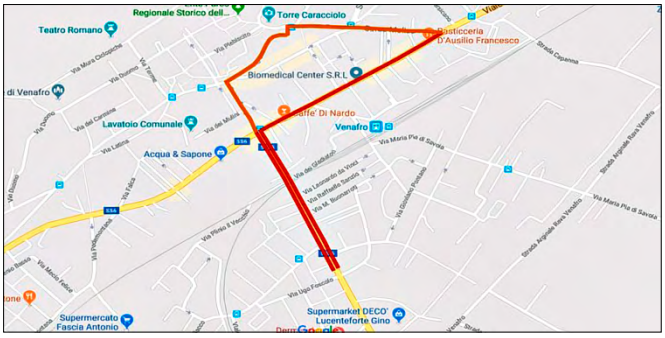

Figure 4. The city route of Venafro where the red line indicates a residential area with high traffic intensity, and the orange line indicates a residential area with medium traffic intensity

The concentrations of atmospheric particulate matter are different between the summer and winter periods, as shown in Table 4. In the summer period, PM concentrations are on average higher than those in the afternoon. This difference could be due to the heavy vehicular traffic of trucks and road transporters, which, can walk freely on urban and extra-urban roads during the night hours, and then have limitations during the daytime hours to reduce the risks for cars. This gap decreases during the

Table 4. Average concentrations of the different sizes of atmospheric particulate matter (μg m^{-3}) relating to the summer and winter periods; standard deviation (SD); minimum (min) and maximum (max) value determined; 60, 80, 95 percentiles (*mor.* = morning; *aft.* = afternoon)

	Concentration mean (μg m^{-3})															
	Summer								Winter							
	PM_1		$PM_{2.5}$		PM_4		PM_{10}		PM_1		$PM_{2.5}$		PM_4		PM_{10}	
	mor.	*aft.*	*mor.*	*aft.*	*mor.*	*aft.*	*mor.*	*aft.*	*mor.*	*aft.*	*mor.*	*aft.*	*mor.*	*aft.*	*mor.*	*aft.*
mean	23.1	13.1	23.9	13.6	25.1	14.6	28.3	17.1	35.5	32.5	47.3	40.9	50.9	45.9	58.4	66.5
SD	39.9	35.1	40.5	35.3	43.2	36.4	57.3	43.9	20.0	23.9	20.5	25.3	20.9	33.4	31.5	125.1
min	0.0	5.0	8.0	6.0	8.0	7.0	8.0	7.0	13.9	16.9	23.7	24.5	26.3	26.3	30.1	29.4
max	1090.0	1080.0	1100.0	1090.0	1130.0	1130.0	1720.0	1430.0	135.5	155.0	147.0	165.0	149.7	170.3	215.9	738.6
60 %	20.0	10.0	21.0	11.0	22.0	12.0	24.0	13.0	35.3	28.9	47.7	35.6	50.7	37.3	54.9	39.8
80%	25.0	13.0	26.0	14.0	27.0	15.0	31.0	18.0	43.3	39.0	55.7	48.4	61.1	50.5	67.5	53.9
95%	43.8	26.0	45.0	27.0	46.8	28.0	53.0	33.0	59.4	46.6	72.5	64.4	76.0	106.5	95.1	110.0

winter period. The maximum values appear to be occasional when compared to respective 95% values. During the summer period, considering the standard deviation, the average values are comparable to those of 95%. While in the winter period, the correspondence is 80%. Furthermore, in the winter period, the concentrations between morning and afternoon become broadly comparable, since in addition to the emissions due to heavy vehicle traffic, there are also emissions linked to the use of heating systems.

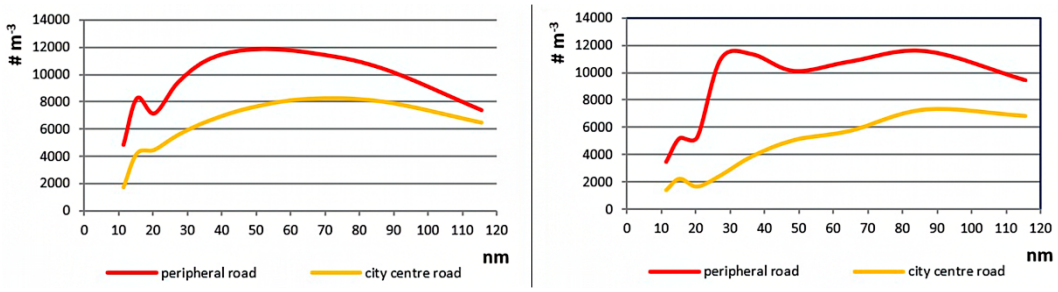

Figure 5. Comparison between the average distribution of ultrafine particles (# m^{-3}) VS the diameter of the particles (nm) between the summer and winter periods in the two types of routes

Table 5. Pearson correlation coefficient between submicron particles in different size fractions. Values> 0.7 are highlighted

11.5	15.4	20.5	27.4	36.5	48.7	64.9	86.6	115.5	
1	0.666	0.782	0.928	0.959	0.945	0.806	0.298	0.162	**11.5**
	1	0.909	0.564	0.582	0.714	0.816	0.589	0.520	**15.4**
		1	0,802	0,782	0,815	0,792	0,576	0,456	**20.5**
			1	0,985	0,894	0,813	0,418	0,179	**27.4**
				1	0,949	0,856	0,334	0,107	**36.5**
					1	0,922	0,354	0,195	**48.7**
						1	0,609	0,614	**64.9**
							1	0,920	**86.6**
								1	**115.5**

The UFP concentrations, as shown in Figure 5, are comparable in the two periods. In both types of path, the distribution curves show similar trends and are lower than 12000 # m^{-3} for the path highlighted by the red line and lower than 8000 # m^{-3} for the path highlighted by the orange line. It was decided to carry out Pearson correlations only for this reason since the ultrafine particles present significantly higher values compared to the other sites examined.

Table 5. shows the relative Pearson correlation coefficients (r) determined for all sizes: the coefficients highlighted in blue, *i.e.*, those with a value greater than 0.7, highlight a good correlation between the two fractions considered. Correlations are good for sizes ranging from 11.5 to 64.9 nm, which means that fresh aerosol is emitted from the same sources.

Termoli

The last sampling was carried out in the municipality of Termoli, the only seaside town in the region. Four samplings were also carried out in this municipality, two during the winter period and two during the summer period.

Routes carried out during the sampling campaign in Termoli are represented in Figure 6. The route is traced based on the type of vehicular traffic and housing structures present. The red route represents the streets with intense vehicular traffic and represents the main entrance to the city, while the orange route represents the city centre, characterized by larger spaces and a small limited traffic area.

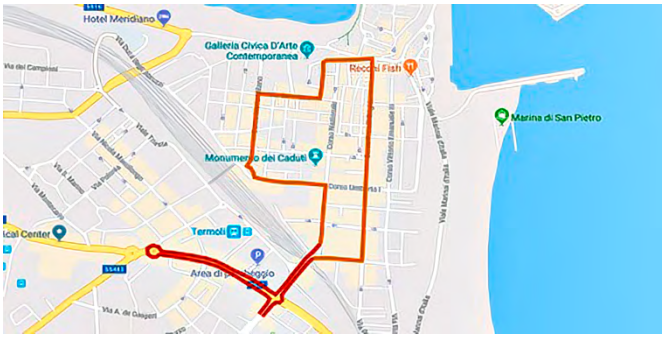

Figure 6. City route of Termoli where the red line indicates a residential area with high traffic intensity whereas the orange line indicates a residential area with medium traffic intensity

Table 6. Average concentrations of the different sizes of atmospheric particulate matter (μg m^{-3}) relating to the summer and winter periods; standard deviation (SD); minimum (min) and maximum (max) value determined; 60, 80, 95 percentiles. (*mor.* = morning; *aft.* = afternoon)

	Concentration mean (μg m^{-3})															
	Summer								Winter							
	PM_1		$PM_{2.5}$		PM_4		PM_{10}		PM_1		$PM_{2.5}$		PM_4		PM_{10}	
	mor.	*aft.*	*mor.*	*aft.*	*mor.*	*aft.*	*mor.*	*aft.*	*mor.*	*aft.*	*mor.*	*aft.*	*mor.*	*aft.*	*mor.*	*aft.*
mean	15.1	11.4	15.6	11.8	16.6	12.5	18.7	14.1	8.8	18.5	18.5	35.5	24.0	44.9	39.5	64.0
SD	7.4	10.8	7.5	10.9	8.2	11.3	10.8	12.9	2.5	3.2	2.6	3.9	3.1	5.1	6.9	10.1
min	8.0	3.0	9.0	4.0	9.0	4.0	9.0	4.0	6.8	12.6	16.2	30.1	20.4	38.2	28.5	51.7
max	122.0	164.0	135.0	165.0	169.0	166.0	276.0	184.0	22.6	27.0	32.4	50.0	38.3	64.3	58.8	101.9
60 %	14.0	9.0	14.0	10.0	15.0	10.0	18.0	12.0	8.5	18.7	18.2	35.7	23.7	44.7	39.5	63.2
80%	17.0	14.0	18.0	14.0	19.0	15.0	22.0	18.0	9.6	20.9	19.7	37.5	25.6	47.8	44.0	67.9
95%	26.0	26.0	27.0	27.0	29.0	28.0	33.0	32.0	11.5	24.3	21.5	42.6	28.5	55.4	52.1	85.2

Table 6 shows a variation in average concentrations between the summer period and the winter period. The concentrations of atmospheric particulates in the summer period are comparable within the day, while in the winter period, an increase in the concentration of the various fractions of PM is observed in the afternoon compared to the morning. This variation could be influenced by the presence of the sea breeze, which rises in the summer period and participates in the exchange of air. During the summer period, there is a greater delta between the minimum value and maximum value in the various fractions of the particulate matter. But even in this case, these values are occasional when compared to the 95% average values. In the afternoon sampling the average values of both $PM_{2.5}$ and PM_{10} exceed the permitted limit, 35.5 μg m^{-3} and 64 μg m^{-3} respectively. However, if this value is averaged with the average morning value, 11.8 μg m^{-3} for $PM_{2.5}$ and 14.1 μg m^{-3} for PM_{10}, the average daily values are 23.7 μg m^{-3} for $PM_{2.5}$ and 39.05 μg m^{-3} for PM_{10}, values that fall within the permitted limits. As regards the winter period, it should be underlined that the municipality of Termoli is crossed by a highly travelled stretch of motorway, which connects the south with the north of Italy. It is possible to suppose that in the winter period, the colder climatic conditions limit the exchange of air linked to convective motions and consequently, there is an increase in fine dust concentrations.

Figure 7 shows the comparison between the average distribution of ultrafine particles between the summer and winter periods in the two types of routes. It could be observed that the concentrations of UFP are comparable to those of atmospheric particulates. They appear to be 2000 # m^{-3} and 6000 # m^{-3} respectively lower in the summer and winter periods. Furthermore, on this site, the trend of UFPs in both the red path and the orange path assumes a comparable trend.

This paper aimed to characterize the air quality of some sites in the Molise region with data collected experimentally. The analysis of the data collected has underlined an important influence of air quality due to vehicular traffic and the use of heating systems, highlighting significant gaps between the summer period and the winter period. The geographical and demographic characteristics of Campobasso make the city comparable in terms of quality of life to many small Italian towns. In Italy the PM_{10} evaluation parameter is the daily average: according to Legislative Decree 155/2010 this limit is equal to 50 μg m^{-3}, not to be exceeded more than 35 times per year. The same decree also establishes an average annual limit of 40 μg m^{-3}. In April 2008 the European Union definitively adopted a

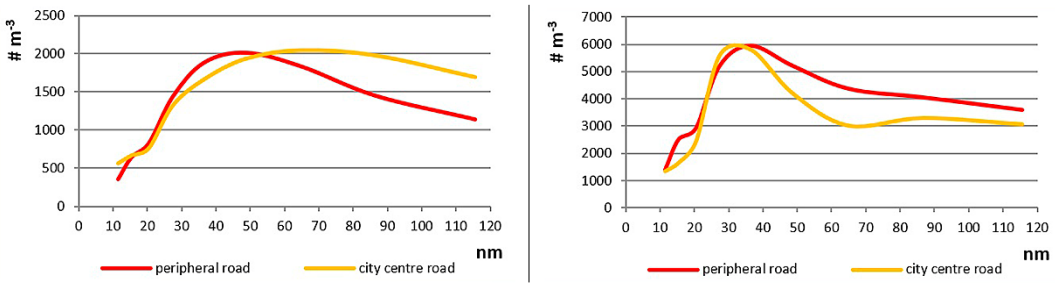

Figure 7. Comparison between the average distribution of ultrafine particles (# m^{-3}) VS the diameter of the particles (nm) between the summer and winter periods in the two types of routes

new directive (2008/50/EC) which sets air quality limits with concerning $PM_{2.5}$, considered the most dangerous for our health. As regards $PM_{2.5}$, only the average annual limit of 25 μg m^{-3} is established. There is currently no regulation on exposure limits for PM_4, PM_1 and ultrafine particles. The overall picture shows an almost ideal climatic situation, with concentrations of atmospheric particulates and ultrafine particles which in most cases are below the limit concentrations established by law. The presence of anomalous peaks is resolved over time.

The results of concentrations of $PM_{2.5}$ and PM_{10} in Campobasso were compared with those of atmospheric particulate matter in some Italian cities. There are approximately 15 common demographically comparable results, but only three present works in the literature regarding the monitoring of $PM_{2.5}$ and PM_{10} in different atmospheric and climatic conditions. The municipality of Lodi (Urso et al., 2015) is approximately 580 km from Rome in the North-West direction (45°19'N 9°30'E), approximately 44700 inhabitants, 41.38 km^2, 87 m above sea level, 1080.45 inhabitants km^{-2}. The municipality of Biella (Diana et al., 2022) is approximately 670 km from Rome in a North-West direction (45°33'59"N 8°03'12"E), approximately 42800 inhabitants, 46.69 km^2, 420 m above sea level, 917.22 inhabitants km^{-2}. Finally, the municipality of Avellino (Capozzi et al., 2022), about 250 km from Rome in a south-east direction (40°54'55"N 14°47'23"E), approximately 52100 inhabitants, 30.55 km^2, 348 m above sea level, 1,706.58 inhabitants km^{-2}. Table 7 compares the concentrations reported in the literature with those obtained experimentally with this work in the municipality of Campobasso.

In all the municipalities examined there is a variation in the concentration of the various dimensions of atmospheric particulate matter between the summer and winter periods linked to the variation in climatic conditions. The work carried out in the municipality of Biella presents concentration values relating only to PM_{10} and the reasons that explain the difference in concentrations between the summer and winter periods are widely discussed by the authors in the article [Diana et al., 2022]. It is possible to note how the concentrations of the two fractions of particulate matter, respectively the inhalable fraction (PM_{10}) and the respirable fraction ($PM_{2.5}$), present lower values in the municipality of Campobasso compared to the cities examined. Furthermore, the average concentrations obtained during the entire sampling campaign are decidedly lower when compared with those reported in the literature [Manigrasso et al., 2017] regarding large metropolises such as Rome (Table 8).

Table 7. Comparison of the average concentrations (μg m^{-3}) of $PM_{2.5}$ and PM_{10} in four comparable Italian cities. (*sum.* = summer, *win.* = winter)

	Concentration mean PM (μg m^{-3})			
	$PM_{2.5}$		PM_{10}	
	sum.	*win.*	*sum.*	*win.*
Lodi	19.8	38.3	28.3	65.2
Biella	/	/	4.0	80.0
Avellino	35.0	36.1	31.9	39.2
Campobasso	8.2	14.6	10.5	23.9

Table 8. Comparison between the average values of the three most populated areas of the entire sampling (μg m^{-3}) with the city of Rome

	Concentration mean PM (μg m^{-3})			
	PM_1	$PM_{2.5}$	PM_4	PM_{10}
Campobasso	8	11	12	16
Termoli	14	21	25	35
Venafro	26	31	40	45
Roma	129	130	131	137

Although the average concentrations of the various fractions of atmospheric particulate matter in Venafro are greater than those in Termoli or Campobasso, they become small (about a quarter) when compared to those of metropolises such as Rome.

Conclusions

In conclusion, this work began to demonstrate the quality of the air in the Molise region, starting from the measurement of the respirable and inhalable fraction of atmospheric particulate matter. The data collected is only a starting point. The authors examined the importance of respirable and non-respirable fractions and ultrafine particles for air quality monitoring. Studies on this topic are constantly updated and are not always sufficient to describe a correct public health assessment. It remains confirmed by the literature, the danger of submicron particles, which manage to reach the deepest part of the human respiratory system and are responsible for various pulmonary and cardiovascular diseases. They should represent, together with atmospheric particulate matter, the new assessment target for air quality.

References

Arfin, T., Pillai, A. M., Mathew, N., Tirpude, A., Bang, R., & Mondal, P. (2023). An overview of atmospheric aerosol and their effects on human health. *Environmental Science and Pollution Research*, 30, 125347–125369. https://doi.org/10.1007/s11356-023-29652-w

Avino, P., Casciardi, S., Fanizza, C., & Manigrasso, M. (2011). Deep Investigation of Ultrafine Particles in Urban Air. *Aerosol and Air Quality Research*, 11(6), 654–663. https://doi.org/10.4209/aaqr.2010.10.0086

Avino, P., Lopez, F., & Manigrasso, M. (2013). Regional Deposition of Submicrometer Aerosol in the Human Respiratory System Determined at 1-s Time Resolution of Particle Size Distribution Measurements. *Aerosol and Air Quality Research*, 13(6), 1702–1711. https://doi.org/10.4209/aaqr.2013.06.0189

Avino, P., & Manigrasso, M. (2017). Dynamic of submicrometer particles in urban environment. *Environmental Science and Pollution Research*, 24(16), 13908–13920. https://doi.org/10.1007/s11356-016-6752-8

Borrow, D. J., Van Netten, K., & Galvin, K. P. (2018). Ultrafine Particle Recovery Using Thin Permeable Films. *Frontiers in Chemistry*, 6, 220. https://doi.org/10.3389/fchem.2018.00220

Buonanno, G., & Morawska, L. (2015). Ultrafine particle emission of waste incinerators and comparison to the exposure of urban citizens. *Waste Management*, 37, 75–81. https://doi.org/10.1016/j.wasman.2014.03.008

Buonanno, G., Stabile, L., Avino, P., & Belluso, E. (2011). Chemical, dimensional and morphological ultrafine particle characterization from a waste-to-energy plant. *Waste Management*, 31(11), 2253–2262. https://doi.org/10.1016/j.wasman.2011.06.017

Capozzi, V., Raia, L., Cretella, V., De Vivo, C., & Cucciniello, R. (2022). The Impact of Meteorological Conditions and Agricultural Waste Burning on PM Levels: A Case Study of Avellino (Southern Italy). *International Journal of Environmental Research and Public Health*, 19(19), 12246. https://doi.org/10.3390/ijerph191912246

Costa, S., Ferreira, J., Silveira, C., Costa, C., Lopes, D., Relvas, H., Borrego, C., Roebeling, P., Miranda, A. I., & Paulo Teixeira, J. (2014). Integrating Health on Air Quality Assessment—Review Report on Health Risks of Two Major European Outdoor Air Pollutants: PM and NO_2. *Journal of Toxicology and Environmental Health*, Part B, 17(6), 307–340. https://doi.org/10.1080/10937404.2014.946164

Diana, A., Bertinetti, S., Abollino, O., Giacomino, A., Buoso, S., Favilli, L., Inaudi, P., & Malandrino, M. (2022). PM10 Element Distribution and Environmental-Sanitary Risk Analysis in Two Italian Industrial Cities. *Atmosphere*, 14(1), 48. https://doi.org/10.3390/atmos14010048

Donaldson, K., Stonea, V., Cloutera, A., Renwicka, L. & MacNee, W. (2001). Ultrafine particles. *Occupational and Environmental Medicine*, 58(3), 211–216. https://doi.org/10.1136/oem.58.3.211

Dondi, A., Carbone, C., Manieri, E., Zama, D., Del Bono, C., Betti, L., Biagi, C., & Lanari, M. (2023). Outdoor Air Pollution and Childhood Respiratory Disease: The Role of Oxidative Stress. *International Journal of Molecular Sciences*, 24(5), 4345. https://doi.org/10.3390/ijms24054345

Dongarrà, G., Manno, E., Varrica, D., Lombardo, M., & Vultaggio, M. (2010). Study on ambient concentrations of PM_{10}, $PM_{10-2.5}$, $PM_{2.5}$ and gaseous pollutants. Trace elements and chemical speciation of atmospheric particulates. *Atmospheric Environment*, 44(39), 5244–5257. https://doi.org/10.1016/j.atmosenv.2010.08.041

Du, Y., Xu, X., Chu, M., Guo, Y., Wang, J. (2016). Air particulate matter and cardiovascular disease: The epidemiological, biomedical and clinical evidence. *J. Thorac. Dis.*, 8. https://doi: 10.3978/j.issn.2072-1439.2015.11.37

Famiyeh, L., Jia, C., Chen, K., Tang, Y. T., Ji, D., He, J., & Guo, Q. (2023). Size distribution and lung-deposition of ambient particulate matter oxidative potential: A contrast between dithiothreitol and ascorbic acid assays. *Environmental Pollution*, 336, 122437. https://doi.org/10.1016/j.envpol.2023.122437

Feng, S., Gao, D., Liao, F., Zhou, F., & Wang, X. (2016). The health effects of ambient $PM_{2.5}$ and potential mechanisms. *Ecotoxicology and Environmental Safety*, 128, 67–74. https://doi.org/10.1016/j.ecoenv.2016.01.030

Fernández-Camacho, R., Rodríguez, S., De La Rosa, J., Sánchez De La Campa, A. M., Alastuey, A., Querol, X., González-Castanedo, Y., Garcia-Orellana, I., & Nava, S. (2012). Ultrafine particle and fine trace metal (As, Cd, Cu, Pb and Zn) pollution episodes induced by industrial emissions in Huelva, SW Spain. *Atmospheric Environment*, 61, 507–517. https://doi.org/10.1016/j.atmosenv.2012.08.003

Han, S. C., Wang, G. Z., & Zhou, G. B. (2023). Air pollution, EGFR mutation, and cancer initiation. *Cell Reports Medicine*, 4(5), 101046. https://doi.org/10.1016/j.xcrm.2023.101046

Heusinkveld, H. J., Wahle, T., Campbell, A., Westerink, R. H. S., Tran, L., Johnston, H., Stone, V., Cassee, F. R., & Schins, R. P. F. (2016). Neurodegenerative and neurological disorders by small inhaled particles. *NeuroToxicology*, 56, 94–106. https://doi.org/10.1016/j.neuro.2016.07.007

Hill, W., Lim, E. L., Weeden, C. E., Lee, C., Augustine, M., Chen, K., Kuan, F. C., Marongiu, F., Evans, E. J., Moore, D. A., Rodrigues, F. S., Pich, O., Bakker, B., Cha, H., Myers, R., Van Maldegem, F., Boumelha, J., Veeriah, S., Rowan, A., Lombardelli, C, N., Karasaki, T.,... Swanton, C. (2023). Lung adenocarcinoma promotion

by air pollutants. *Nature*, 616(7955), 159–167. https://doi.org/10.1038/s41586-023-05874-3

Jiang, B., Xie, Y., Xia, D., & Liu, X. (2019). A potential source for PM2.5: Analysis of fine particle generation mechanism in Wet Flue Gas Desulfurization System by modeling drying and breakage of slurry droplet. *Environmental Pollution*, 246, 249–256. https://doi.org/10.1016/j.envpol.2018.12.001

Johannson, K. A., Balmes, J. R., & Collard, H. R. (2015). Air Pollution Exposure. Chest, 147(4), 1161–1167. https://doi.org/10.1378/chest.14-1299

Kelly, F. J., & Fussell, J. C. (2019). Improving indoor air quality, health and performance within environments where people live, travel, learn and work. *Atmospheric Environment*, 200, 90–109. https://doi.org/10.1016/j.atmosenv.2018.11.058

Li, N., Sioutas, C., Cho, A., Schmitz, D., Misra, C., Sempf, J., Wang, M., Oberley, T., Froines, J., & Nel, A. (2003). Ultrafine particulate pollutants induce oxidative stress and mitochondrial damage. *Environmental Health Perspectives*, 111(4), 455–460. https://doi.org/10.1289/ehp.6000

Lodovici, M., & Bigagli, E. (2011). Oxidative Stress and Air Pollution Exposure. *Journal of Toxicology*, 2011, 1–9. https://doi.org/10.1155/2011/487074

Madureira, J., Slezakova, K., Silva, A. I., Lage, B., Mendes, A., Aguiar, L., Pereira, M. C., Teixeira, J. P., & Costa, C. (2020). Assessment of indoor air exposure at residential homes: Inhalation dose and lung deposition of PM10, PM2.5 and ultrafine particles among newborn children and their mothers. *Science of The Total Environment*, 717, 137293. https://doi.org/10.1016/j.scitotenv.2020.137293

Maher, B. A., Ahmed, I. A. M., Karloukovski, V., MacLaren, D. A., Foulds, P. G., Allsop, D., Mann, D. M. A., Torres-Jardón, R., & Calderon-Garciduenas, L. (2016). Magnetite pollution nanoparticles in the human brain. *Proceedings of the National Academy of Sciences*, 113(39), 10797–10801. https://doi.org/10.1073/pnas.1605941113

Manigrasso, M., Costabile, F., Liberto, L. D., Gobbi, G. P., Gualtieri, M., Zanini, G., & Avino, P. (2020). Size resolved aerosol respiratory doses in a Mediterranean urban area: From PM10 to ultrafine particles. *Environment International*, 141, 105714. https://doi.org/10.1016/j.envint.2020.105714

Manigrasso, M., Natale, C., Vitali, M., Protano, C., & Avino, P. (2017). Pedestrians in Traffic Environments: Ultrafine Particle Respiratory Doses. *International Journal of Environmental Research and Public Health*, 14(3), 288. https://doi.org/10.3390/ijerph14030288

Marini, S., Buonanno, G., Stabile, L., & Avino, P. (2015). A benchmark for numerical scheme validation of airborne particle exposure in street canyons. *Environmental Science and Pollution Research*, 22(3), 2051–2063. https://doi.org/10.1007/s11356-014-3491-6

Notardonato, I., Manigrasso, M., Pierno, L., Settimo, G., Protano, C., Vitali, M., Mattei, V., Martellucci, S., Di, F., Boccia, P., & Avino, P. (2019). The importance of measuring ultrafine particles in urban air quality monitoring in small cities. *Geographica Pannonica*, 23(4), 347–358. https://doi.org/10.5937/gp23-24447

Settimo, G., Yu, Y., Gola, M., Buffoli, M., & Capolongo, S. (2023). Challenges in IAQ for Indoor Spaces: A Comparison of the Reference Guideline Values of Indoor Air Pollutants from the Governments and International Institutions. *Atmosphere*, 14(4), 633. https://doi.org/10.3390/atmos14040633

Soggiu, M. E., Inglessis, M., Gagliardi, R. V., Settimo, G., Marsili, G., Notardonato, I., & Avino, P. (2020). PM10 and PM2.5 Qualitative Source Apportionment Using Selective Wind Direction Sampling in a Port-Industrial Area in Civitavecchia, Italy. *Atmosphere*, 11(1), 94. https://doi.org/10.3390/atmos11010094

Stabile, L., Buonanno, G., Avino, P., Frattolillo, A., & Guerriero, E. (2018). Indoor exposure to particles emitted by biomass-burning heating systems and evaluation of dose and lung cancer risk received by population. *Environmental Pollution*, 235, 65–73. https://doi.org/10.1016/j.envpol.2017.12.055

Turpin, B. J., Saxena, P., & Andrews, E. (2000). Measuring and simulating particulate organics in the atmosphere: Problems and prospects. *Atmospheric Environment*, 34(18), 2983–3013. https://doi.org/10.1016/S1352-2310(99)00501-4

Urso, P., Cattaneo, A., Garramone, G., Peruzzo, C., Cavallo, D. M., & Carrer, P. (2015). Identification of particulate matter determinants in residential homes. *Building and Environment*, 86, 61–69. https://doi.org/10.1016/j.buildenv.2014.12.019

Vahlsing, C., & Smith, K. R. (2012). Global review of national ambient air quality standards for PM10 and SO2 (24 h). *Air Quality, Atmosphere & Health*, 5(4), 393–399. https://doi.org/10.1007/s11869-010-0131-2

Wang, G., Bai, X., Wu, C., Li, W., Liu, K., & Kiani, A. (2018). Recent advances in the beneficiation of ultrafine coal particles. *Fuel Processing Technology*, 178, 104–125. https://doi.org/10.1016/j.fuproc.2018.04.035

Word Health Organization - WHO. (2010). *Guidelines for indoor air quality: selected pollutants*. Copenhagen, Denmark.

Wright, L. P., Zhang, L., Cheng, I., Aherne, J., & Wentworth, G. R. (2018). Impacts and Effects Indicators of Atmospheric Deposition of Major Pollutants to Various Ecosystems—A Review. *Aerosol and Air Quality Research*, 18(8), 1953–1992. https://doi.org/10.4209/aaqr.2018.03.0107

Xing, Y. F., Xu, Y. H., Shi, M. H., Lian, Y. X., (2016). The impact of PM2.5 on the human respiratory system. *Journal of Thoracic Disease*, 8(1), E69 - E742016. https://doi:10.3978/j.issn.2072-1439.2016.01.19

INTERNATIONAL SCIENTIFIC JOURNAL
GEOGRAPHICA PANNONICA
Volume 28, Issue 3, 169–181 (September 2024)
Journal homepage: http://www.dgt.uns.ac.rs/en/homepage/pannonica/

Lateral Meander Migration of a Medium-sized Lowland River: Case Study on the Rába River, Hungary

Alexandra Pusztai-Eredics[A*], Gábor Kovács[B], Gábor Tóth[B], Tibor Lenner[B], Tímea Kiss[C]

[A] *ELTE Doctoral School of Environmental Sciences, Egyetem sq. 1-3, 1053 Budapest, Hungary*
[B] *Department of Geography, ELTE Savaria University Centre, Károlyi Gáspár sq. 4, 9700 Szombathely, Hungary*
[C] *Independent researcher, Horváth Gy. str. 80, 6630 Mindszent, Hungary*

KEYWORDS

meandering
lateral channel migration
human impact
QGIS
topographic maps

ABSTRACT

Engineering works greatly influence the lateral channel migration (LCM) of meandering rivers. We aimed to characterise the spatiotemporal characteristics of LCM during the last 174 years of the almost freely meandering Upper Rába (Hungary) and to identify units with distinctive LCM histories. The studied Rába's reach has been regulated just at some points. Due to the free meandering, its length varied between 119 and 133 km. The most intensive length increase (+291 m/y) took place between 2005 and 2008, and by the end of the process, the sinuosity had reached its historical maximum (SI_{2018}= 1.93). The mean LCM was 3.3 m/y (1844–2018). The periods with intensive channel migration (max: 24–27 m/y) were followed by periods with low migration rates. Based on local channel morphology and LCM rates, 14 units were identified. The highest LCM rate was measured in the freely migrating units (R5: 5.8 m/y; R3: 4.4 m/y and R6 4.0 m/y).

Introduction

Lateral channel migration (LCM) is a fundamental process governing the channel dynamics of meandering rivers (Blanka & Kiss, 2008; Bertalan et al., 2016) and contributing to the sediment budget (Nagy & Kiss, 2020; Kiss et al., 2022, 2024). However, bank erosion can cause severe damage to agricultural lands, settlements, or infrastructure, depending on its extent and intensity (Lawler et al., 1997; Das et al., 2012; Bertalan et al., 2019; Langović et al., 2024). The horizontal channel shift of free or partially controlled meandering rivers could have a significant LCM up to several meters per year. Therefore, monitoring the spatiotemporal extent and driving factors of channel changes is crucial, especially along some highlighted reaches and sections (Blanka & Kiss, 2008; Hooke, 2008; Mirijovsky et al., 2015; Bertalan et al., 2016; Bertalan et al., 2019), allowing the prediction of the lateral migration process, providing a basis for sustainable channel and floodplain management, e.g., to determine the necessary floodplain width (Sipos et al., 2022).

Historical maps of the last two to three centuries and modern sources provide valuable sources for analysing past processes and could be used to determine the direction and rate of channel development (Goudie, 1990; Hudson & Kesel, 2000; Dragicevic et al., 2017). Geoinformatics completed by remote sensing methods and field geodetic measurements allow fast and accurate data collection and systematization to reveal the characteristics of horizontal channel development (Clerici et al., 2015; Schwendel et al., 2015; Yousefi et al., 2018; Bertalan et al., 2019). The increasing availability of remotely sensed and topographic

[*] Corresponding author: Alexandra Pusztai-Eredics, email: eredics.alexandra@sek.elte.hu
doi: 10.5937/gp28-49989
Received: March 22, 2024| Revised: June 26, 2024| Accepted: August 29, 2024

databases has significantly boosted spatiotemporal studies with increasingly smaller errors (Blanka & Kiss, 2008, 2011; Michalková, 2009; Michalková et al., 2011; Bertalan & Szabó 2015; Pavlek, 2023; Langović et al., 2021).

Meandering is a common channel pattern of alluvial rivers (Rhoads & Welford, 1991; Thorne, 1997; Hooke, 2007; Blanka, 2010). Especially in the middle of the Carpathian Basin, where most rivers are embedded into alluvial deposits, their slope and discharge characteristics allow the development of a meandering channel pattern (Timár & Telbisz, 2005). Although most meandering rivers in Hungary have been regulated, there are sections where the channel is still unregulated. The intensive meander development is the main problem, often endangering settlements and infrastructure (Laczay, 1972), justifying the need for comprehensive studies.

The Rába River is a tributary of the Danube. Formerly, its lower reach (downstream of Sárvár) was studied in detail from a hydro-morphological point of view (Károlyi, 1962; Laczay, 1972). However, no mapping or morphometric study has been conducted on the upper Hungarian reach. The main problem is that the free meander migration erodes arable lands and destroys roads and infrastructure. Thus, to carry out sustainable floodplain and channel management, it is necessary to understand the characteristics of the long-term channel evolution. Therefore, we aimed to collect spatial data over a long time (1844–2018) and to identify the most intensively migrating sections of the Upper Rába River in Hungary. The following research questions were raised: (1) What were the main spatial and temporal characteristics of the LCM during the last 174 years? (2) Could the studied reach be divided into smaller units with distinctive LCM histories? (3) How did the local engineering works influence the long-term evolution of the river?

Study area

The Rába River (length: 287 km) is one of the main rivers in Western Hungary (Bergmann et al., 1996). The Upper Rába (from its source in Austria to Sárvár) has been regulated only at a few points, mainly at settlements; thus, it meanders freely on its floodplain. The local works aimed to protect the settlements, transport infrastructure, and flood defence works from flooding and lateral erosion. Besides, five dams were built on the Upper Rába (Bergmann et al.,

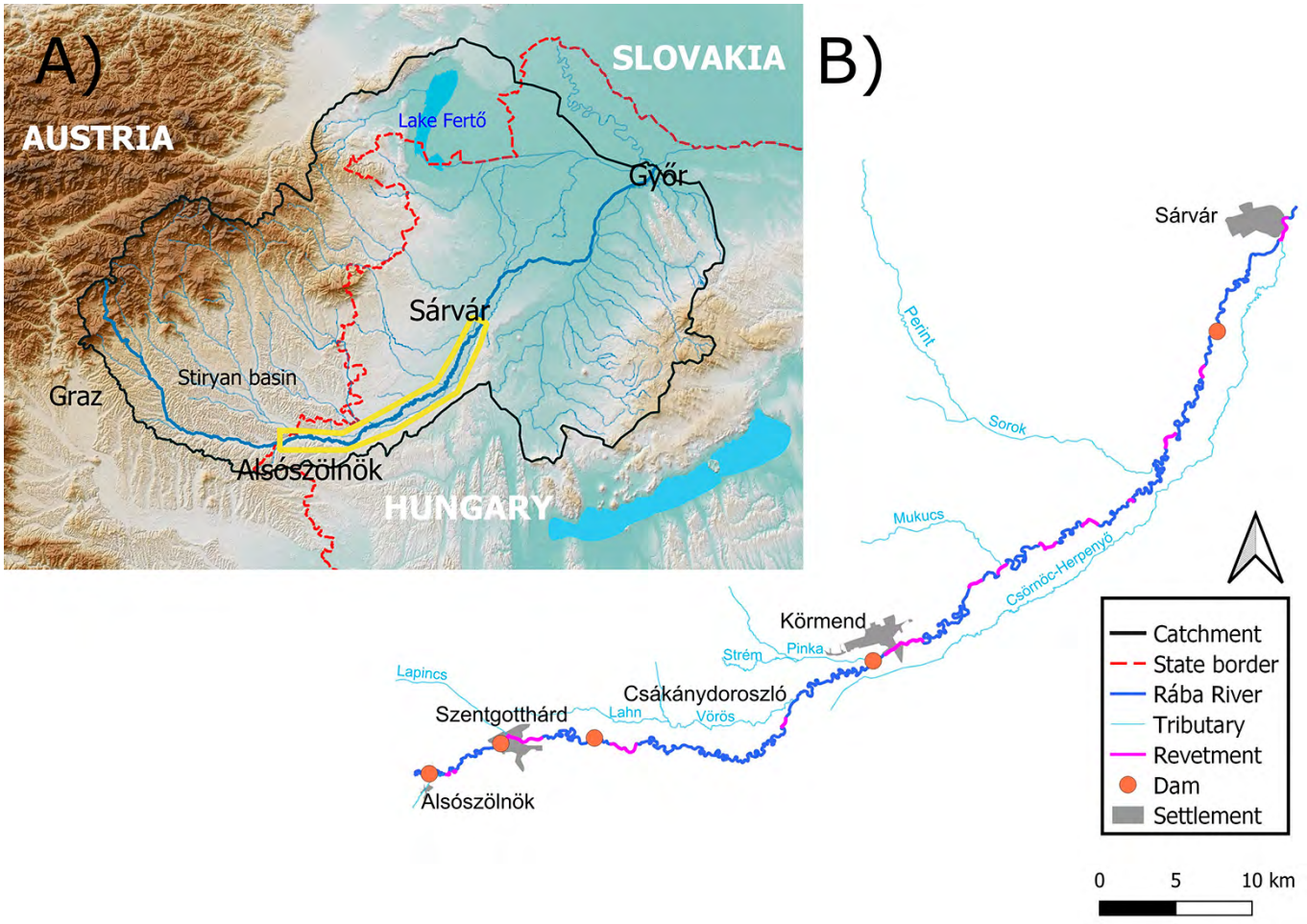

Figure 1. The catchment of the Rába River is located in Austria and Hungary (A). The upper part of the Hungarian reach was studied in detail (B)

1996). On the contrary, the Lower Rába is confined by artificial levees, and its channel is regulated by cut-offs and revetments to a large extent (Laczay, 1972). This study aimed to analyse the channel development of the Hungarian Upper Rába reach (Figure 1).

The catchment of the Rába River (10,113 km^2) is shared by Austria and Hungary. The Alpine sub-catchments have a key influence on the regime of the Rába. The first flood of the river in March is initiated by snowmelt and rainfall, then heavy rainfalls trigger rapid floods in July. In November, a smaller flood is related to Mediterranean cyclones. Based on the characteristic discharge values (Q_{min}= 2.6 m^3/s and Q_{max}= 471 m^3/s measured at Szentgotthárd), the Rába River is a medium-sized river. It contributes to the mean discharge of the Danube by 1.3% (Bergmann et al., 1996).

The hydrology of the Hungarian Upper Rába is determined by the tributaries draining the mountainous sub-catchments in the Eastern Alps (Figure 1). On the other hand, the Upper Rába has no significant right-side tributary (Laczay, 1972). The Lapincs Brook has the greatest influence on the water and sediment transport of the Upper Rába since the mean discharge of the Lapincs is three times greater than the mean discharge of the Rába, and its coarse sediments also have a major influence on the formation of the riverbed (Károlyi, 1962).

The Hungarian Upper Rába is located in a 2–3 km wide valley, influenced by tectonic displacements. The mean gradient of the upstream part of the Upper Rába valley is 1‰, then decreases to 0.85‰, and finally increases to 0.90–0.86‰ in the downstream section (Bergmann et al., 1996).

The large amount of sediment transported by the Rába decreases significantly along the studied reach (Bogárdi, 1971). Bedload transport starts at Q ≥12 m^3/s, reaching its maximum at 30 m^3/s (EDUVIZIG, 2024). Large amounts of the bedload and suspended sediment are deposited on the valley floor during floods (Bergmann et al., 1996).

Materials and Methods

Data sources

Military maps, civilian maps, and orthophotos were used to analyse the horizontal channel shift (Table 1). They have different sources with different formats and projections; thus, they had to be integrated into the same projection system (EPSG:23700–HD72/EOV) using QGIS (3.28/Firenze). Georeferencing was performed using control points (e.g., bridges, road crossings, and churches).

The error in georeferencing (Table 1) of the Second Military Survey (1844–1855) (Timár et al., 2006) was greater than that of the Third Military Survey (1878–1880) (Biszak et al., 2007; Jankó, 2007). The military maps of the 20th century (made in 1951, 1955–1956, and 1983–1984) were provided by the Hungarian Military History Institute and Museum. To create the 1951 map, the sheets of the Third Military Survey were re-edited based on field survey data or by visual interpretation of aerial photographs (Jankó, 2007; Hegedüs, 2007). The next detailed survey of the Rába valley was completed in 1955–1956, so it became the next accurate mapping after the Third Military Survey. In or-

Table 1. Main characteristics of maps and orthophotos used in the present study

Source	Survey date	Scale	Resolution (m/px)	Horizontal error (m) of the original source		Mean error (m) after georeferencing
				Mean	Maximum	
Second Military Survey	1844–1855	1: 28,800		70–80*	200** / 140–300*	2.2±1.3
Third Military Survey	1878–1880	1: 25,000		5–10***	80–120***	1.8±0.9
Military Topographical Map	1951	1: 25,000		5–10***		0.8±0.4
Military Topographical Map	1955–1956	1: 25,000		5–10***		0.8±0.4
Civil topographical map	1960–1961	1: 10,000		neglible		
Military Topographical Map	1983–1984	1: 25,000		neglible		
Civil topographical map („EOTR")	1983, 1996–1998	1: 10,000		neglible		
Orthophoto	2000		0.5	neglible		
Orthophoto	2005		0.5	neglible		
Orthophoto	2008		0.5	neglible		
Orthophoto	2012		0.4	neglible		
Orthophoto	2015		0.4	neglible		
Orthophoto	2018		0.4	neglible		

*Source: * Kovács, 2010; **Timár & Molnár, 2003; ***Kovács et al., 2024a*

der to avoid the horizontal errors of the various maps, the method proposed by Timár & Molnár (2003) was followed, and control points (100 points/survey) were applied for each map sheet. Topographic maps (1960–1961, 1983, and 1996–1998) have also been produced for civilian purposes. These map series were optimised for the territory of Hungary, so their projection inaccuracies are neglectable.

The projection inaccuracies of the orthophoto images (taken in 2000, 2005, 2008, 2012, 2015, and 2018) are negligible; they were orthorectified by the provider (Lechner Knowledge Centre).

The main error of the remotely sensed dataset originates in the canopy cover of deciduous trees, as the woody riparian vegetation could hide the bankline during digitisation. To solve the problem, the image processing method *Classification* (plugin) within QGIS was used to classify the pixels of a given orthophoto. The created pixel classes with the same or similar properties supported the separation of the land from the water so that the bankline of the channel could be delineated (Pusztai-Eredics et al., 2024).

Calculation of sinuosity and lateral migration rate of the bankline

The banklines and the centre line were determined (midpoints of the distance between the banks) on each map and orthophoto. The Sinuosity Index (SI) was calculated as the ratio of the length of the centre line and the length of the meander belt (Brierley & Fryirs, 2005).

The vectorized banklines were overlapped in QGIS using the NNjoin module. The new polygon between two subsequent banklines in the direction of the displacement indicates the area eroded from the floodplain by the channel. In contrast, the polygon on the other side refers to the area of accumulation.

Geometrical and statistical methods were used to determine the extent of the LCM rate. First, a perpendicular line was constructed on a digitised bankline every 2 m all along the studied reach (Figure 2A). Along these lines, the lateral channel shift was measured. The annual LCM rate (m/y) was expressed as the ratio of the length of perpendicular lines and the years between two surveys.

To determine the maximum LCM rates, circles with a diameter of 500 m were placed along the centre line. The circles overlap by 90 m, approximately equal to the doubled channel width (Figure 2B). The maximum LCM rates within the circles were determined by applying a moving average.

Delimitation of the units of the Upper Rába section in Hungary

Based on the LCM rate and the degree of human influence, 14 units with similar channel characteristics were identified on the Upper Rába. The unit boundaries were set at inflexion points (following Bertalan et al., 2019), where the channel evolution rate showed a clear shift. The unit length, the proportion (%) of bank protection, and average and maximum LCM rates (m/y) were calculated in each unit. The joining tributaries were also considered, as they could substantially influence the water and sediment dynamism of a unit. The slope of each unit was determined based on the longitudinal profile provided by the Water Directorate.

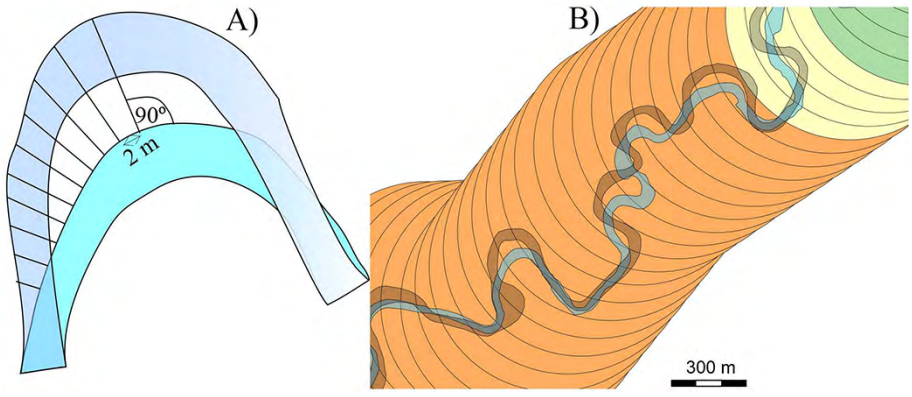

Figure 2. The method used to quantify lateral channel changes in every 2 meters (A) and to identify the rate and location of the greatest lateral erosion

Results

Based on the spatial data, the LCM of the Hungarian Upper Rába was studied in detail over 174 years.

Changes in river length

The length of the centre line of the Upper Rába was 127.5±4.5 km during the studied period (Figure 3). The reach length has changed dramatically in some periods due to natural or artificial cut-offs. The most extensive shortening was observed between 1844 and 1879, as the river was shortened by 7.7 km or 6% (–266 m/y) by artificial cut-offs. Therefore, its originally high sinuosity (SI_{1844}=1.84) decreased (SI_{1878}=1.73). By the 1960s, the original length of the channel had almost recovered, as well as its sinuosity (SI_{1960}=1.84). However, several meanders were artificially cut off between 1968 and 1977, and some natural meander cut-offs also happened. Thus, by the early 1980s, the 24 cut-offs had shortened the Hungarian Upper Rába by about 2.7 km, or 2% (–117 m/y). Since the late 1990s, the reach length increased again (by 2.6%, +235 m/y) as intensive meander development started, as reflected by the increasing sinuosity (SI_{1996}=1.85). The most intensive length increase (+291 m/y) took place between 2005 and 2008, thus in 2018 the sinuosity had reached its historical maximum (SI_{2018}= 1.93).

Temporal changes in lateral channel migration (LCM) rate

The regulation works were very limited along the studied reach of the Upper Rába; therefore, the channel could almost freely develop by bank erosion and point-bar accumulation. As a result, the mean LCM rate over the entire studied period (1844–2018) was 3.3 m/y.

However, the LCM showed considerable spatiotemporal variability (Figure 4). During the 1950s (1951–1959) and late 1990s (1996–1999), the LCM was high and changeable compared to other periods (Figure 5), as reflected by the box plots with many outliers and a wide range between extreme values. In these periods, the mean LCM was 4.1–4.9 m/y; however, it was as high as 15–20 m/y at some bends. The lateral channel shift was especially intensive in the late 1990s, as some meanders were displaced by 24–27 m/y, reaching the maximum values of the entire studied period. The direction of the LCM is also interesting, as in the 1950s, the channel mostly migrated towards its left bank (west), but later, in the late 1990s, the channel shifted towards the right bank.

The periods of intensive LCM were always followed by periods when the LCM became moderate or slow (Figure 5). Low LCM rates (2.2–2.8 m/y) were measured in five periods (1878–1950, 1960–1982, 2000–2004, 2005–2007 and 2015–2018). During these periods, the box plots reflect that the individual bends migrated almost uniformly, as the boxes are narrow and outliers are almost missing.

The periods with intensive LCM were preceded by periods with gradually increasing values. For example, the 20th century started with a very limited LCM rate (mean: 2.1 m/y). However, after 2005 a gradually increasing trend is visible until 2012–2014 (mean: 3.5 m/y). Then, the cycle started again, as moderate LCM (mean: 2.6 m/y) between 2015 and 2018 followed the last intensive migration phase.

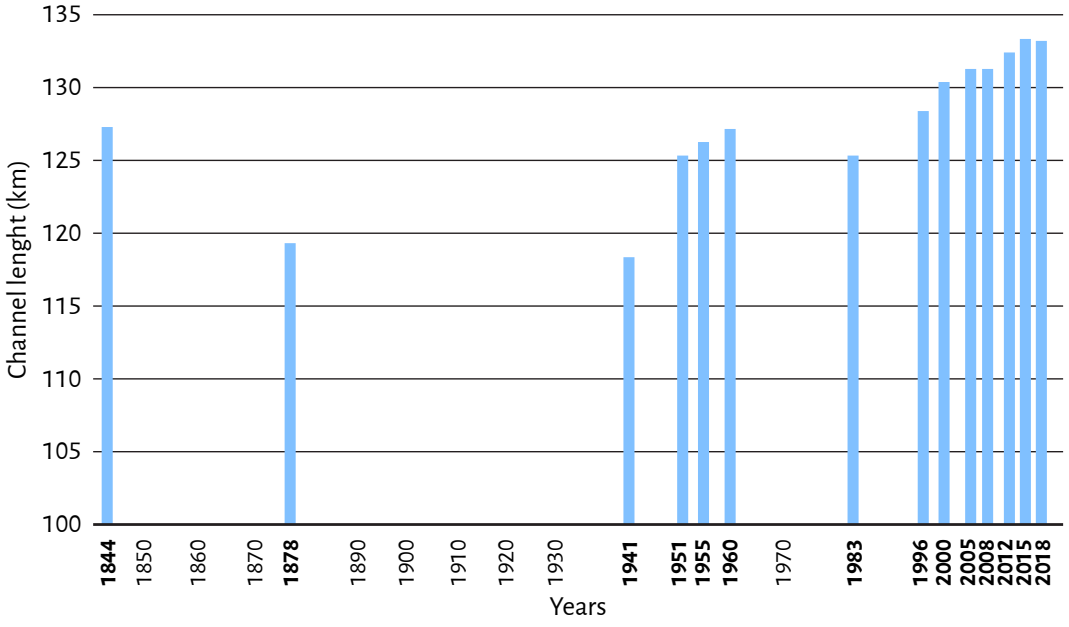

Figure 3. Changes in reach length (km) of the Hungarian Upper Rába between 1844 and 2018

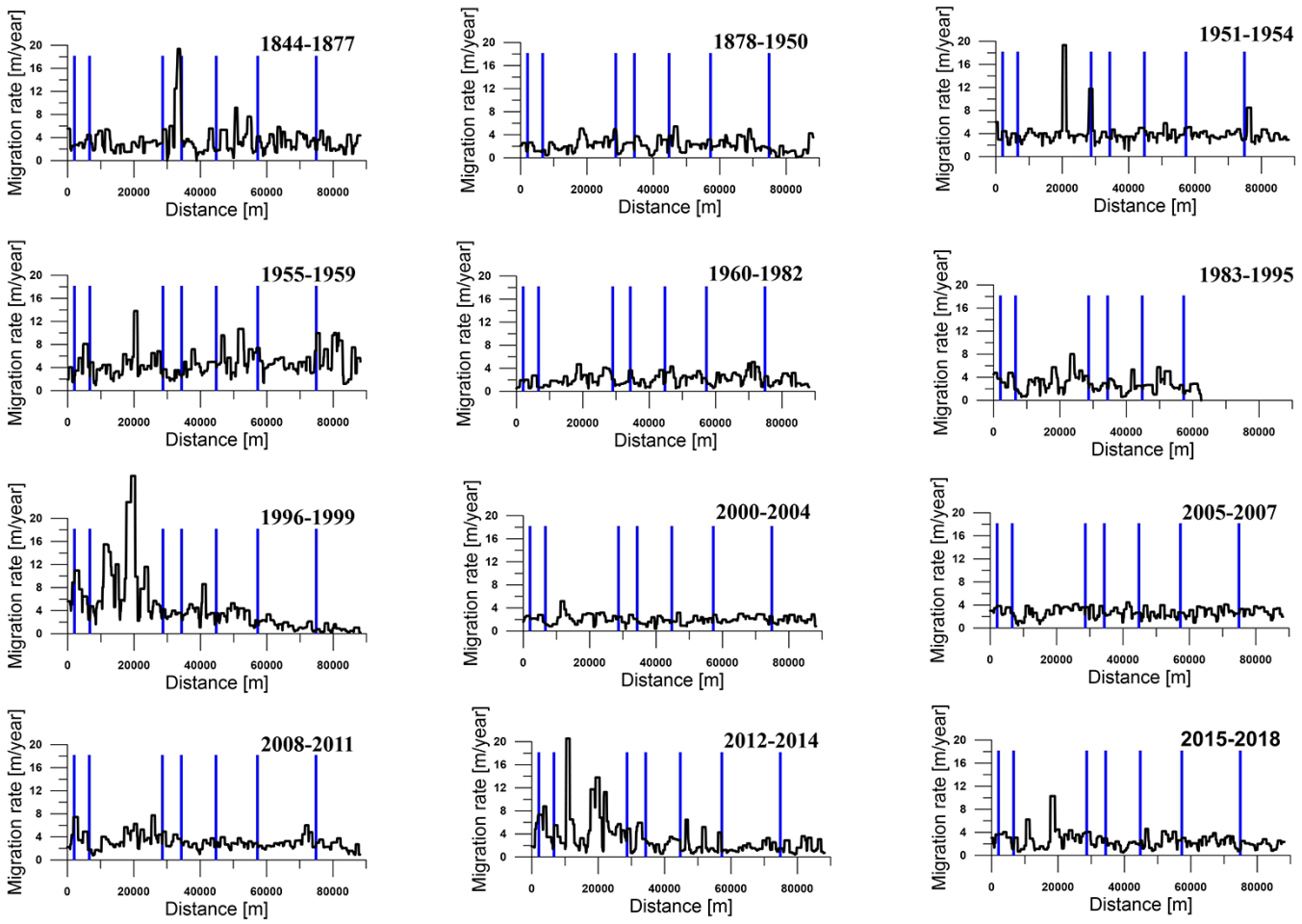

Figure 4. Changes in lateral channel migration rate between subsequent surveys along the Hungarian Upper Rába. Blue bars indicate the location of confluences. On the horizontal axis, the distance refers to the distance from the Austro-Hungarian border, where the Rába enters Hungary

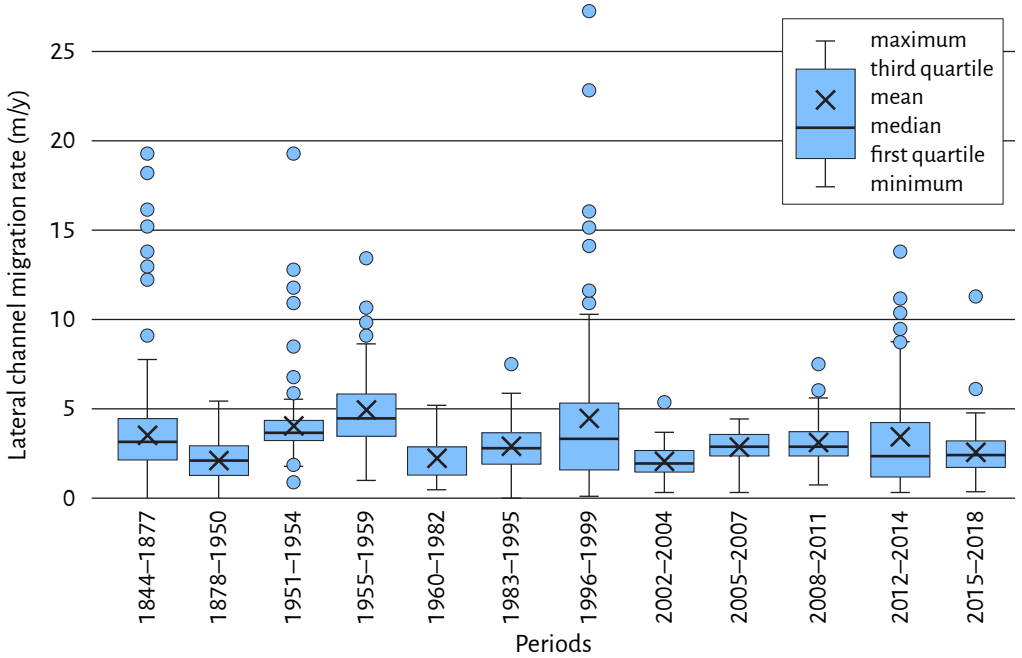

Figure 5. Temporal characteristics of the LCM of the Upper Rába. The input data of the box plots are the LCM of single bends

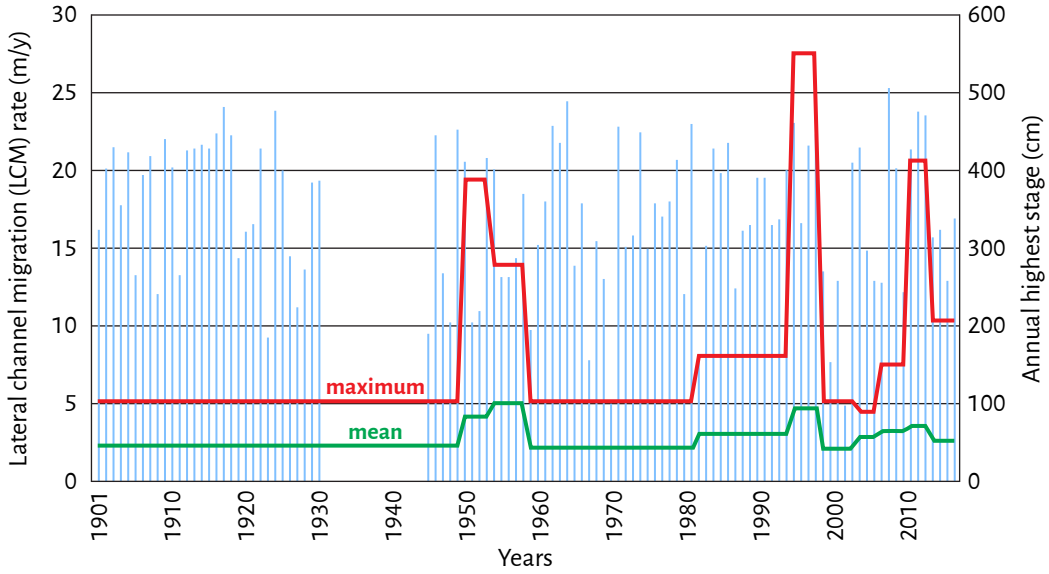

Figure 6. Connection between mean and maximum lateral migration rate and annual highest water levels measured at Körmend gauging station

Hydrological background of the lateral channel migration

The occurrence of floods was compared to the channel shifts of the Upper Rába. Four major floods occurred in 1883, 1900, 1910, and 1925; however, their effects on LCM were unclear (Figure 6), as the LCM rates were probably levelled during the long interval (72 y) between the subsequent surveys. The next major flood was registered in 1963, and another large flood followed it in 1965 when the highest water level on record was measured. However, despite the two consecutive floods, there was no evidence of more intensive LCM between 1960 and 1982 (22 y).

However, since 1996, more frequent spatial data on LCM have been available. Thus, the effect of floods in 1996, 2009, and 2013 could be identified on lateral erosion. After the 1996 flood, the maximum LCM rate was 27.3 m/y for the four years (1996–1999). The 2009 flood resulted in a maximum displacement of 7.7 m/y (for 2008–2011), while after the 2013 flood the maximum value was again quite high, as it was 20.5 m/y (2012–2014).

These contradictory results suggest that a long period between surveys could hide the effects of hydrology on LCM. In contrast, if the surveys were made with shorter intervals, the effects of floods could be detected. Besides, the LCM seems to have a cyclic pattern: it gradually increases until it reaches a peak value, and then – regardless of the floods – a relaxation period comes with low bank erosion rate.

Spatial changes in lateral channel migration (LCM) rate

The detailed analysis of the temporal variations in LCM rate revealed periods with intensive or moderate channel changes. However, it was hypothesised that there were spatial variations, as local variables influence the bed morphology (e.g., confinement, slope, revetments, and tributaries). Based on local variables and LCM rates, 14 units with similar meander characteristics were identified on the Upper Rába (Figure 7; Table 2).

Some units could be considered as "near-natural" ones (R3, R5, R6, R8, and R13), as they experienced no or minimal human impact. However, even these units could not develop naturally, as the effects of upstream or downstream human impacts might propagate toward them. These units represent 84% (111.5 km) of the studied Upper Rába. They are far from settlements, and the valley sides do not impede meander development. Therefore, these units had the highest LCM (Figure 8). The Unit R5 had the highest LCM rate (5.8 m/y) with the greatest variability (from 2.6 m/y to 27.5 m/y). Also, a high average migration rate was measured in Units R3 (4.4 m/y) and R6 (4.0 m/y).

The "heavily modified" group of units (R2, R4, R7, R9, R11, and R14) have been affected by human interventions to a great extent. In several bends, the concave bank was stabilised by revetments between 1968 and 1977, and many meanders were artificially cut off. Before these engineering works, these meanders also developed freely (Figure 8). Thus, they had intensive LCM (1844–1959: 2.5-3.6 m/y). However, LCM became negligible after the bank stabilisation and cut-offs, the (1983–2018: 1.6-2.6 m/y). Consequently, the long-term average LCM rate of these units with bank stabilisations became low (2.0-3.0 m/y).

The third group of units belongs to the "slightly modified" class (R1, R10, and R12). These units had moderate LCM rates, as the long-term average varied between 2.9 and 3.6 m/y. Due to their medium character, these units had significant variations in LCM between the lowest (1.7–1.9 m/y) and highest (5.4–7.8 m/y) rates.

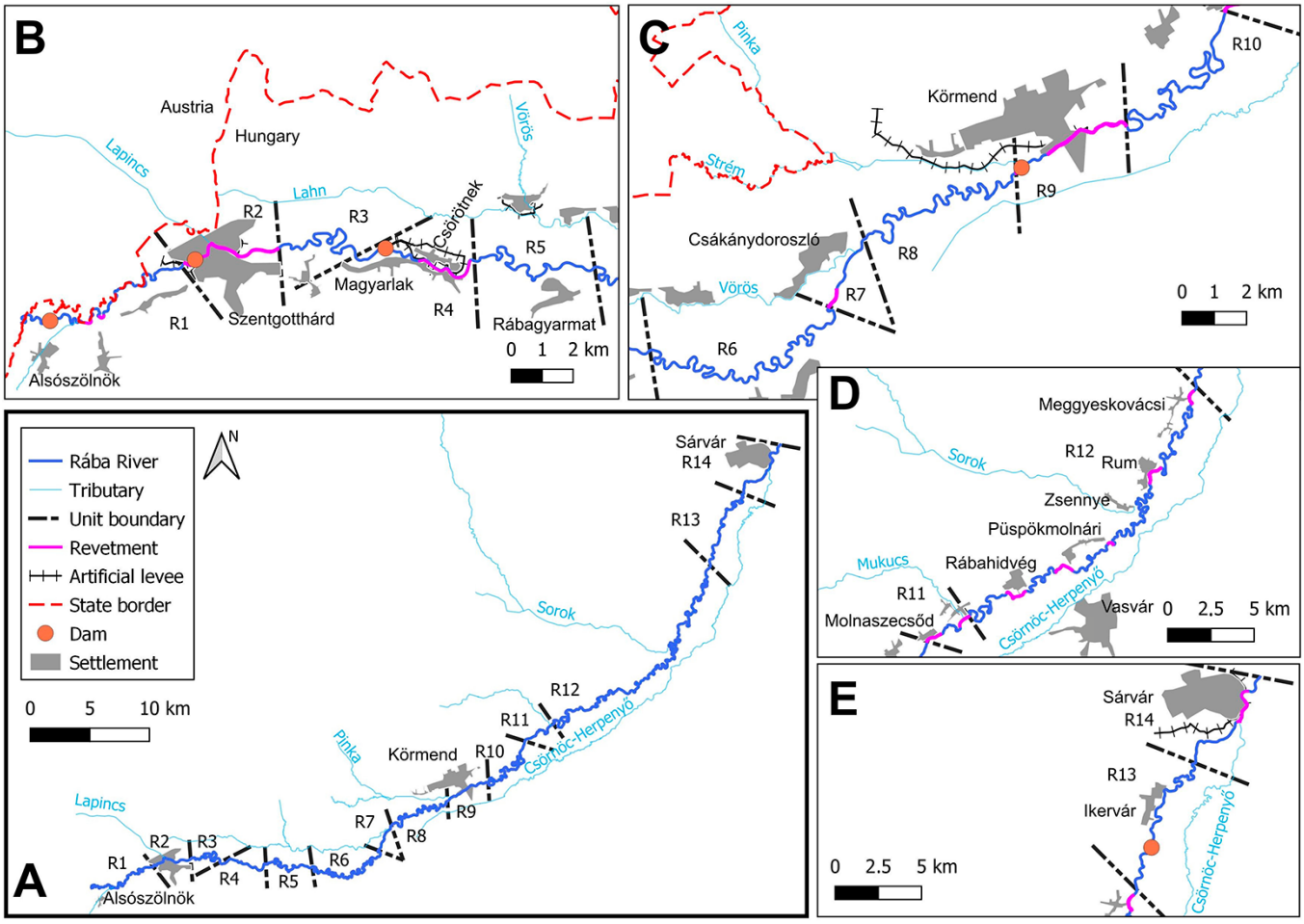

Figure 7. Fourteen morphologically uniform units were identified along the Hungarian reach of the Upper Rába (A). Some units have higher sinuosity, greater lateral migration, and more human impact than others (B–E)

Table 2. Main characteristics of the units identified along the Upper Rába

Unit (river km)	Length in 2018 (km)	Confinement	Slope in 2023 (m/km)	Number of bends	Proportion of revetments (%)	Migration rate (m/y) (1844-2018)	
						mean	max.
R1 (216.3-207.5)	8.8	none	1.06	40	5.7	3.6	10.9
R2 (207.5-203.7)	3.8	great	1.32	8	95	2.1	5.6
R3 (203.7-197.9)	5.9	none	0.58	14	0	4.4	20.5
R4 (197.9-193)	4.9	great	0.9	14	44.9	2.6	12.0
R5 (193-186.2)	6.8	none	0.76	22	0	5.8	27.3
R6 (186.2-173.6)	13.9	none	0.56	48	0	4.0	11.8
R7 (173.6-171.1)	2.5	none	0.52	6	24	2.1	9.3
R8 (171.1-160.8)	10.7	partial	0.46	36	0	3.3	19.4
R9 (160.8-156.7)	4.1	great	0.73	9	75.6	2	12.8
R10 (156.7-145.2)	11.9	none	0.4	31	0	3.0	9.6
R11 (145.2-141.6)	3.6	none	0.64	12	47.2	3.0	17.6
R12 (141.6-102.9)	39.2	none	0.42	125	13.3	2.9	10.7
R13 (102.9-93.1)	10.3	none	0.93	29	0	2.8	10.0
R14 (93.1-86.6)	6.5	great	0.58	18	29.2	2.2	7.5

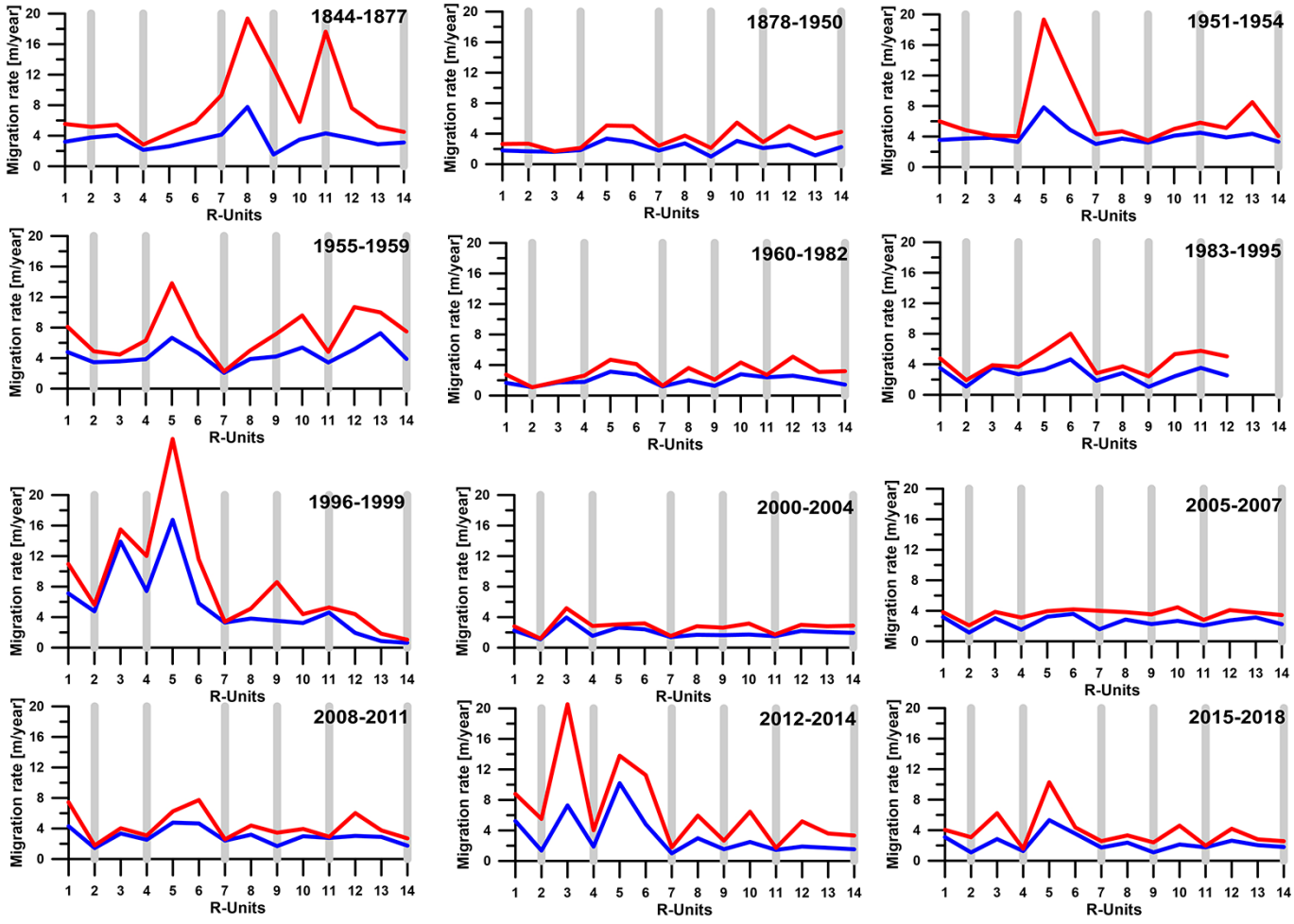

Figure 8. Mean (blue) and maximum (red) lateral channel migration rates of the units during the studied periods. (Grey bars indicate "heavily modified" units)

It is also interesting to note that, in terms of LCM direction, units directly affected by human interventions tended to move towards the right bank, while naturally developing stretches tended to migrate towards the left bank.

Discussion

Significant lateral erosion and LCM have been detected along the bends of the Hungarian Upper Rába reach over the last 174 years. However, their magnitude and direction were not uniform, neither in space nor in time, as there are significant differences between the different periods and between the identified units of the studied reach.

The studied reach has been significantly shaped by local river management works, particularly between 1968 and 1977, highlighting the substantial role of human intervention. Based on the extent of this influence and meander migration characteristics, 14 units were identified and later classified into three groups (Figure 9).

Most of the reach develops without direct human impact (84% of the total length) or with limited human impact (16%). However, these bends could not have developed completely freely either, as these units are located between units that have been heavily modified by direct interventions (e.g., cut-offs, revetments, dams). The cut-offs increase the slope, the revetments increase the flow velocity by reducing the channel friction, and dams could impound the channel. These effects propagate both upstream and downstream. Thus, they may also have affected the flow and sediment transport conditions of the freely developing units.

Spatiotemporal changes in reach length and lateral migration rate

The studied parameters reflect intensive LCM, especially in naturally developing units. The most intensive increase in reach length was observed between 2005 and 2008 (291 m/y). However, this lengthening varied in space, as the

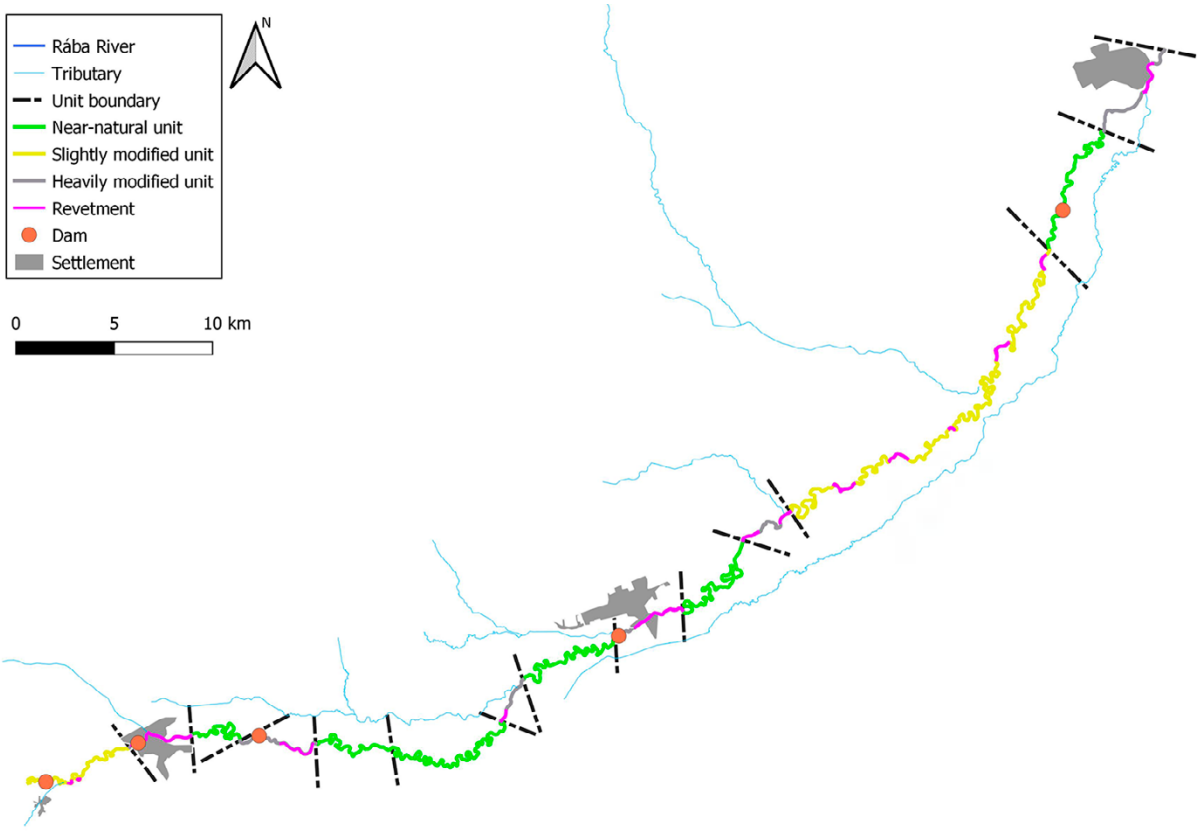

Figure 9. Based on the human impact and the lateral channel migration three types of units were identified along the Hungarian Upper Rába

units without direct human impact (e.g., R3, R5, and R6) had a markedly higher centre line increase than the units with human impacts. In the naturally developing units, nothing impeded the lateral erosion. Thus, the meanders could migrate freely, and the sinuosity increased.

The fluvial evolution and LCM were particularly active in the 1950s and the late 1990s. An average LCM rate of 4.1 to 4.9 m/y was measured in these active periods, whereas the long-term mean LCM rate was 3.3 m/y. These values are considerably higher than observed along other rivers in the Carpathian Basin. For example, along the Tapoly and Ondava Rivers (Slovakia), the LCM ranged between 0.8–1.5 m/y and 1.15–1.45 m/y, respectively (Rusnák et al., 2014; 2016). Though, along the Sajó River in Hungary the LCM was higher, reaching 5-7 m/y (Bertalan et al., 2019). It must be noted that along the Upper Rába, exceptionally high maximum rates were detected, especially in Unit R5, where the maximum LCM rate was 27.5 m/y, and the greatest variability in channel shift was also found. This value is much higher than the maximum LCM (17.9 m/y) measured on the Sajó River (Bertalan et al., 2019). During the intensively forming periods, the LCMs were widely changeable, referring to some individual meanders with very high migration rates. According to our hypothesis, in these meanders and these periods, all environmental parameters were favourable for the rapid migration (e.g., loose bank material, sparse vegetation, thalweg diverted to the bank). In contrast, other meanders reached areas with dense vegetation or compacted bank material. Besides, the collapsed bank material at the foot of the bank could also slow down the erosion at some points.

Spatiotemporal changes in sinuosity

Human interventions could also affect a river's sinuosity (Timár, 2003). Along the Upper Rába reach, cut-offs made in the late 19th century resulted in a significant decrease in sinuosity along the entire reach until 1878. As a result of these engineering works, the length of the river decreased by 6%. Thus, the sinuosity was reduced (SI_{1844}=1.84; SI_{1878}=1.73). Similar changes in sinuosity were detected later on because 24 artificial or natural meander cut-offs occurred (1960–1982). They shortened the reach by 2%, so the sinuosity of the channel decreased again from 1.84 to 1.80.

The effects of human impacts were also evident in the unit scale. The "heavily modified" units had lower sinuosity (SI: 1.04–1.30) than the "near-natural" and "slightly modified" units (SI: 1.54–2.53). Usually, the human impact decreases the sinuosity of a channel. Thus, the channel pattern of the heavily modified units (e.g., R2, R7, and R9) changed from meandering to slightly sinuous (SI: 0.3–0.4). Conversely, the channel pattern of the almost natural and slightly modified units (e.g., R1 and R6) changed from

slightly sinuous to meandering as their sinuosity index increased from l.3 and l.5 to l.6 and 2.4, respectively.

Thus, all the studied parameters indicate that there is a gradual evolution along the units with little or no human disturbance, as has been shown in other studies of similar European rivers (Keesstra et al., 2005; Blanka & Kiss, 2011; Dragicevic et al., 2017; Bertalan et al., 2019).

Effect of slope conditions and tributaries on lateral channel movements

The Rába River's unique characteristics, such as its high sinuosity and free meander development, are key to understanding its high LCM rates. As Schumm (1985) pointed out, the moderate slope (0.5-0.9 m/km) is a crucial factor in supporting the formation of high sinuosity. This specific slope range is found along the Upper Rába, which in turn promotes high sinuosity and intensive LCM, making the Rába a fascinating subject of study.

In Unit R3, the accelerated meander migration might also be influenced by the confluence of the largest tributary of the Rába River. The Lapincs Brook has higher discharge than the Rába, as their mean discharge ratio is 3:1; besides, it transports large amounts of bed load. Thus, the erosion accelerated downstream of the confluence, especially because here, meanders develop freely; thus, nothing impedes the LCM. The other tributaries have no similar effect on the LCM of the Rába, as they have very low discharges.

Conclusion

The study has revealed significant LCM of the Hungarian Upper Rába during the last ca. 180 years. Some extremely migrating meanders have been eroded at 20-27 m/y, indicating significant floodplain reworking. This does not imply that bank erosion was always significant in a given area, as periods of intensive LCM (e.g., 1950s) were interspersed with periods (e.g., 1960s) when LCM became slower in the whole system. The temporal pattern shows that the LCM gradually gets more and more intensive until reaching its maximum. Then, a period of relaxation appears with very limited bank retreat. Then the cycle starts again. However, this natural cycle is influenced by various human impacts in some units, while the meanders freely develop in other units.

However, further research will be needed to investigate the driving factors of the intensive changes in sinuosity and LCM rate. Thus, the effects of hydrological changes, influence and dynamism of tributaries, and bank material should be studied in greater detail. In addition, the channel evolution of the Rába is probably influenced by active tectonism, which changes the slope and the flow velocity (Miall, 1996; Keller & Pinter, 2002; Timár, 2003), and influences sinuosity (Blanka, 2010). Therefore, the LCM should be compared with available tectonic data in the future.

The identified units with characteristic LCM rates could be applied to develop effective solutions for sustainable channel and floodplain management for the Upper Rába. Preserving freely developing banks is important to maintain the natural bank processes, which contribute to the healthy sediment budget of the river and provide valuable habitats. In the case of artificially modified channel sections, the hydro-morphological consequences of interventions should be carefully considered. As revetments could lead to incision and channel narrowing, they could increase flow velocity and greater flood risk (Kiss et al., 2019).

Acknowledgement

The acquisition of the 2012 orthophotos was supported by the ELTE BDPK Institutional Excellence Framework Programme in 2021.

References

Bergmann, H., Kollmann, W., Vasvári, V., Ambrózy, P., Domokos, M., Goda, L., Laczay, I., Neppel, F., & Szilágyi, E. (1996). *Hydrologische Monographie des Einzugsgebietes der Oberen Raab. [Hydrological monograph of the Upper Raab catchment area]* Graz University of Technology, Graz, Austria, 257.

Bertalan, L., & Szabó, G. (2015). Mederfejlődési vizsgálatok a Sajó hazai szakaszán. [Studies of river bed evolution on the Sajó River in Hungary] In: Boda, J. (Ed.): *Az elmélet és a gyakorlat találkozása a térinformatikában VI.* Debreceni Egyetemi Kiadó, Debrecen, 61-68. https://doi.org/10.13140/RG.2.1.1070.7048

Bertalan, L., Szabó, G. & Szabó, S. (2016). Soil degradation induced by lateral erosion of a non-regulated alluvial river (Sajó River, Hungary). In Zapletalová, J. & Kirchner, K. (Eds.): *Current Environmental Threats and Their Impact in the Landscape Brno.* Ústav geoniky AV CR, Brno, pp. 8-9. 10.13140/RG.2.2.20748.31362

Bertalan, L., Rodrigo-Comino, J., Surian, N., Šulc Michalková, M., Kovács, Z., Szabó, S., et al. (2019). Detailed assessment of spatial and temporal variations in river channel changes and meander evolution as a preliminary work for effective floodplain management. The example of Sajó River, Hungary. *Journal of Environmental Management*, 248, 109277. 10.1016/j.jenvman.2019.109277

Biszak, S., Timár, G., Molnár, G., Jankó, A. (2007). Digitized maps of the Habsburg Empire - The third military survey, Ungarn, Siebenbürgen, Kroatien-Slawonien, 1869-1887, 1:25000. DVD. Arcanum Adatbázis Kiadó.

Blanka, V. (2010). *Kanyarulatfejlődés dinamikájának vizsgálata természeti és antropogén hatások tükrében*. [Dynamics of meander development in response to natural and human impacts]. PhD dissertation, Szeged University, Szeged, Hungary, 145.

Blanka, V., & Kiss, T. (2008). A kanyarulatfejlődés jellegének és mértékének vizsgálata a Hernád Alsódobsza feletti szakaszán, 1937 és 2002 között. [Meander development of the Hernád River upstream of Alsódobsza, between 1937 and 2003] In: Szabó, J., & Demeter, G. (Eds.): *Tanulmányok a Kádár László születésének 100. évfordulóján rendezett tudományos konferenciára*. Kossuth Egyetemi Kiadó, Debrecen, Hungary, 147-154.

Blanka, V., & Kiss, T. (2011). Effect of different water stages on bank erosion, case study on River Hernád, Hungary. *Carpathian Journal of Earth and Environmental Sciences* 6(2), 101-108.

Bogárdi, J. (1971). *Vízfolyások hordalékszállítása. [Sediment transport of rivers]* Akadémiai Kiadó, Budapest, Hungary, 837.

Brierley, G.J., & Fryirs, K.A. (2005). *Geomorphology and River Management: Applications of the River Styles Framework*. Blackwell Publishing, Malden, 398.

Clerici, A., Perego, S., Chelli, A., & Tellini, C. (2015). Morphological changes of the floodplain reach of the Taro River (Northern Italy) in the last two centuries. *Journal of Hydrology*, 527, 1106-1122. 10.1016/j.jhydro1.2015.05.063

Das, A. K., Sah, R. K., & Hazarika, N. (2012). Bankline change and the facets of riverine hazards in the floodplain of Subansiri-Ranganadi Doab, Brahmaputra Valley, India. *Natural Hazards*, 64(2), 1015-1028. 10.1007/s11069-012-0283-5

Dragićević, S., Pripužic, M., Živković, N., Novković, L, Kostadinov, S., Langović, M., Milojković, B., & Čvorović, Z. (2017). Spatial and temporal variability ofbank erosion during the period 1930-2016: Case study-Kolubara River Basin (Serbia). *Water*, 9(10), 748. 10.3390/w9100748

EDUVIZIG (2024). *Rába [The Rába River]*. North-Transdanubian Hydrological Directorate (EDUVIZIG), Győr, Hungary. https://www.eduvizig.hu/eszak-dunantuli/vizgazdalkodas-vizszolgaltatas/vizkeszlet-gazdalkodas/felszini-vizeink/folyoink/raba (assessed on 15.03.2024)

Goudie, A. (1991). *Geomorphological techniques*. Routledge, London, 592. https://doi.org/10.4324/9780203430590

Hegedüs, Á. (2007). Tükörcserepek a térképtörténetből: A gyorshelyesbítés (1950-52). [Mirror tiles from map history: The swift adjustment (1950-52)] *Tájoló*, 25(2), 38-39.

Hooke, J. M. (2007). Complexity, self-organisation and variation in behaviour in meandering rivers. *Geomorphology*, 91(3-4), 236-258.

Hooke, J.M. (2008). Temporal variations in fluvial processes on an active meandering river over a 20-year period. *Geomorphology*, l00(1-2), 3-13.

Hudson, P. F. & Kesel, R. H. (2000). Channel migration and meander-bend curvature in the Lower Mississippi River prior to major human modification. *Geology*, 28(6), 531-534. 10.1130/0091-7613(2000)28<531:CMAMCI>2.0.CO;2

Jankó, A. (2007). *Magyarország katonai felmérései 1763-1950.* [*The military surveys of the Hungarian Kingdom 1763–1950*] Argumentum Kiadó, Budapest, Hungary, 196.

Károlyi, Z. (1962). A Kisalföld vizeinek földrajza [Hydrography of the Little Plain]. *Földrajzi Közlemények*, 10(86), 157-174.

Keesstra, S. D., van Huissteden, J., Vandenberghe, J., Van Dam, O., de Gier, J., & Pleizier, I. D. (2005). Evolution of the morphology of the river Dragonja (SW Slovenia) due to land-use changes. *Geomorphology*, 69(1-4), 197- 207. l0.1016/j.geomorph.2005.01.004

Keller, E.A., & Pinter, N. (2002). *Active Tectonics: Earthquakes, Uplift and Landscape*. Prentice Hall, New York, 432.

Kiss, T., Amissah, G. J., & Fiala, K. (2019). Bank Processes and Revetment Erosion of a Large Lowland River: Case Study of the Lower Tisza River, Hungary. *Water,* 11(6), 1313. 10.3390/w11061313

Kiss, T., Sipos, G., & Vass, R. (2022). Alluvial ridge development and structure: Case study on the Upper Tisza, Hungary. *Geographica Pannonica*, 26(3), 230-240. 10.5937/gp26-38365

Kiss, T.; Tóth, M.; Török, G.T.; Sipos, G. 2024. Reconstruction of a long-term, reach-scale sediment budget using lateral channel movement data as a proxy: A case study on the lowland section of the Tisza River, Hungary. *Hydrology*, 11(5), 67. 10.3390/hydrology11050067

Kovács, G. (2010). The advantages of using the second military survey maps in fluvial studies. *Acta Geodaetica et Geophysica Hungarica*, 45(1), 64–70.

Kovács, G., Pusztai-Eredics, A., & Varga, N. (2024a). Településfejlődési vizsgálatokhoz (is) használható topográfiai adatforrások Magyarországon: 1950 előtti topográfiai térképművek. [Topographical sources in Hungary used for settlement development studies: Topographical maps made before 1950] *Településföldrajzi Tanulmányok*, 13(1), 224-237.

Kovács, G., Pusztai-Eredics, A., & Varga, N. (2024b). Településfejlődési vizsgálatokhoz (is) használható

topográfiai adatforrások Magyarországon: 1950 utáni topográfiai térképművek. [Topographical sources in Hungary used for settlement development studies: Topographical maps made after 1950] In: Horváthné Molnár, K., Fűzfa, B. (Eds.): *Teremtő tudomány*. Szombathely, Savaria University Press, Hungary, 80-94.

Laczay, I. (1972). A Rába vízgyűjtője és vízrendszere. A Rába szabályozása és kanyarulati viszonyai. [Catchment and hydrology of the Rába. Regulation and meanders of the Rába] *Vízrajzi Atlasz 14: A Rába*. VITUKI, Budapest, Hungary, 4-7, 24-30.

Langović, M., Popović, S., Dragićević, S., Stojanović, Ž., & Manić, E. (2024). Assessment of the Economic Consequences of Riverbank Erosion: The Case of the South Morava River, Serbia. *Water Economics and Policy*, 10(2). 10.1142/S2382624X24500036

Langovic, M., Dragicevic, S., Novkovic, I., Zivkovic, N., Tosic, R., Milojkovic, B., & Cvorovic, Z. (2021). Assessment of the soil loss caused by riverbank erosion in Serbia. *Glasnik Srpskog Geografskog Drustva*, 101(1), 31–47. 10.2298/GSGD2101031L

Lawler, D.M., Thorne, C.R., & Hooke J.M. (1997). Bank erosion and instability. In: Throne, C.R. (Ed.): *Applied Fluvial Geomorphology for River Engineering and Management*. Wiley, Chichester, 137-173.

Miall, A.D. (1996). *The geology of fluvial deposits: Sedimentary Facies, Basin Analysis, and Petroleum Geology*. Springer, Berlin, 582.

Michalková, M. (2009). Analysis of lateral channel activity of the Sacramento River from aerial photos. *Geographic Journal*, 61, 199-213.

Michalková, M., Piégay, H., Kondolf, G.M., & Greco, S.E. (2011). Lateral erosion of the Sacramento River, California (1942–1999), and responses of channel and floodplain lake to human influences. *Earth Surface Processes and Landforms*, 36(2), 257–272. 10.1002/esp.2106

Mirijovsky, J., Sulc Michalková, M., Petyniak, O., Mácka, Z., & Trizna, M. (2015). Spatial-temporal evolution of the unique preserved meandering system in central Europe - The Morava River near Litovel. *Catena*, 127(11), 300-311.

Nagy, J., & Kiss, T. (2020). Point-bar development under human impact: Case study on the Lower Tisza River, Hungary. *Geographica Pannonica*, 24(1), 1-12. 10.5937/gp24-23011

Pavlek, K. (2023). Geomorphological change in rivers: research approaches, results and challenges. *Hrvatski Geografski Glasnik/Croatian Geographical Bulletin*, 85(1), 5–39. 10.21861/HGG.2023.85.01.01

Pusztai-Eredics, A., Varga, N., & Kovács, G. (2024). Településfejlődési vizsgálatokhoz (is) használható topográfiai adatforrások Magyarországon: modern topográfiai és térinformatikai adatforrások. [Topographical sources in Hungary used for settlement development studies: Modern topographical and geoinformatical data sources] *Savaria Természettudományi és Sporttudományi Közlemények*, 21, 49-69.

Rhoads, B. L., & Welford, M.R. (1991). Initiation of river meandering. *Progress in Physical Geography*, 15(2), 127–156.

Rusnák, M., Lehotsky, M., & Kidová, A., (2016). Channel migration inferred from aerial photographs, its timing and environmental consequences as responses to floods: A case study of the meandering Topla River, Slovak Carpathians. *Moravian Geographical Reports*, 24(3), 32-43. 10.1515/mgr-2016-0015

Schumm, S.A. (1985). Patterns of alluvial rivers. *Annual Review of Earth and Planetary Sciences*, 13, 5-27. https://doi.org/10.1146/annurev.ea.13.050185.000253

Schwendel, A. C., Nicholas, A. P., Aalto, R. E., Sambrook Smith, G. H., & Buckley, S. (2015). Interaction between meander dynamics and floodplain heterogeneity in a large tropical sand-bed river: The Rio Beni, Bolivian Amazon. *Earth Surface Processes and Landforms*, 40(15), 2026-2040. 10.1002/esp.3777

Sipos, G., Blanka-Végi, V., Ardelean, F., Onaca, A., Ladányi, Z., Rácz, A., & Urdea, P. (2022). Human nature relationship and public perception of environmental hazards along the Maros/Mureș River. *Geographica Pannonica*, 26(3), 297-307. 10.5937/gp26-39657

Slowik, M. (2012): Changes of river bed pattern of a lowland river: effect of natural processes or anthropogenic intervention? *Geografiska Annaler Series A, Physical Geography*, 94(3), 301–320. https://doi.org/10.1111/j.14680459.2011.00432.x

Thorne, C.R. (1997). Channel Types and Morphological Classification. In: Thorne, C.R., Hey, R.D., & Newson, M.D. (Eds.): *Applied Fluvial Geomorphology for Engineering and Management*. Wiley, Chichester. 175-221.

Timár, G., (2003). Controls on sinuosity changes: a case study of the Tisza River, the Great Hungarian Plain. *Quaternary Science Review*, 22(20), 2199-2207. http://dx.doi.org/10.1016/S0277-3791%2803%2900145-8

Timár, G., & Telbisz, T. (2005). A meanderező folyók alakváltozása és az alakváltozás sebessége. [Changes in meandering and its rate] *Hidrológiai Közlöny* 85, 48-54.

Timár, G., Molnár, G., Székely, B., Biszak, S., Varga, J., & Jankó, A. (2006). Digitized maps of the Habsburg Empire: The map sheets of the second military survey and their georeferenced version. DVD. Arcanum Adatbázis Kiadó, Hungary.

Yousefi, S., Mirzaee, S., Keesstra, S., Surian, N., Pourghasemi, H.R., Zakizadeh, H.R., & Tabibian, S. (2018). Effects of an extreme flood on river morphology (case study: Karoon River, Iran). *Geomorphology*, 304, 30-39. 10.1016/j.geomorph.2017.12.034

INTERNATIONAL SCIENTIFIC JOURNAL
GEOGRAPHICA PANNONICA
Volume 28, Issue 3, 182–204 (September 2024)
Journal homepage: http://www.dgt.uns.ac.rs/en/homepage/pannonica/

Assessment of the Spatial Configuration Pattern in Tiruchirappalli City for Energy Studies through Generative Urban Prototype Models: A Case for Warm and Humid Climate

G. R. Madhavan[A*], Dr D. Kannamma[A]

[A] *Department of Architecture, National Institute of Technology, Tiruchirappalli, Tamil Nadu, India*

KEYWORDS

local climatic zones
image classification
urban morphology
cooling load consumption
machine learning
climate change

ABSTRACT

Developing countries with complex urban spatial configurations strive to control urbanization and its impact on energy consumption. The current study has used Tiruchirappalli city in India as a study area to demonstrate the impact on cooling energy consumption by complex urban spatial configurations. To comprehend the complexity, sixty-five urban prototypes were generated through permutation and combination using local climatic zones scheme. The image-based binary classification model was used to categorize the morphologies in the city. The study aims to investigate the cooling energy consumption of a heterogeneous urban spatial configuration through prototype models. The urban prototypes were grouped using the unsupervised machine learning approach. The validation for the prototypes was conducted through the RMSE method, and the errors lie between 0.45 and 0.68. The results indicated that increasing the green cover ratio on the combination of high and mid-rise spatial configurations is ineffective in reducing the cooling energy. In contrast, the combination of low-rise and mid-rise spatial configurations consumed less energy for air-conditioning when the green cover ratio was increased. The results conclude that the combination of high-rise with open low-rise spatial configuration is unsuitable for warm and humid climate. The high frequency of the cooling energy was between 120Gjs to 250Gjs which explains that the complexity of the spatial configuration in the city helps to reduce the energy utilized for air conditioning. This research aids planners and energy policymakers in the decision-making process of city spatial planning.

Introduction

In the last few decades, the world has undergone high urbanization as a result of population growth and the rise of cities (Sun et al., 2020). The life expectancy of the citizens living in highly populated cities has been reduced drastically. Urban population encounters major difficulties pertaining to thermal conditions and the energy sources necessary for sustaining a comfortable indoor environment (Ellena et al., 2020). Since the urban population has increased over the past few decades, temperatures in cities have been rising rapidly (Rajagopal et al.,

* Corresponding author: G. R. Madhavan, e-mail: madhavangr3@gmail.com

doi: 10.5937/gp28-50781

Received: May 01, 2024| Revised: August 31, 2024| Accepted: September 06, 2024

2023). Several cities have seen increased temperatures due to urbanization and climate change (Hood, 2005). In the 21st century, high-temperature occurrences are expected to become more frequent and longer (Dosio et al., 2018; Perkins-Kirkpatrick & Lewis, 2020). A study conducted by Heaviside et al. (2017) demonstrates that urban inhabitants have greater health risks than rural populations, particularly during high temperatures. The occurrence of heat waves further intensifies this risk. Numerous research has been conducted on the urban environment and microclimate to reduce the high-temperature occurrence in the coming years (Abougendia, 2023). The spatial arrangements of the built environment create thermal anomalies between cities and rural landscapes, which is deduced by the urban heat island intensity (Abougendia, 2023; Taha, 1997). UHI phenomenon is explained by different cooling rates between urban and rural areas (Klysik & Fortuniak, 1999). UHI intensity has been studied and reported by various authors (Arnfield, 2003; Masson et al., 2020; Oke, 2004; Stewart, 2011), and the temperature differences recorded in the research were based on urban morphology, land use pattern and climate (Nastran et al., 2019; Yue et al., 2019). Previous research on UHI addressed thermal anomalies up to 10°C (Alcoforado et al., 2014; Warren et al., 2016). The UHI intensity causes heat-related health risks in the residents of cities, along with increased cooling load consumption (Barrao et al., 2022). In the wave of urbanization, reducing cooling load consumption in the cities is the top priority (Vallati et al., 2015). Urban energy performance has become a worldwide environmental conversation in every decennial since global urbanization is expected to reach about 70% by 2050 (United Nations, 2019). The urban morphology significantly increases energy usage (Katal et al., 2022). A study by X. Li et al. (2019) shows that the cooling load of residences increases substantially for a 3°C rise in standard effective temperature (SET). So, it is essential to control the cooling load consumption in the cities by optimizing the urban morphologies and reducing the UHI intensity. The phenomenon of climate change presents significant obstacles to the energy consumption of buildings, as outdoor weather conditions influence the energy and thermal performance of structures (Huo et al., 2022). To adequately address the issue of climate change, it is imperative to gain a comprehensive understanding of the forthcoming regional and temporal trends in energy use alongside the implementation of energy efficiency measures for building stocks (Deng et al., 2023). Urban Building Energy Models (UBEMs) are derived from Building Energy Models (BEMs), which can analyse energy demand and assess the effects of prospective retrofits on building stock at a city or district level. These models utilize Energy Plus as the simulation engine for analysis and evaluation purposes (Hong et al., 2020). The present study has used UBEMS to investigate the cooling load consumption of residential buildings in complex spatial configurations of a city. Urbanization and population expansion in developing countries have a significant impact on climate change (Parmesan & Yohe, 2003). To analyze the impacts, the urban planners have designed a few schemes. The local climatic zone is one such scheme invented by Oke and Stewart. The local climate zone scheme is a system for classifying urban areas into distinct local climates based on morphological and land cover characteristics (Stewart & Oke, 2012). Several investigators have conducted LCZ classification studies (Alexander & Mills, 2014; Kotharkar & Bagade, 2018; Leconte et al., 2015; Nassar et al., 2016; Skarbit et al., 2017). LCZ classification scheme helps to find the urban morphological patterns of the cities through which researchers can create models for urban energy studies (Cao et al., 2022). The LCZ technique facilitates the classification of spatial configuration within urban areas, which helps to finalize suitable urban designs in the climate change mitigation and adaptation process. The present study has used the LCZ scheme to create urban prototypes to classify complex spatial configurations of the city. Various studies were conducted on the classification of LCZs in different cities. However, most of them are microscale classifications limited to small urban patches. The LCZ classification study conducted in Nagpur indicates that cities with complex urban forms need separate LCZ subcategories. The intra-urban heterogeneity is high in complex urban forms due to unplanned settlement patterns (Kotharkar & Bagade, 2018). Numerous cities in India come under unplanned settlements since their urban morphologies are heterogeneous in nature. The need for classifying the city at the local scale level helps to capture more regional features compared to microscale classification. A multitude of studies have been conducted to examine the correlation between urban form and environmental factors, with the aim of equipping designers and planners with performative indicators that can be utilized during the initial stages of design (Natanian & Auer, 2020). Previous studies have used several classification methods to classify the urban forms and create archetypes to assess performance in terms of energy and microclimate. A study by Joshi et al. (2022) used urban morphological parameters as the independent variable in clustering the urban archetypes. Recent years have seen a rise in studies related to intra-urban heterogeneity in order to enhance urban planning regulations. It is imperative to minimize the number of simulations conducted in these studies during a large-scale calibration process (Deng et al., 2023). Most research has primarily examined the influence of climatic change on the energy efficiency of archetypal or prototype buildings (Deng et al., 2023; Heidelberger & Rakha, 2022; Nagpal et al., 2019; Nik, 2016; Wang et al., 2018;

Yang et al., 2021). However, there is a dearth of comprehensive research on the variations of spatial configuration across the unplanned settlements present in cities, which needs to be adequately elucidated. The complexity of spatial configuration varies for each city, particularly for cities in developing countries where the unplanned settlements are high in ratio, so the division of distinct morphological features is not possible in such cities. To overcome this issue, the current study focuses on an Indian metropolis and presents a detailed process of analyzing the spatial configuration, as well as investigating energy usage for cooling purposes. The study seeks to accomplish two research objectives: (a) To comprehend the spatial geography of the urban area in a highly heterogeneous mixed urban setting. (b) To conduct a quantitative analysis on the spatial configuration of a complex metropolitan area to determine the most efficient urban forms that minimize the energy usage for Air-conditioning. The present study aims to categorize urban prototypes with respect to their energy consumption and analyze them to develop urban planning energy regulation policies.

Research Area

Tiruchirappalli is situated in Tamil Nadu, India, and has a tropical savanna or tropical wet and dry climate, as classified by the Koppen climate classification. Tiruchirappalli is classified as a warm and humid climatic zone according to the National Building Code (NBC-2016). The year is divided into four distinct seasons: winter, which spans the months of January and February, and summer, which encompasses the period from March to June. The monsoon season occurs from June to September, followed by the post-monsoon season from October to December. The city comprises high-rise, midrise and low-rise structures with highly vegetated to bare soil land covers. The city comes under one of the complex-built environments with a mixture of all built-cover and land-cover typologies. The city was chosen for the study for its highly heterogeneous built settings and hot summers. A study by Bhatnagar et al. (2018) indicates that Tiruchirappalli has the highest cooling degree days in India. So, the current study is essential to understand the impact of spatial configuration on cooling load reduction potential.

Methodology

The methodology section is subdivided into five phases as follows.

Phase 1: Sub-classification system

In the initial stage, a novel subclassification system using the Local climatic zones was introduced to segregate the urban morphology into different classes. For classification purpose, we have utilized permutation and combination method to curate different possibilities of spatial configuration with nine LCZ classes (Figure 2).

Phase 2: Model Preparation

Using the sub-classification model, sixty-five different morphologies were obtained (Figure 3). Each morphology was re-arranged into four combinations based on the proportion of land cover and build cover zones (Figure 2b). The LCZ models were configured as per the development control regulations of Tiruchirappalli city. The obtained morphologies and their combinations were modelled in Rhino 7 to export it for simulation.

Phase 3: Image processing

We have used pixel-based segregation (binary classification) in python to find the LCZ classes in the study area. Initially, the training images from the study area of size 40,000 Sq.m were utilized for training the model (Figure 4). The images were converted into two-dimensional binary pixels, and for testing, the high-resolution Google image of the city was divided into numerous urban patches. With the help of a random shuffle, both training and testing binary data were equated to find the LCZ classes of the study area.

Phase 4: Energy Simulation

The model imported from Rhino 7 was used to conduct energy simulation for the study. Rhino 7 helps the researchers as a computational design tool that connects the gap between modelling and simulation (Anton & Tănase, 2016). URBANopt components from ladybug tools are utilized to calculate the cooling load since ladybug is an environmental analysis tool from Grasshopper, which accounts for complex building geometry and weather information (Bajšanski et al., 2024). The standard effective temperature was fixed for all models, which was obtained through a survey of the residents in the city. The model's simulation settings and physical properties are provided in Table 1 and Table 2.

Phase 5: Clustering and Validating

The sixty-five different spatial configurations were clustered through their UMI values using the k means clustering method (Figure 1), and validation was conducted through a one-way ANOVA test. The optimal number of clusters was determined using silhouette scores. The distribution of urban configurations in the clusters was plotted in the area graph and pie-chat for further investigation.

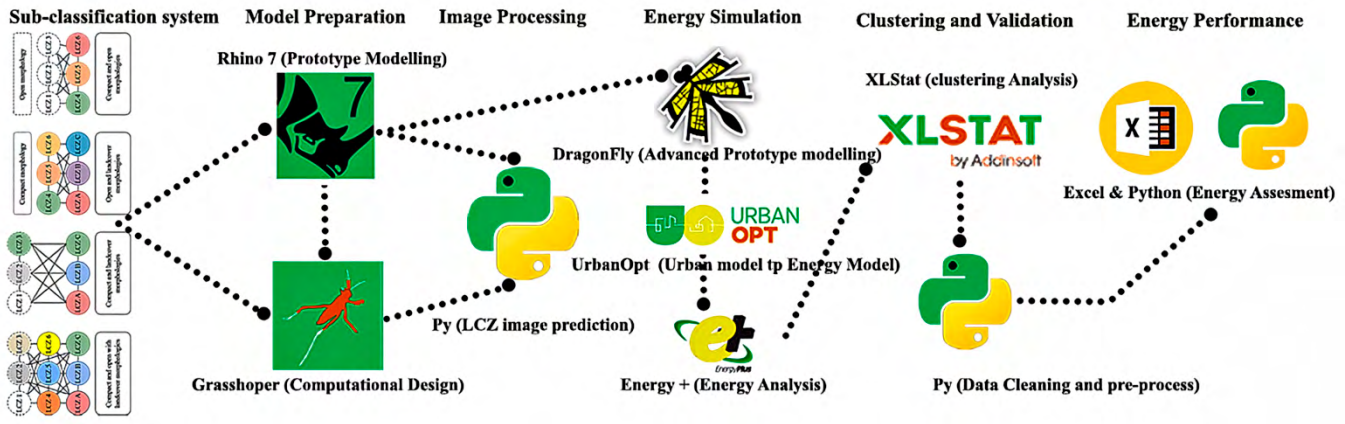

Figure 1. Workflow representation of research phases

Phase 6: Energy performance assessment

In the final stage, the data collected from the URBANopt simulation was analyzed to determine the low-performing built environment present in the city, and the best-performing morphologies were identified and ranked based on their cooling load consumption.

Sub-classification system

A novel subclassification system was introduced in this research for cities that are highly heterogeneous and have complex spatial configurations. This sub-classification helps to capture more complex features compared to the traditional method. A study conducted in China indicates that fine-scale mapping has potential, but we can retain more region-level features from the larger grid size (170 m × 170 m) (Ma et al., 2023). Analyzing a minimal area of 50 m × 50 m is efficient, but large-scale patches are more reliable and efficient for investigating the impact of urban morphological features on building energy consumption. This classification system was created based on the permutation and combination of LCZs (Figure 2a). In this combination, LCZ 7, LCZ 8, LCZ 9, LCZ D, LCZ F and LCZ G were excluded since these LCZs present in the lowest ratio in Tiruchirappalli city. This study aims to cluster the LCZs of an ideal central business district so the most prominent LCZs, which come under compact types (LCZ 1, LCZ 2 and LCZ 3), Open configurations (LCZ 4, LCZ 5 and LCZ 6) and land cover configurations (LCZ A, LCZ B and LCZ C) were chosen for the permutation and combination. In this classification, not more than one land cover was used to define the typology since the study focuses on the energy consumption data of built morphologies.

Model Preparation

Urban blocks are sections of one or more buildings encircled by streets (Schirmer & Axhausen, 2016). The sample city chosen for the model was Tiruchirappalli in South India, which comes under warm and humid climate. The development control regulations of the city were used for the designing of blocks. The minimum plot size allowed for the building was 300 Sq.m., used in the study to create the building blocks (Figure. 2c). Thirty plots were created for one module with a module size of 9000 Sq.m (Figure 2b). Each module was modelled with four different combinations, and the four modules were combined to create one neighbourhood of 38,709 Sq.m. Four combinations of the neighbourhood were designed based on the distribution of morphologies. The first combination has an equal distribution of all morphologies, followed by a 60-20-10 ratio of three zones for the rest of the combinations (Figure 2b). The neighbourhood designed for the study consists of 1200 plots with the distribution of different land cover and built cover types. A block model was designed in Rhino 7 with fixed floor heights for low, mid, and high-rise buildings (Table 1). The number of floors for the low-rise building is 1, the mid-rise building is 3.5, and the high-rise building is 7. The distribution of the buildings in the plot was determined by giving random seed values in the scripting so that for every LCZ, the variations in arrangements of the building block can be achieved. The Final model consisted of 65 zones grouped into six configurations: compact and open with landcover configurations, compact and open configurations, compact with landcover configurations, open with landcover configurations, compact configurations, and open configurations. The open configuration has one zone (LCZ 456), and the compact configuration has one zone (LCZ 123). Compact open with landcover configuration has 27 zones, compact and open configuration has 18 zones, compact with landcover configuration has 9 zones and open with landcover configuration has 9 zones (Figure 3).

Urban Morphology Indicators

Numerous urban morphological indicators (UMIs) have been reported in previous studies, and they are broadly categorized as building block indicators, open space indicators, street indicators, and plot indicators (Elzeni et al., 2022). The selected urban morphology indicators for the current study were Aspect ratio, Sky view factor, Perme-

able surface fraction, Floor area ratio, Height of rough element, Standard deviation of building height, Ground space index and open space ratio. The indicators were selected based on the literature review from published research articles (Apreda et al., 2020; Heris et al., 2020; Palusci et al., 2022; Stewart & Oke, 2012b; Teller & Azar, 2001). These indicators were used in a study conducted in Belgium, where they found that the difference in UMI values between the zones significantly impacts microclimate (Joshi et al., 2022). The urban district model from the Dragonfly was used to calculate the UMI values. The formulas used to calculate the indicator values are given in Figure 2d. In the correlation matrix we found that OSR (Open space ratio) was highly co-relating with Permeable surface fraction and Ground space index, so it was not used for the clustering process since it would alter its results Figure 5.

Image Processing

The area of Tiruchirappalli city constitutes 167.2 Sq.km, of which 8 Sq.km was taken for study from the region of KK Nagar zone (Figure 4d). The city was divided into five zones for administrative purposes and KK Nagar is populated high compared to other zones (Figure 4c) (Karthik, 2021). To conduct image classification, the study area was divided into urban grids with two fixed grid sizes, one larger (400m × 400m) and another smaller (200m × 200m). High-resolution Google map images of the identified LCZs in the city were fed as input to the image classifier model. The images were converted to the binary matrix, and the values were reshuffled multiple times to train the model for every probability. Ultimately, the Python program was utilised to determine the appropriate zone for the test data, which consisted of Google photos measuring 200m x 200m. Each smaller grid (200m × 200m) comprises three different morphologies, which were difficult to process through the GIS model and prone to errors while calculating for a large area. This approach provides a comprehensive understanding of the morphology distribution with higher accuracy. The method to convert the Google images into binary matrices is given in Figure 4a. For each LCZ class, 10 images from the study area were used to train the model for classification. A total of 650 images were used to train the model, and their binary data were collected to classify the test images, as shown in Figure 4d.

Simulation

The energy simulation method used in this study was divided into three sub-stages: (a) Importing the urban models, (b) Energy plus weather file generation from UWG (Urban weather generator) for all urban prototypes, (c) Cooling load calculation Figure 1. The energy plus weather file (city code: 433440) was obtained from climate.onebuilding.org website under WMO Region 2. By modelling the LCZs in the Urban Weather Generator (UWG), EPW data were collected for all 65 prototypes. Using meteorological data from the rural weather station, UWG generates a new urban EPW file and determines the hourly air temperature and humidity within the urban canopy. The article by Bueno et al. (2014) describes the workflow and the four UWG modules. The evaluation of the UWG against field data from Basel, Switzerland, and Toulouse, France, has yielded satisfactory results (Bueno et al., 2013). Generally, urban energy evaluation is conducted through statistical data, physical models, and degree days (Li et al., 2021). The physical model method has high accuracy in calculating energy data when compared with the other two methods (Chen et al., 2018). The influence of the microclimate in the cooling load can be calculated with better accuracy in simulation models (Li et al., 2021). The district cooling load of the LCZ was obtained from the URBANopt component through the geoJSON file. Dragonfly was used to calculate the district cooling load data by converting the simulation model into a geoJSON file. The blocks in the urban prototypes were divided into seven zones (Z1-Foyer, Z2 - Guest room, Z3 - Office space, Z4 - Living room, Z5 - Pantry, Z6 - Bed Room, Z7 - Bath and Z8 - Bed Room) (Figure 2c). Zone 6 and Zone 8 were fixed as air-conditioned space for the simulation. The model's simulation settings and physical parameters were presented in Table 1 and Table 2, adapted from (Kolhatkar et al., 2022).

Table 1. Building Properties

Properties		Inputs
Floor height	All floors	4 m
No of Floors	Low, Mid and High	1, 3.5 and 7
Wall thickness		0.23 m
Construction Type	Bricks and Concrete	
U-Value of wall	For all the Zones	0.38 W/Sq.m. K
U-Value of roof		0.25 W/Sq.m. K
U -Value of glazing		2.60 W/Sq.m. K
WWR		0.25 (All directions)
SHGC of glazing		0.65
Air-conditioned zones	65 Prototypes	Zone 6 and Zone 8

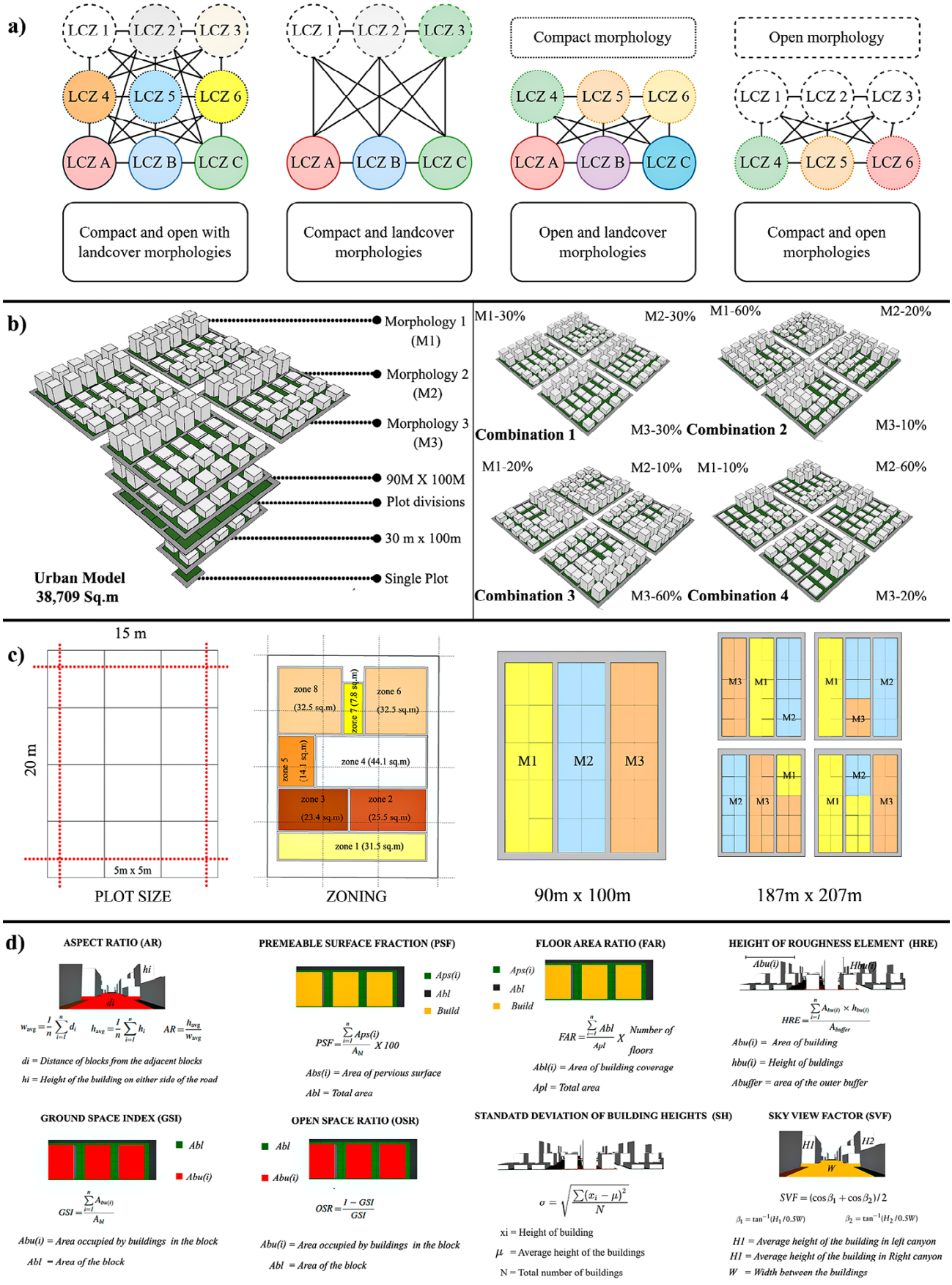

Figure 2. Prototype classification through LCZ method a) Sub-classification system b) Urban morphology model c) Model preparation method d) Urban morphology indicators

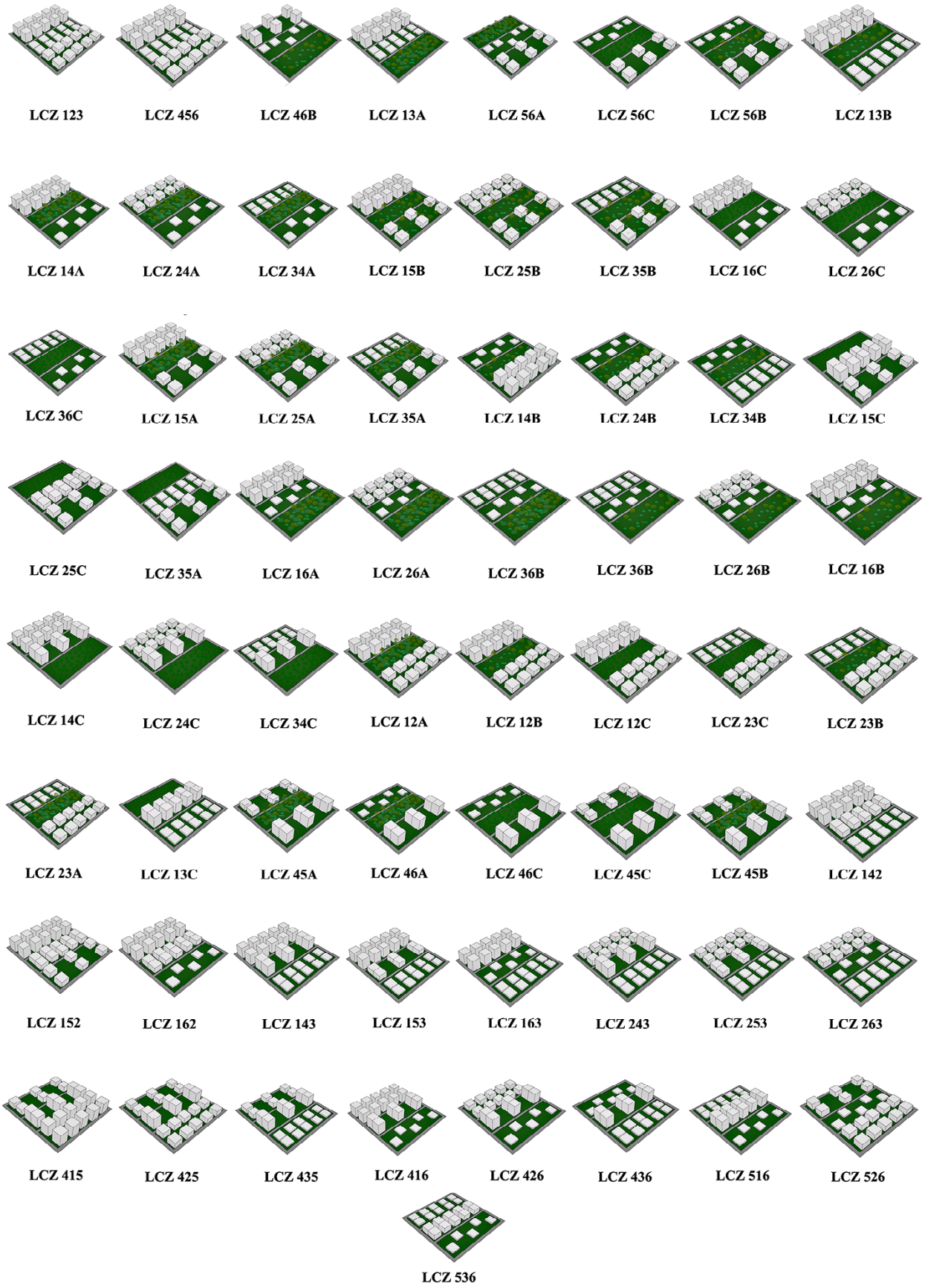

Figure 3. Urban prototypes of local climatic zones

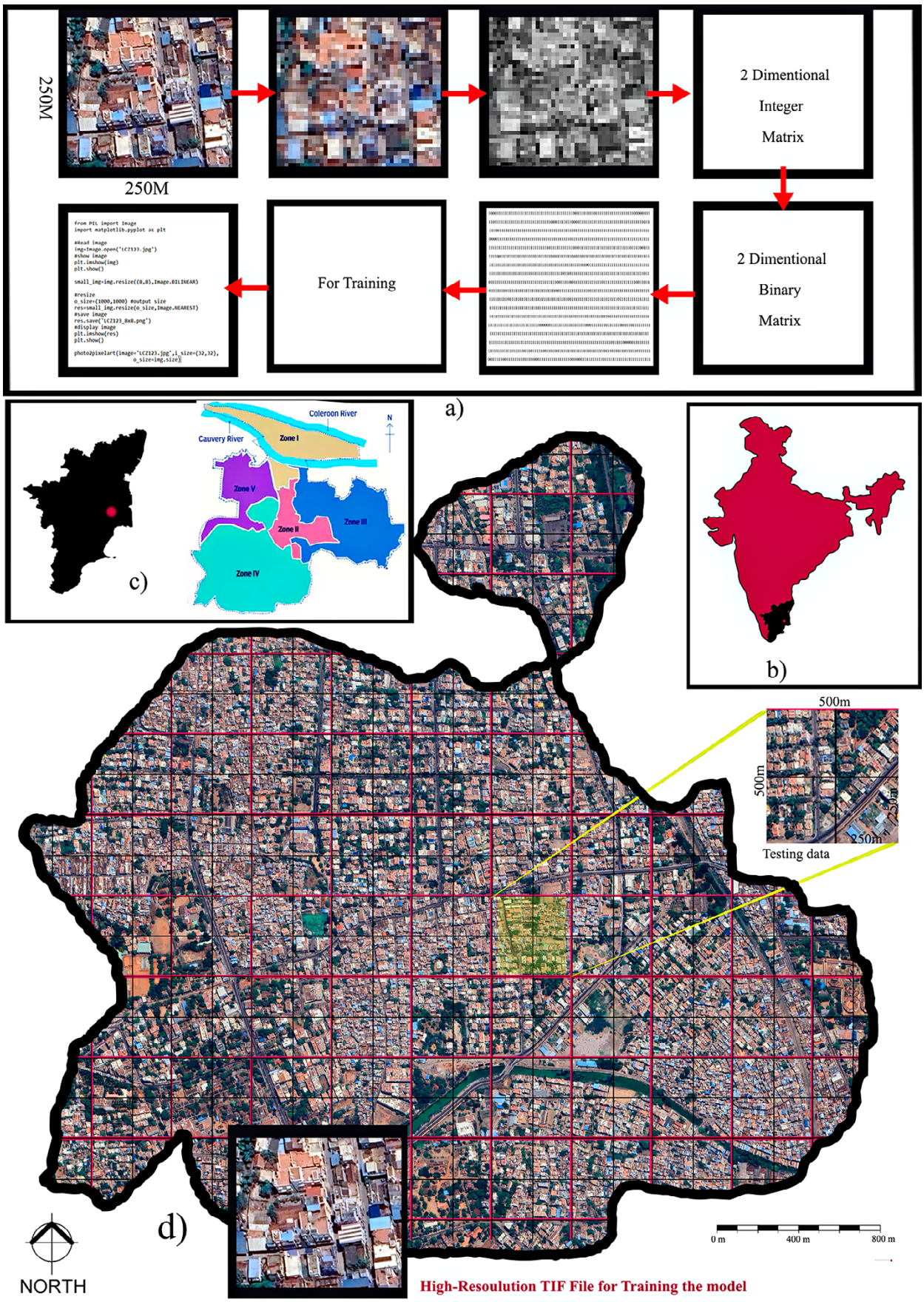

Figure 4. Mapping method (a) Image processing method (b) Map of Tamil Nadu state in India (c) Map of Tiruchirappalli city (KK Nagar) (d) Satellite image of the study area

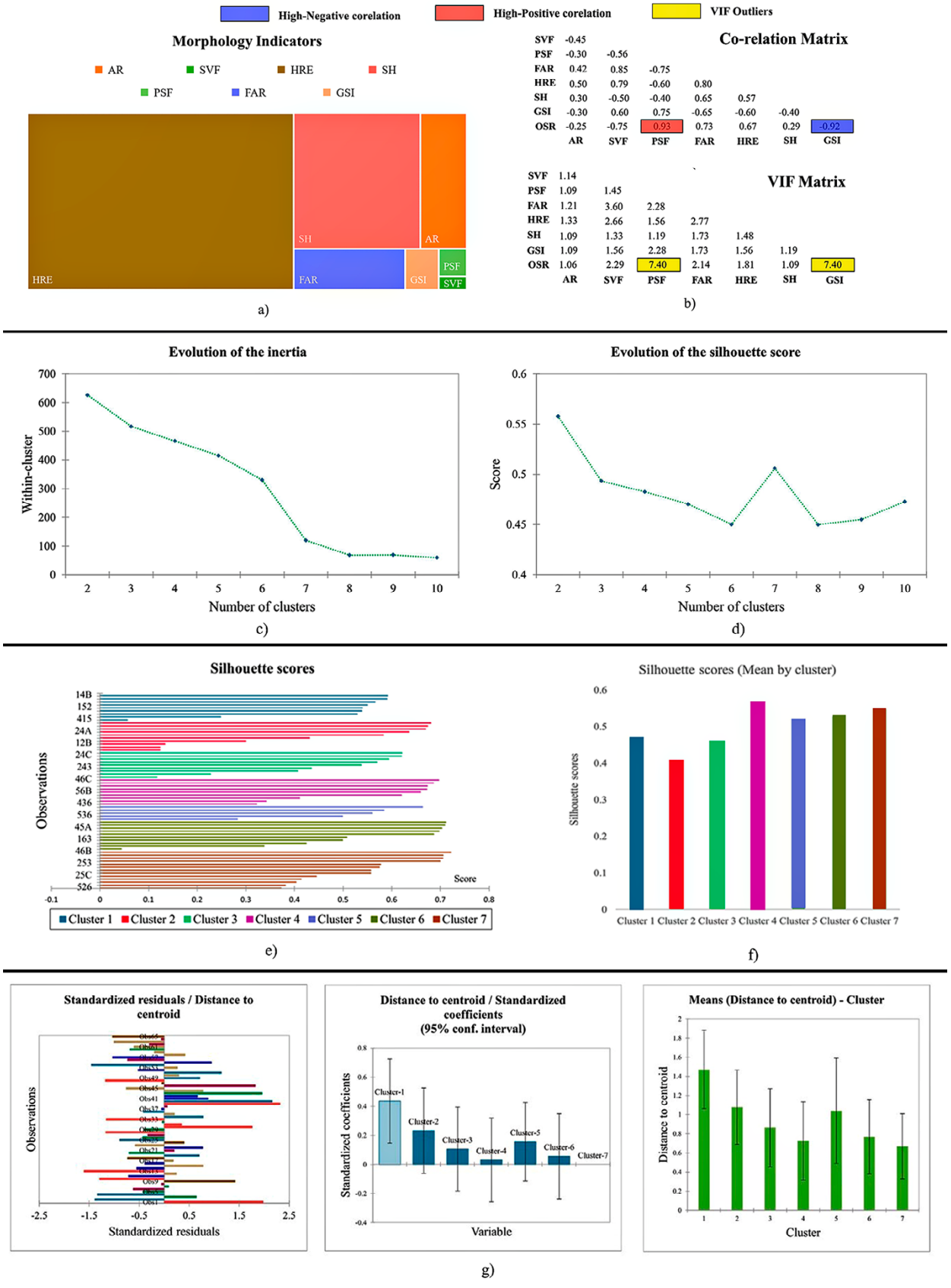

Figure 5. Clustering Results (a) UMIs (b) Co-relation and VIF Matrix of UMIs (c) Inertia values (d) Silhouette scores (e) Individual silhouette scores (f) Distance from the average silhouette scores (Clusters) (g) ANOVA Results

Table 2. Simulation settings

UWG parameters		Inputs
Building program	Midrise Apartment's	
ASHRAE Climate zone	2 - Hot	
Building Age	1980 - 2004	
Construction Type	(Mass) Bricks and Concrete	
Urban Patch size	210 M X 210 M	
Boundary conditions	UBL at Daytime	1000 m
	UBL at Nighttime	450 m
	Inversion height	200 m
Previous Layer	Thickness	0.95
	Conductivity	1 W/m-K
	Volumetric heat capacity	1.6e6 J/cu.m-k
Impervious layer	Thickness	0.95
	Conductivity	1 W/m-K
	Volumetric heat capacity	1.6e6 J/cu.m-k
Anthropogenic Heat capacity	Same for all Zones	4 W/Sq.m
Occupation Schedule	Midrise_Appartment_Occ	
Simulation Period	Summer (1st -Mar – 31st May) TMY	
Set Temperature	Based on the survey taken from residents	26.3°C (Summer)

Clustering and Validation

An unsupervised machine learning method (K-means) was used in this study, which groups the n observation into k clusters. It starts with a predetermined number of clusters (k) and n data points; the algorithm chooses cluster centres randomly. In this method, data points are categorized according to the closest cluster centre, and the process is achieved by minimizing the sum of square distances between any data point and its closest cluster centre within the cluster, as indicated by the equation presented in Jain (2010). Generally, the centroids are chosen randomly by the K-means algorithm. To avoid this, we have employed the centroid initialization technique known as k-means initialization to avoid the random selection of centroids. The most optimal initial centroid was chosen using this method, and the XLSTAT tool was used for this process. Many different approaches have been used to determine the number of clusters. For clustering analyzes, finding the ideal number of clusters is essential to avoid errors in the clustering process. For this research, we used the silhouette score method, which calculates an overall representative score to test the effectiveness of the clustering. It works based on the compactness of individual clusters (intra-cluster distance) and the separation between clusters (inter-cluster distance) as given in equation 1.

$$si = \frac{bi - ai}{max(bi, ai)} \tag{1}$$

ANOVA and MANCOVA are the primary criteria for validating previous studies' clustering results (Panuwatwanich & Nguyen, 2017). For the external criterion analysis, we selected the average air temperature (Ta) of the LCZs as the dependent variable. The external variable in this study cannot be a factor influencing or providing information about urban morphology indicators. One-way ANOVA was used in several studies to validate the results of clustering analyses. So, one-way ANOVA is utilized to confirm the clustering results by finding whether the mean air temperature (Ta) fluctuates among the clusters.

Results and Discussion

Validating the clustering results

It is essential to determine the suitable number of clusters for the k means in the clustering algorithm. Unlike the hierarchical clustering method, k means cannot independently determine the number of clusters. The silhouette score method was used to fix the final number of clusters. The maximum value of the cluster was fixed as 10 (k) since increasing the k value decreases the inertia within the cluster (Figure 5). In various studies Silhouette score helps to find the effectiveness of the clustering algorithm. In the evolution of the silhouette score, a sharp rise was observed at k=7 (Figure 5d). In contrast, the inertia score steeply decreases at k=7, near 100 (Figure 5c). There was no significant decrease in the inertia level after 7, from which the results concluded that the data can be divided into 7 clusters (Table 2). The average silhouette score was 0.475; Figure 5e denotes that a significant number of individual silhouette score were higher than the average, which explains that the clustering algorithm was well performed. To validate the clustering results, one-way ANOVA was used in this research. Figure 5g demonstrates the distance of the air temperature data from the centroid for all prototypes. The research concludes that there is a significant amount of deviation between the data with a 95% confidence interval. The specifics of the ANOVA test are denoted in Table 4 and Table 5.

Analyzing the clustering results.

Seven Groups (G1-G7) were acquired through clustering results. Cluster 5 has the lowest number of zones (Z=5), while Cluster 7 has the highest number of zones (Z=13) (Table 6). The zones deprived of land cover were grouped along with those with land cover configurations. low-rise configurations were grouped along with the high-rise. The combination of open configurations and compact configurations was found in G6 and G7. Since the intra-cluster difference is less than the inter-cluster difference, the clustering results were fit to further analyze (Table 7). Aspect ratio (AR), Sky view factor (SVF), Height of roughness element (HRE), Stand deviation of building height (SH), Permeable surface fraction (PSF), Floor area ratio ((FAR), Ground space index (GSI) and Urban district cooling load (UDCL) were the variables used for the cluster analysis. The highest aspect ratio and lowest sky view factor were found in compact and open built with landcover configurations and compactly built configurations. The height of the roughness element (HRE) and Standard deviation of building heights (SH) were high in compact-built forms and low in open-built forms. The values of the PSF were between 0.2 and 0.4, which shows that the mixed morphologies were similar in the distribution of permeable surfaces. The GSI values were high in compact-built configurations compared to open-built configurations, and a distinct difference was seen between the configurations with land cover and those deprived of land cover. The floor area ratio was high in LCZ 142 (Compact high rise and mid-rise with open high-rise category) and low in LCZ 36A (Compact low rise and open low rise with dense trees category). The clustering results indicate that unrelated mixed spatial configurations can be grouped due to the similarities in the distribution of the classes. Thus, it explains that when dealing with complex urban forms, larger grid sizes are essential to capture the regional geographical features of the city.

Inter-cluster variation

The clustering results indicated that 65 typologies can be clustered into seven groups (G1-G7). The minimum and maximum distance between the cluster centroids were 2.4 and 18.9 (Table 7). Among all the groups, G1 has high AR, HR, FAR and SH due to the distribution of morphologies within the group (Figure 6a & Figure 7). Similarly, G1 has a high urban cooling load (284.13 Gjs) in summer, and 40% of the zones in G1 come under compact with open-built con-

Table 3. Numbers of Iterated clusters

Clusters	C1	C2	C3	C4	C5	C6	C7	C8	C9
Silhouette scores	0.56	0.49	0.47	0.46	0.45	0.52	0.45	0.46	0.47
No of clusters	k=2	k=3	k=4	k=5	k=6	k=7	k=8	k=9	k=10

Table 4. ANOVA Results

Source	DF	Sum of squares	Mean squares	F	Pr > F
Model	9.000	5.266	0.585	2.343	0.026

Table 5. Cluster centroid data.

Variable	Obs. with missing data	Obs. without missing data	Minimum	Maximum	Mean	Std. deviation
Distance to centroid	0	65	0.000	2.495	0.792	0.545

Table 6. Clustering Result

Cluster	G1	G2	G3	G4	G5	G6	G7
Number of objects by cluster	9	10	9	9	5	10	13
Within-cluster variance	3.414	1.891	1.107	0.801	1.706	0.862	0.609
Minimum distance to centroid	0.487	0.185	0.433	0.277	0.408	0.137	0.053
Average distance to centroid	1.471	1.078	0.862	0.725	1.040	0.767	0.668
Maximum distance to centroid	2.890	2.402	2.062	1.841	1.908	1.346	1.143
Urban Prototypes	14A	24A	34A	35B	36C	25A	35A
	15A	15B	25B	26C	35C	24B	34B
	14B	16A	16C	36A	36B	15C	25C
	123	14C	26A	34C	536	16B	26B
	142	153	24C	263	56C	163	253
	143	162	456	436		516	526
	152	416	243	23C		425	435
	415	13A	426	46C		13B	23A
	12A	12B	46A	56B		13C	23B
		12C				45A	45B
							45C
							46B
							56A

figuration. G1 has low SVF and GSI due to the distribution of fewer landcover zones within the cluster. G2 has high GSI and low FAR since 40 % of them were compact low and mid-rise configurations (Figure 6b & Figure 8). The difference in the PSF between the groups was insignificant due to repetitive urban prototypes. The difference between G3 and G5 was also insignificant due to the distribution of similar morphologies in the groups except the open-built type, which was present for 15% (Figure 6b). Similarly, G4 and G7 have low differences, which can be comprehended by the difference between the centroids (Table 7). The GSI was similar between the groups except for G2 since it was the only cluster with fewer land cover types. G1 and G5 have high differences in the values of the variables selected for the clustering. Similarly, G4 and G1 have high dissimilarities when compared with other groups. Open-built type was present only in G3, and compact-built morphology only in G1. The difference between the centroids of G1 and G3 proves that the clusters were separated far from each other (Table 8). Similarly, the G2 and G5 clusters were separated far from each other, which can be understood by the distribution of cluster centroids. Compact with open built and land cover typology has maximum share with G5 (70%) and G1 (30%). The results conclude that the variations between the clusters were due to the distribution of urban morphology within the spatial arrangements. The current study provides a novel approach in LCZ modelling for complex city forms, and using this approach, researchers can benefit by finding suitable morphology for the cities under warm and humid climate. This study also helps to create morphological clusters for the cities to research the distribution of UHI in different clusters.

Table 7. Distance between the cluster centroids

Clusters	G1	G2	G3	G4	G5	G6	G7
G1	0						
G2	4.013	0					
G3	10.088	6.078	0				
G4	15.417	11.405	5.335	0			
G5	18.989	14.977	8.908	3.574	0		
G6	7.328	3.319	2.761	8.093	11.666	0	
G7	13.023	9.011	2.938	2.397	5.971	5.697	0

Table 8. Variation between and within the clusters

Variation inertia	Absolute	Percent
Within-cluster	81.473	3.75%
Between-clusters	2089.268	96.25%
Total inertia	2170.741	100.00%

Identified LCZs in the Research area

The study area was divided into 195 urban patches using 200 m x 200 m grids. Each urban patch was tested through image classification model in Python by randomly generating the images. Out of 195 urban patches, 15 images were not able to be classified due to the absence of build cover configurations. 180 images were classified successfully, and their representative groups were provided in Figure 9a. G5 and G6 were in small ratios with LCZ 56C, LCZ 45A and LCZ 13B configurations. Similarly, G1 and G3 were distributed for 15% of the study area. LCZ 34A and LCZ 12A were the configurations under the G1 and G3. 32.2% of the distribution was under G7 and 34.4% under G2 (Figure 9b). The confusion matrix of the group indicates the image classification accuracy was high in G2, G7 and G4 since they share 80.4% of the study area. The precision, recall and F1 scores of the 3 groups are given in Table 9. LCZ 12A, LCZ 12B, LCZ 12C, LCZ 13A, LCZ 416, LCZ 153, LCZ 34A, LCZ 35B, LCZ 23C, LCZ 34C, LCZ 56C, LCZ 45A, LCZ 13B, LCZ 53A, LCZ 23A, LCZ 45B, LCZ 23B and LCZ 56A were present in the study area (Figure 10a). The morphology characters of the classified urban patches were extracted and co-related with the UMI values of Urban prototypes. For validation, 18 LCZ configurations in the study area were compared with their urban prototypes. The RMSE values for the respective indicators are given in Figure 10b. The classification results conclude that 90% of the study area has configurations with dense and scattered trees. The presence of open high-rise and compact high-rise urban configurations was less than 7%. The confusion matrix presented in Figure 10c denotes the total number of images classified accurately under each group.

Table 9. Classification validation table

Groups	Precision	Recall	F1-score
Group 2	82.85%	85.51%	84.91%
Group 7	88.50%	83.79%	85.32%
Group 4	55.82%	59.37%	56.63%

Energy Performance Investigation

Investigation of energy performance was conducted through 2 objectives: (a) analyzing the cooling load consumption for all combinations of 65 zones and (b) Analyzing and ranking the performance of the classified spatial configurations present in the city. The cooling load consumption for each LCZ was calculated through a simulation model in URBANopt. The SET temperature was fixed constant for all zones so that the results could be compared without deviation of occupant's behaviour. The heat map of the energy consumption is shown in Figure 11e. The spatial configurations deprived of vegetation have higher energy consumption than other types of configurations. Compared to other zones, open high-rise configurations and compact high-rise configurations with dense trees consume high energy for cooling the indoor spaces. Compact midrise configurations and compact low-rise configurations (23A, 23B and 23C) consume less than open morphologies in a few combinations (Figure 11a). Densely vegetated configurations like 15A and 14B classes reflect high variation in the energy consumption between the combinations. The impact of vegetation in reducing the cooling load was significantly low in high-rise zones compared to low-rise zones. Open configuration with a combination of compact configurations consumes high energy when there is a lack of dense or scattered trees. Further analyzes were conducted on the morphologies present in the city. The simulated data were plotted against the real-time cooling energy data to validate the urban prototype model. TNEB (Tamil Nadu Electricity Board) data were used to calculate the rest time cooling load for the buildings. The RMSE value was 0.55, and all 18 morphologies were used for the validation (Figure 11c). The distribution of the groups was analysed and mapped in Figure 11. We found that approximately G2, G4 and G7 were present in over 80% of the study area. So, the study was further conducted by analyzing of the morphologies in G2, G4 and G7. LCZ 416 (open high rise and compact high rise with open low-rise zones) consume high energy for cooling the spaces. Combination 2, which is 60% of the first class, 20% of the second class, and 10% of the third class, has high cooling load consumption in most morphologies. The lowest cooling was found at 23C (compact mid-rise and low-rise with shrubs), which is 150GJs. The morphologies in Group 2 consume a high cooling load when compared with Group 4 and Group 7 (Figure 11d).

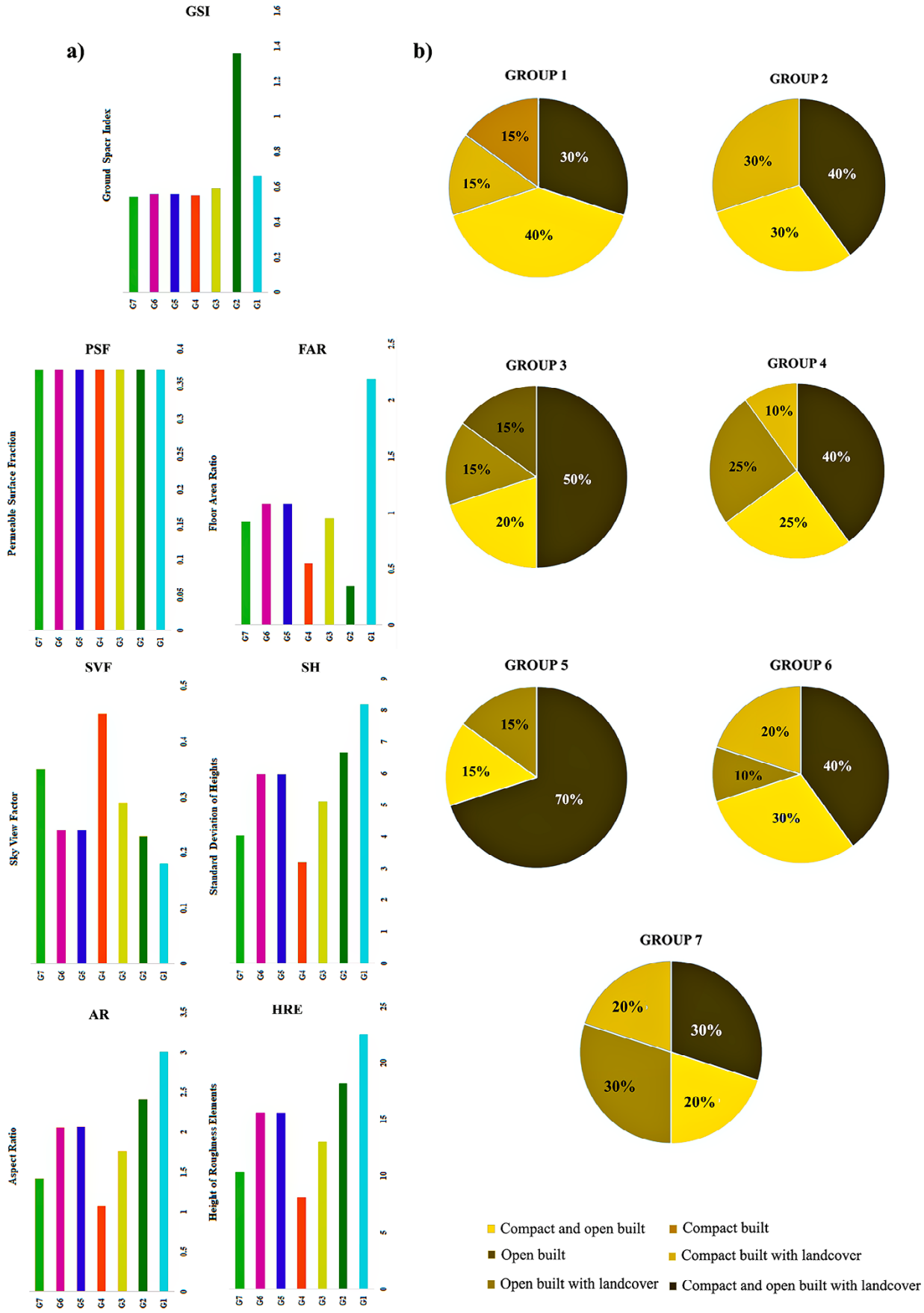

Figure 6. LCZ graphs (a) UMI values for each group (b) LCZ distribution for each group

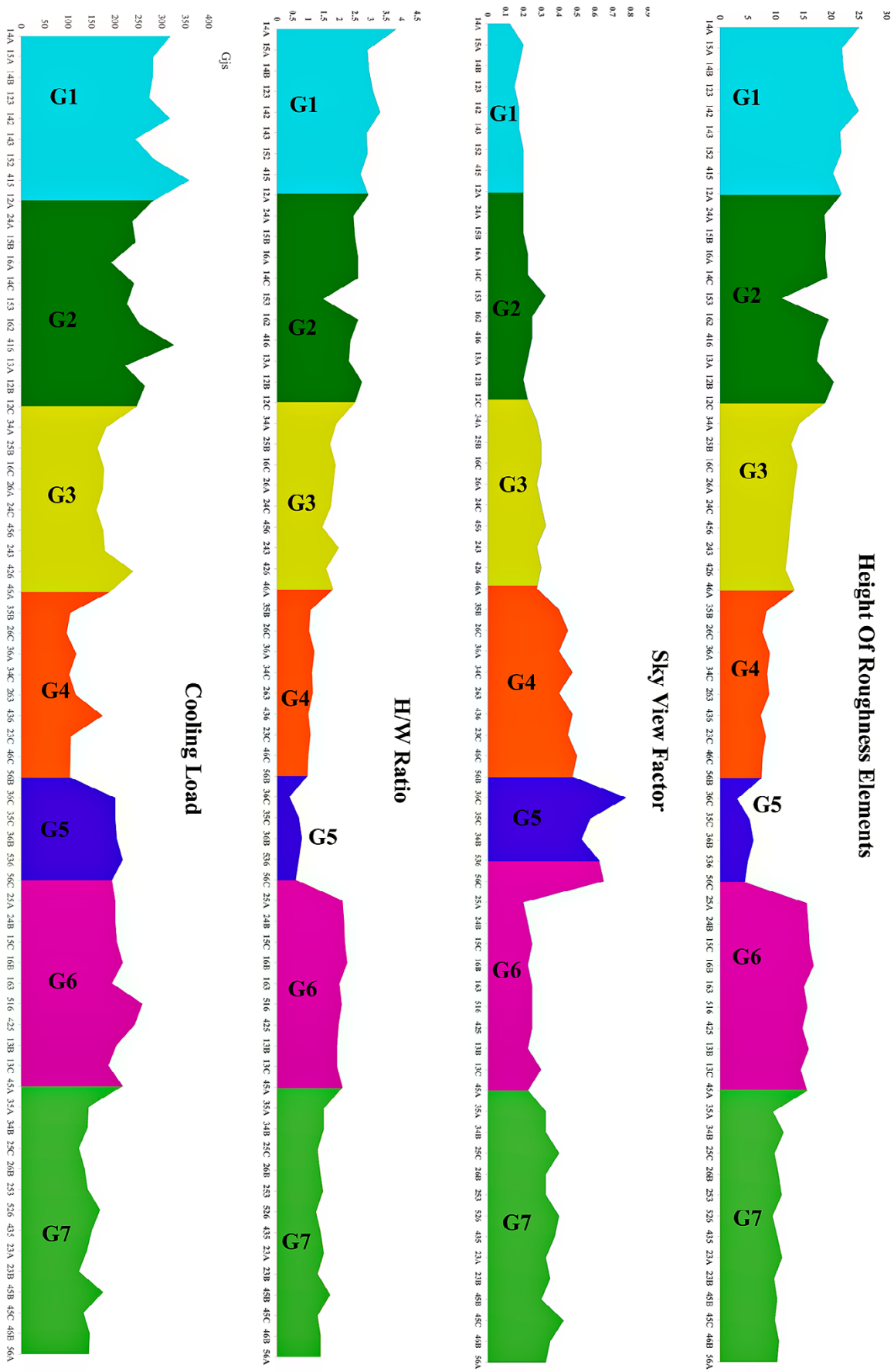

Figure 7. UMI values of urban prototypes

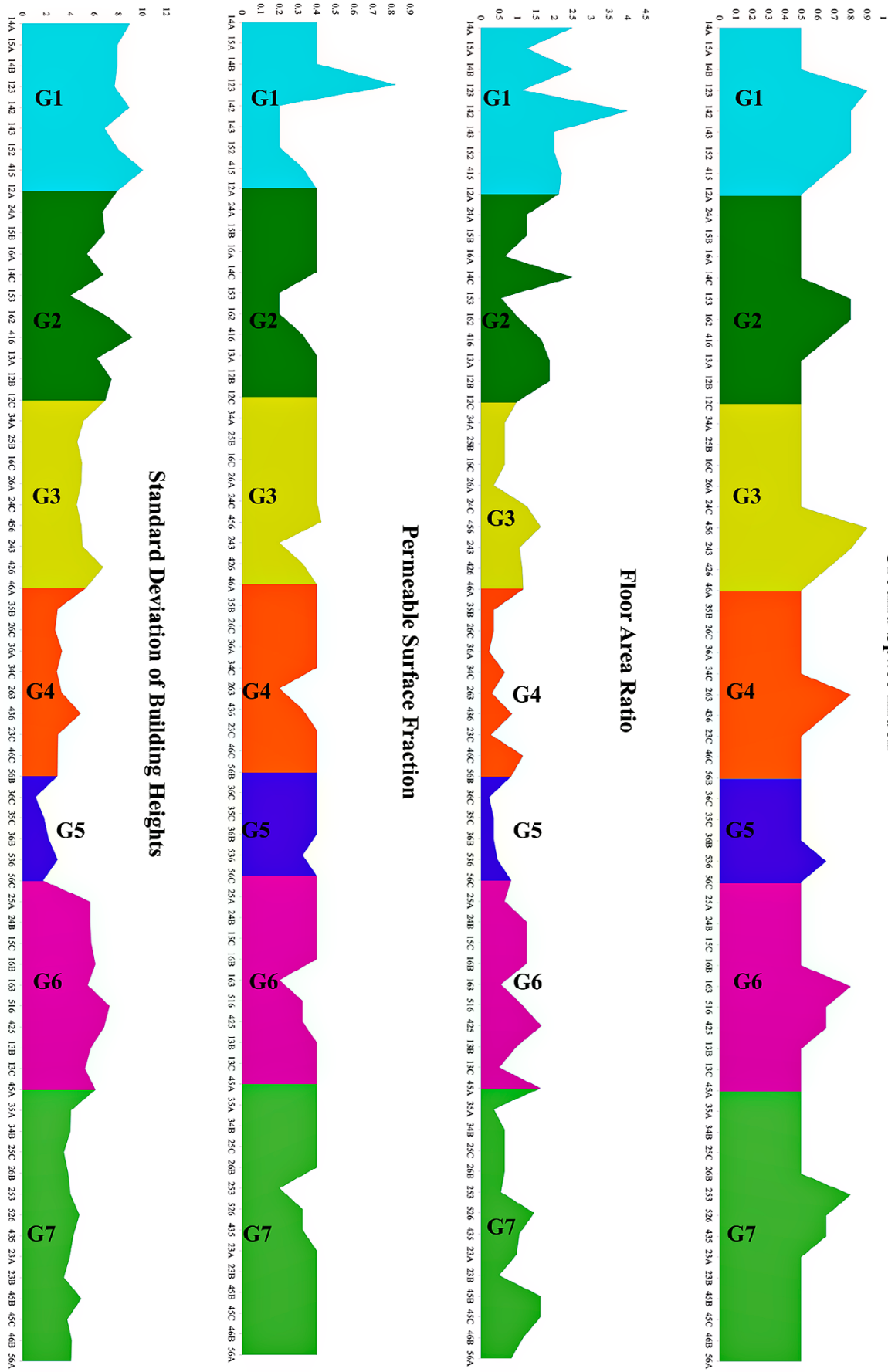

Figure 8. UMI values of urban prototypes

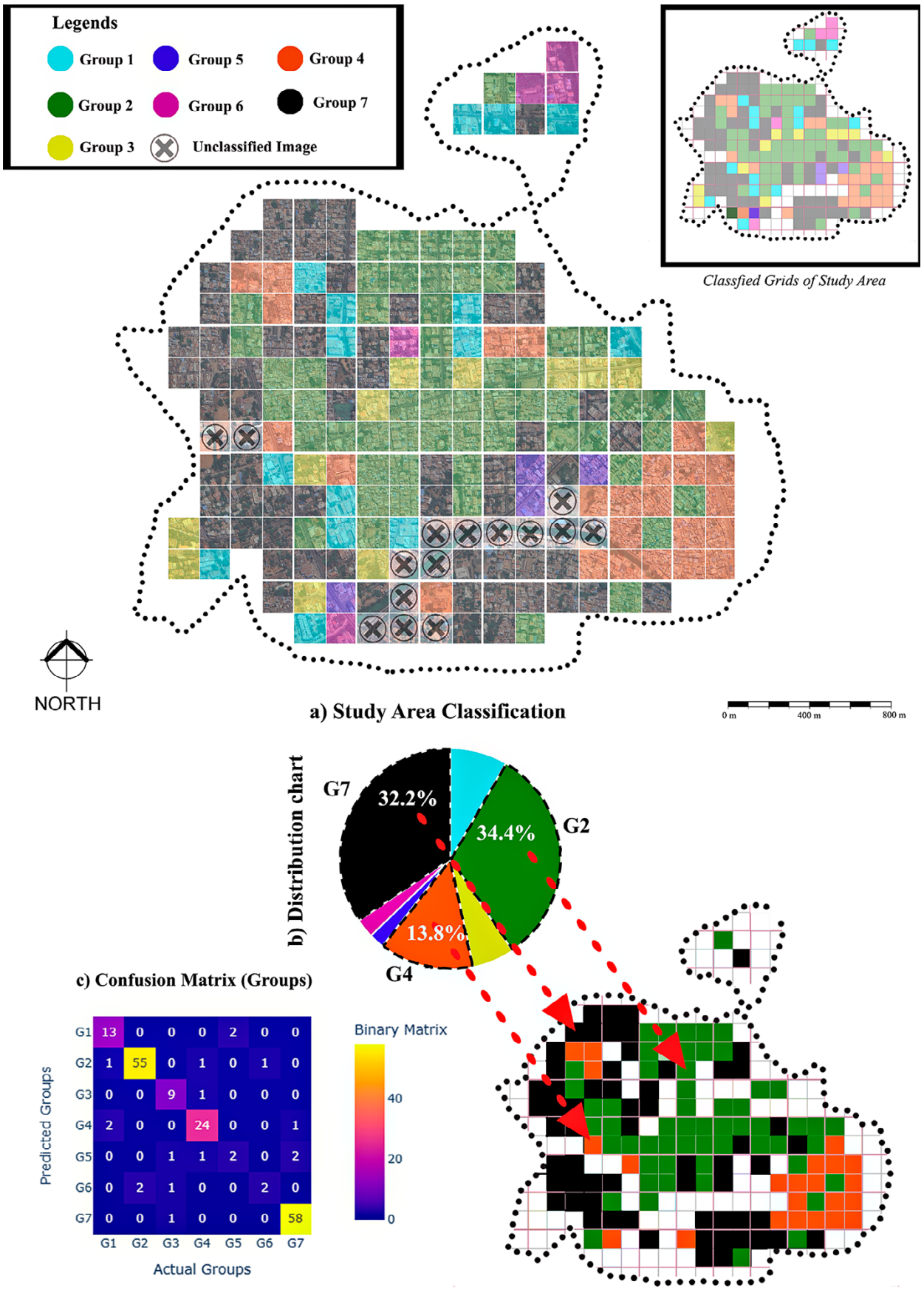

Figure 9. Study area classification results (a) Classification map (b)Distribution of groups in the study area (c) Confusion Matrix of image classification (Groups)

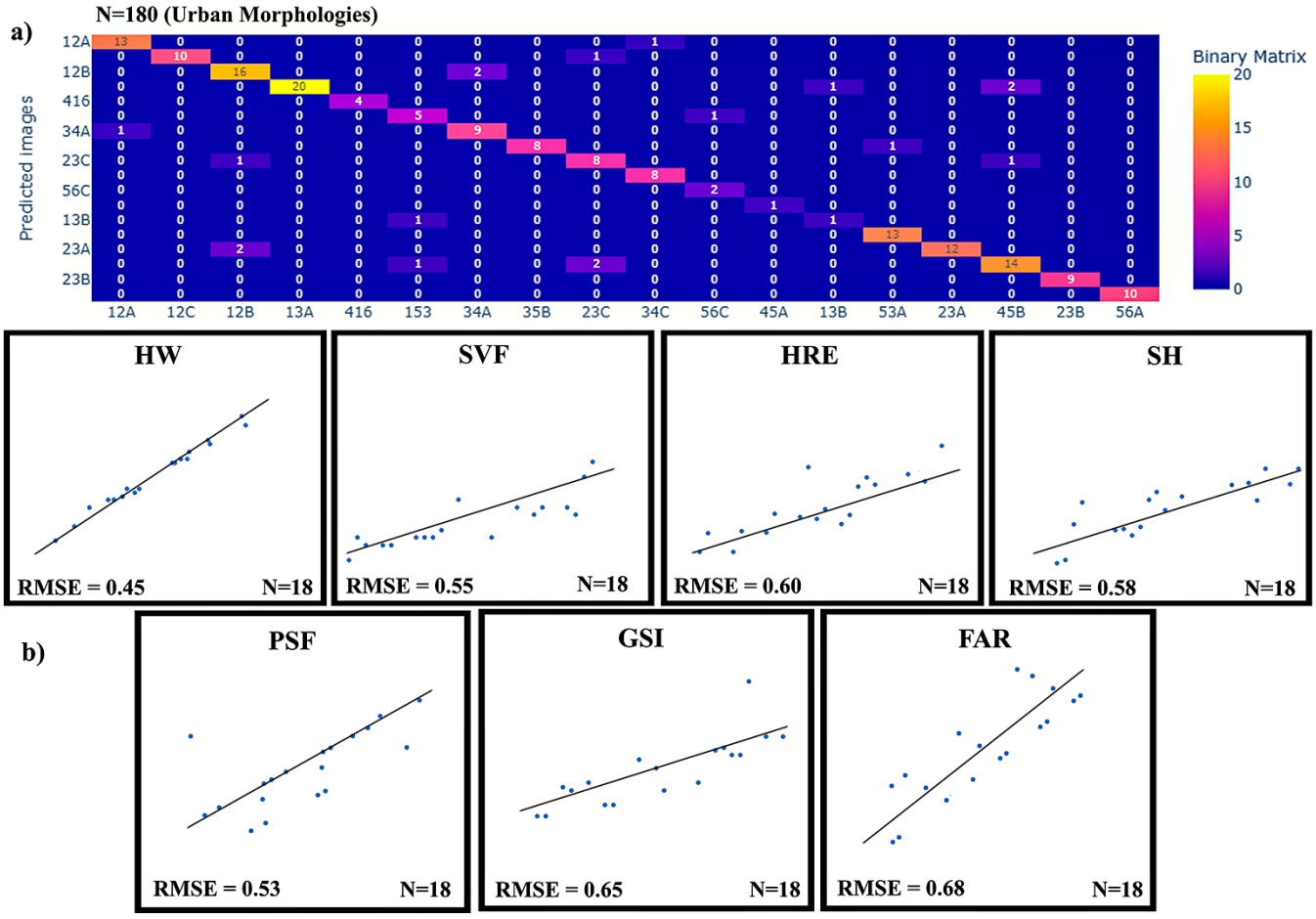

Figure 10. Study area classification results (a) Confusion matrix of classified images (b) RMSE values for validating the urban prototypes

Conclusion

The current study takes KK Nagar in Tiruchirappalli as an example and analyzes the impact of urban spatial geography on the air-conditioning energy usage. In this study, we have proposed a novel method for classifying the city using a two-layer subclassification system. Since major Indian cities are unplanned settlements with more than two LCZ in a grid size of 0.25 sq. km, this study helps classify the highly heterogeneous morphology in cities. The gird size chosen to create the morphology was 38,709 Sq.m. Through this extensive grid size, we can retain more regional geographical features of the city compared to using smaller grids. The research intends to concentrate on the complex urban forms which were not addressed in previous studies to the best of our knowledge. Urban morphology significantly influences the energy consumption of buildings, resulting in a reduction in cooling load Javanroodi et al. (2018). The results of the current study support Javanroodi et al. (2018) statement. The impact of mixed morphologies on energy consumption differed from the planned cities. Compared to the other studies on the impact of urban forms on energy consumption, this research makes a significant contribution in explaining the complex urban structures and their impact on cooling energy consumption. For urban planning, we have found that emphasizing the urban morphology layouts and green cover ratios, such as dense trees (Highly vegetated), Scattered trees (sparsely vegetated) and shrubs (lowly vegetated), is crucial in determining the cooling load consumption in a compact mid-rise and open low-rise morphologies with lands covers. These findings provide insights to urban planners and designers in reducing the energy taken for cooling indoor spaces in mixed morphologies. In policy development, our research can serve as a reference for policymakers. For instance, identifying high energy-consuming urban patches and installing PV panels to reduce the on-grid energy usage. Furthermore, our research demonstrated a workflow for classifying the city morphologies into clusters based on their spatial characteristics. It is worth noting that previous studies have explored the impact of urban morphology on cooling loads, including a study conducted by Kotharkar et al. (2022) in which the author explains that lower cooling loads were seen in open morphologies

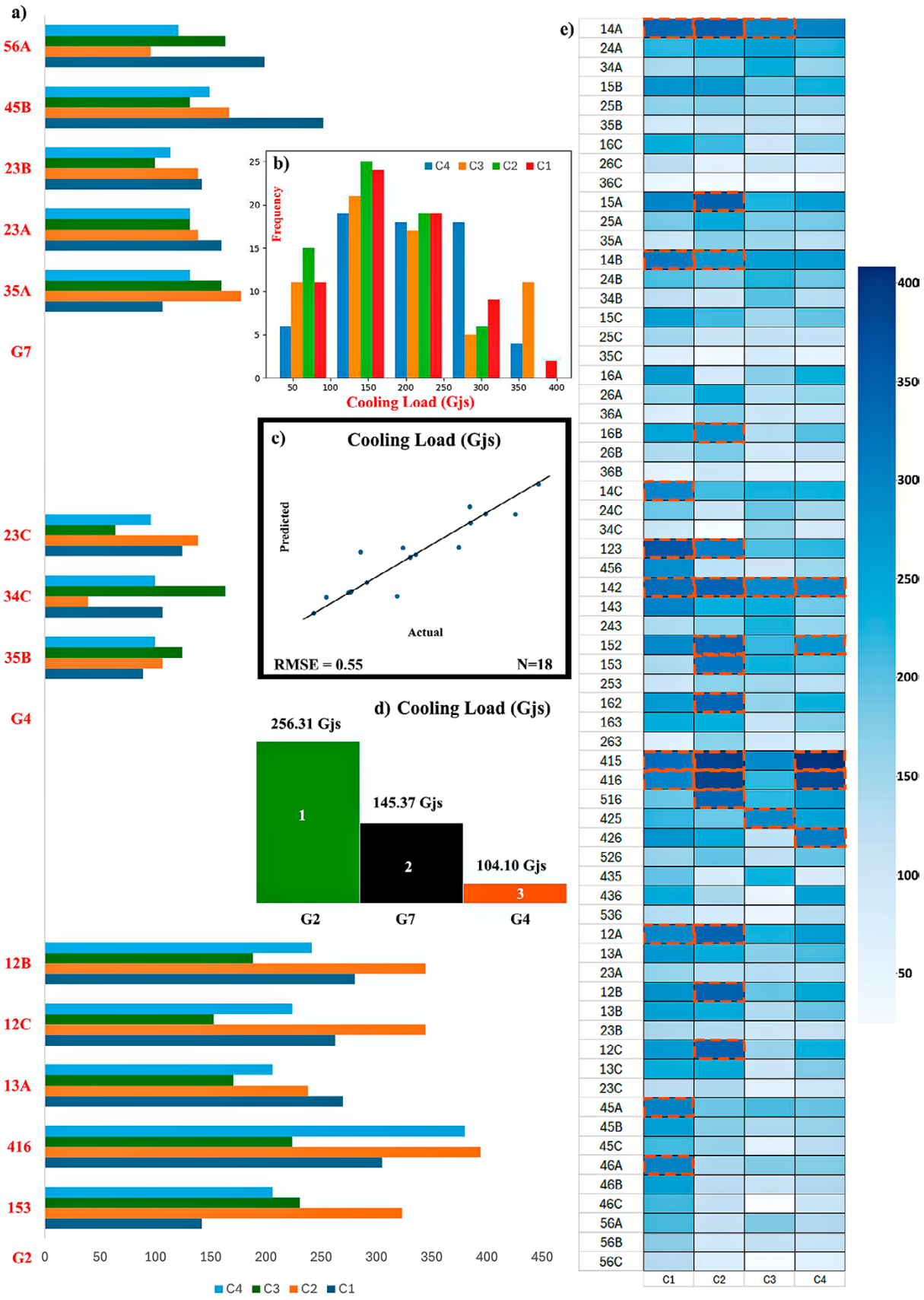

Figure 11. Energy simulation results (a) Cooling load of city LCZs (b) Frequency of cooling loads (c) RMSE values for predicted and actual energy (d) Ranking of groups based on the cooling loads (e) Cooling loads Heat map for all urban prototypes

with high vegetation cover. Similarly, a study conducted in China shows that low and medium-rise structures use more energy for cooling and explains that compact mid-rise configuration's cooling demands were higher than open high-rise (Yang et al., 2022). This study identifies the intricate details in urban morphology at the neighborhood scale through the comparative analysis of different LCZs. It was found that the impact of vegetation on cooling energy consumption of open and compact high-rise along with mid-rise configuration is low. It also explains that increasing the green cover ratio will not help in reducing energy consumption for mixed high and mid-rise morphologies. This study is limited only to residential buildings and hotels, and the results will not be applicable to commercial or office buildings with 8-hour operation slots. There is a scope for future research in studying the arrangement pattern of the buildings and its impact on the reduction of heating loads in cold regions.

The important results of our investigation are as follows:

a) An innovative method for categorizing the complex urban structure of a city. The findings provide valuable design for urban planners and energy policymakers seeking to decrease cooling energy consumption through form-based codes. Our classification approach can be used to classify the morphologies for other cities in future research. This study provides broad insights into sustainable urban development worldwide.
b) In the study area, LCZ 23C (Compact mid-rise and low-rise with sparse vegetation), 34C (Compact low-rise and open high-rise with sparse vegetation) and 35B (Compact low-rise and open mid-rise with scattered vegetation) urban forms needed less energy for air-conditioning in residential neighborhood. The intervention of open or compact low rise in the mixed morphologies reduces the cooling energy consumption drastically.
c) The high frequency of cooling load was between 150Gjs to 200Gjs in the city (Figure 11b). It indicates that the cooling load reduction potential is high in the city when compared to the study area of Nagpur, which was researched by Kotharkar et al. (2022)
d) The Open and compact high-rise with low-rise structures consumes high cooling energy (>400Gjs), which indicates that the high-rise structures with open low-rise combinations are not suitable for warm and humid climate conditions.

Acknowledgement

We are grateful to our institute for providing valuable data and time, inspiring us to complete our research successfully.

References

Abougendia, S. M. (2023). Investigating surface UHI using local climate zones (LCZs), the case study of Cairo's River Islands. *Alexandria Engineering Journal*, 77, 293–307. https://doi.org/10.1016/j.aej.2023.06.071

Alcoforado, M. J., Lopes, A., Alves, E. D. L., & Canário, P. (2014). Lisbon Heat Island. *Finisterra*, 49(98), 61–80.

Alexander, P. J., & Mills, G. (2014). Local climate classification and Dublin's urban heat island. *Atmosphere*, 5(4), 755–774. https://doi.org/10.3390/atmos5040755

Anton, I., & Tănase, D. (2016). Informed Geometries. Parametric Modelling and Energy Analysis in Early Stages of Design. *Energy Procedia*, 85, 9–16. https://doi.org/10.1016/j.egypro.2015.12.269

Apreda, C., Reder, A., & Mercogliano, P. (2020). Urban morphology parameterization for assessing the effects of housing blocks layouts on air temperature in the Euro-Mediterranean context. *Energy and Buildings*, 223, 110171. https://doi.org/10.1016/j.enbuild.2020.110171

Arnfield, A. J. (2003). Two decades of urban climate research: A review of turbulence, exchanges of energy and water, and the urban heat island. *International Journal of Climatology*, 23(1), 1–26. https://doi.org/10.1002/joc.859

Bajšanski, I., Stojaković, V., Tepavčević, B., & Jovanović, M. (2024). A parametric approach for evaluating solar panel insolation in urban areas: Courtyard design case study. *Geographica Pannonica*, 28(2), 115–130. https://doi.org/10.5937/gp28-50098

Barrao, S., Serrano-Notivoli, R., Cuadrat, J. M., Tejedor, E., & Saz Sánchez, M. A. (2022). Characterization of the UHI in Zaragoza (Spain) using a quality-controlled hourly sensor-based urban climate network. *Urban Climate*, 44. https://doi.org/10.1016/j.uclim.2022.101207

Bhatnagar, M., Mathur, J., & Garg, V. (2018). Determining base temperature for heating and cooling degree-days for India. *Journal of Building Engineering*, 18, 270–280. https://doi.org/10.1016/j.jobe.2018.03.020

Bueno, B., Norford, L., Hidalgo, J., & Pigeon, G. (2013). The urban weather generator. *Journal of Building Performance Simulation*, 6(4), 269–281. https://doi.org/10.1080/19401493.2012.718797

Bueno, B., Roth, M., Norford, L., & Li, R. (2014). Computationally efficient prediction of canopy level urban air temperature at the neighbourhood scale. *Urban Climate*, 9, 35–53. https://doi.org/10.1016/j.uclim.2014.05.005

Cao, Q., Huang, H., Hong, Y., Huang, X., Wang, S., Wang, L., & Wang, L. (2022). Modeling intra-urban differences in thermal environments and heat stress based on local climate zones in central Wuhan. *Building and Environment*, 225, 109625. https://doi.org/10.1016/j.buildenv.2022.109625

Chen, M., Ban-Weiss, G. A., & Sanders, K. T. (2018). The role of household level electricity data in improving estimates of the impacts of climate on building electricity use. *Energy and Buildings*, 180, 146–158. https://doi.org/10.1016/j.enbuild.2018.09.012

Deng, Z., Javanroodi, K., Nik, V. M., & Chen, Y. (2023). Using urban building energy modeling to quantify the energy performance of residential buildings under climate change. *Building Simulation*, 16(9), 1629–1643. https://doi.org/10.1007/s12273-023-1032-2

Dosio, A., Mentaschi, L., Fischer, E. M., & Wyser, K. (2018). Extreme heat waves under 1.5 °c and 2 °c global warming. *Environmental Research Letters*, 13(5). https://doi.org/10.1088/1748-9326/aab827

Ellena, M., Breil, M., & Soriani, S. (2020). The heat-health nexus in the urban context: A systematic literature review exploring the socio-economic vulnerabilities and built environment characteristics. *Urban Climate*, 34, 100676. https://doi.org/10.1016/j.uclim.2020.100676

Elzeni, M., Elmokadem, A., & Badawy, N. M. (2022). Classification of urban morphology indicators towards urban generation. *Port Said Engineering Research Journal*, 26(1), 43–56. https://doi.org/10.21608/pserj.2021.91760.1135

Heaviside, C., Macintyre, H., & Vardoulakis, S. (2017). The Urban Heat Island: Implications for Health in a Changing Environment. *Current Environmental Health Reports*, 4(3), 296–305. https://doi.org/10.1007/s40572-017-0150-3

Heidelberger, E., & Rakha, T. (2022). Inclusive urban building energy modeling through socioeconomic data: A persona-based case study for an underrepresented community. *Building and Environment*, 222, 109374. https://doi.org/10.1016/J.BUILDENV.2022.109374

Heris, M. P., Middel, A., & Muller, B. (2020). Impacts of form and design policies on urban microclimate: Assessment of zoning and design guideline choices in urban redevelopment projects. *Landscape and Urban Planning*, 202, 103870. https://doi.org/10.1016/j.landurbplan.2020.103870

Hong, T., Chen, Y., Luo, X., Luo, N., & Lee, S. H. (2020). Ten questions on urban building energy modeling. *Building and Environment*, 168, 106508. https://doi.org/10.1016/J.BUILDENV.2019.106508

Hood, R. (2005). Global Warming. *A Companion to Applied Ethics*, 674–684. https://doi.org/10.1002/9780470996621.ch50

Huo, X., Yang, L., Li, D. H. W., Lun, I., Lou, S., & Shi, Y. (2022). Impact of climate change on outdoor design conditions and implications to peak loads. *Building Simulation*, 15(12), 2051–2065. https://doi.org/10.1007/s12273-022-0913-0

Jain, A. K. (2010). Data clustering: 50 years beyond K-means. *Pattern Recognition Letters*, 31(8), 651–666. https://doi.org/10.1016/j.patrec.2009.09.011

Javanroodi, K., Mahdavinejad, M., & Nik, V. M. (2018). Impacts of urban morphology on reducing cooling load and increasing ventilation potential in hot-arid climate. *Applied Energy*, 231, 714–746. https://doi.org/10.1016/j.apenergy.2018.09.116

Joshi, M. Y., Rodler, A., Musy, M., Guernouti, S., Cools, M., & Teller, J. (2022). Identifying urban morphological archetypes for microclimate studies using a clustering approach. *Building and Environment*, 224, 109574. https://doi.org/10.1016/j.buildenv.2022.109574

Karthik, D. (2021, December 25). *Trichy corporation to have five zones*. Times of India . https://timesofindia.indiatimes.com/city/trichy/trichy-corporation-to-have-five-zones/articleshowprint/88486041.cms

Katal, A., Mortezazadeh, M., Wang, L. (Leon), & Yu, H. (2022). Urban building energy and microclimate modeling – From 3D city generation to dynamic simulations. *Energy*, 251, 123817. https://doi.org/10.1016/j.energy.2022.123817

Klysik, K., & Fortuniak, K. (1999). Temporal and spatial characteristics of the urban heat island of Lodz, Poland. *Atmospheric Environment*, 33(24–25), 3885–3895. https://doi.org/10.1016/S1352-2310(99)00131-4

Kotharkar, R., & Bagade, A. (2018). Local Climate Zone classification for Indian cities: A case study of Nagpur. *Urban Climate*, 24, 369–392. https://doi.org/10.1016/j.uclim.2017.03.003

Kotharkar, R., Ghosh, A., Kapoor, S., & Reddy, D. G. K. (2022). Approach to local climate zone based energy consumption assessment in an Indian city. *Energy and Buildings*, 259, 111835. https://doi.org/10.1016/j.enbuild.2022.111835

Leconte, F., Bouyer, J., Claverie, R., & Pétrissans, M. (2015). Estimation of spatial air temperature distribution at sub-mesoclimatic scale using the LCZ scheme and mobile measurements. In *Proceedings of the 9th International Conference on Urban Climate & 12th Symposium on Urban Environment* (pp. 1–12).

Li, X., Zhou, Y., Yu, S., Jia, G., Li, H., & Li, W. (2019). Urban heat island impacts on building energy consumption: A review of approaches and findings. *Energy*, 174, 407–419. https://doi.org/10.1016/j.energy.2019.02.183

Li, Y., Wang, W., Wang, Y., Xin, Y., He, T., & Zhao, G. (2021). A review of studies involving the effects of climate change on the energy consumption for building heating and cooling. *International Journal of Environmental Research and Public Health*, 18(1), 40. https://doi.org/10.3390/ijerph18010040

Ma, L., Yan, Z., He, W., Lv, L., He, G., & Li, M. (2023). Towards better exploiting object-based image analysis paradigm for local climate zones mapping. *ISPRS Journal of Photogrammetry and Remote Sensing*, 199, 73–86. https://doi.org/10.1016/j.isprsjprs.2023.03.018

Masson, V., Lemonsu, A., Hidalgo, J., & Voogt, J. (2020). Urban climates and climate change. *Annual Review of Environment and Resources*, 45, 411–444. https://doi.org/10.1146/annurev-environ-012320-083623

Nagpal, S., Hanson, J., & Reinhart, C. (2019). A framework for using calibrated campus-wide building energy models for continuous planning and greenhouse gas emissions reduction tracking. *Applied Energy*, 241, 82–97. https://doi.org/10.1016/j.apenergy.2019.03.010

Nassar, A. K., Blackburn, G. A., & Whyatt, J. D. (2016). Dynamics and controls of urban heat sink and island phenomena in a desert city: Development of a local climate zone scheme using remotely-sensed inputs. *International Journal of Applied Earth Observation and Geoinformation*, 51, 76–90. https://doi.org/10.1016/j.jag.2016.05.004

Nastran, M., Kobal, M., & Eler, K. (2019). Urban heat islands in relation to green land use in European cities. *Urban Forestry and Urban Greening*, 37, 33–41. https://doi.org/10.1016/j.ufug.2018.01.008

Natanian, J., & Auer, T. (2020). Beyond nearly zero energy urban design: A holistic microclimatic energy and environmental quality evaluation workflow. *Sustainable Cities and Society*, 56, 102094. https://doi.org/10.1016/j.scs.2020.102094

Nik, V. M. (2016). Making energy simulation easier for future climate – Synthesizing typical and extreme weather data sets out of regional climate models (RCMs). *Applied Energy*, 177, 204–226. https://doi.org/10.1016/J.APENERGY.2016.05.107

Oke, T. R. (2004). Initial guidance to obtain representative meteorological observations at urban sites. *World Meteorological Organization*, 81, 51.

Palusci, O., Monti, P., Cecere, C., Montazeri, H., & Blocken, B. (2022). Impact of morphological parameters on urban ventilation in compact cities: The case of the Tuscolano-Don Bosco district in Rome. *Science of the Total Environment*, 807, 150490. https://doi.org/10.1016/j.scitotenv.2021.150490

Panuwatwanich, K., & Nguyen, T. T. (2017). Influence of Total Quality Management on Performance of Vietnamese Construction Firms. *Procedia Engineering*, 182, 548–555. https://doi.org/10.1016/j.proeng.2017.03.151

Parmesan, C. & Yohe, G. (2003). A globally coherent fingerprint of climate change impacts across natural systems. *Nature*, 421, 37–42 (2003). https://doi.org/10.1038/nature01286

Perkins-Kirkpatrick, S. E., & Lewis, S. C. (2020). Increasing trends in regional heatwaves. *Nature Communications*, 11, 3357. https://doi.org/10.1038/s41467-020-16970-7

Rajagopal, P., Priya, R. S., & Senthil, R. (2023). A review of recent developments in the impact of environmental measures on urban heat island. *Sustainable Cities and Society*, 88, 104279. https://doi.org/10.1016/j.scs.2022.104279

Schirmer, P. M., & Axhausen, K. W. (2016). A multiscale classification of urban morphology. *Journal of Transport and Land Use*, 9(1), 101–130. https://doi.org/10.5198/jtlu.2015.667

Skarbit, N., Stewart, I. D., Unger, J., & Gál, T. (2017). Employing an urban meteorological network to monitor air temperature conditions in the 'local climate zones' of Szeged, Hungary. *International Journal of Climatology*, 37, 582–596. https://doi.org/10.1002/joc.5023

Stewart, I. D. (2011). A systematic review and scientific critique of methodology in modern urban heat island literature. *International Journal of Climatology*, 31(2), 200–217. https://doi.org/10.1002/joc.2141

Stewart, I. D., & Oke, T. R. (2012). Local climate zones for urban temperature studies. *Bulletin of the American Meteorological Society*, 93(12), 1879–1900. https://doi.org/10.1175/BAMS-D-11-00019.1

Sun, L., Chen, J., Li, Q., & Huang, D. (2020). Dramatic uneven urbanization of large cities throughout the world in recent decades. *Nature Communications*, 11(1). https://doi.org/10.1038/s41467-020-19158-1

Taha, H. (1997). Urban climates and heat islands: Albedo, evapotranspiration, and anthropogenic heat. *Energy and Buildings*, 25(2), 99–103. https://doi.org/10.1016/s0378-7788(96)00999-1

Teller, J., & Azar, S. (2001). Townscope II - A computer systems to support solar access decision-making. *Solar Energy*, 70(3), 187–200. https://doi.org/10.1016/S0038-092X(00)00097-9

United Nations. (2019). *World population prospects 2019: Volume I, comprehensive tables*. Department of Economic and Social Affairs.

Vallati, A., De Lieto Vollaro, A., Golasi, I., Barchiesi, E., & Caranese, C. (2015). On the impact of urban micro climate on the energy consumption of buildings. *Energy Procedia*, 82, 506–511. https://doi.org/10.1016/j.egypro.2015.11.862

Wang, D., Landolt, J., Mavromatidis, G., Orehounig, K., & Carmeliet, J. (2018). CESAR: A bottom-up building stock modelling tool for Switzerland to address sustainable energy transformation strategies. *Energy*

and Buildings, 169, 9–26. https://doi.org/10.1016/J.ENBUILD.2018.03.020

Warren, E. L., Young, D. T., Chapman, L., Muller, C., Grimmond, C. S. B., & Cai, X. M. (2016). The Birmingham Urban Climate Laboratory-A high density, urban meteorological dataset, from 2012-2014. *Scientific Data*, 3. https://doi.org/10.1038/sdata.2016.38

Yang, Y., Javanroodi, K., & Nik, V. M. (2021). Climate change and energy performance of European residential building stocks – A comprehensive impact assessment using climate big data from the coordinated regional climate downscaling experiment. *Applied Energy*, 298, 117246. https://doi.org/10.1016/J.APENERGY.2021.117246

Yang, R., Yang, J., Wang, L., Xiao, X., & Xia, J. (2022). Contribution of local climate zones to the thermal environment and energy demand. *Frontiers in Public Health*, 10. https://doi.org/10.3389/fpubh.2022.992050

Yue, W., Liu, X., Zhou, Y., & Liu, Y. (2019). Impacts of urban configuration on urban heat island: An empirical study in China mega-cities. *Science of the Total Environment*, 671, 1036–1046. https://doi.org/10.1016/j.scitotenv.2019.03.421

INTERNATIONAL SCIENTIFIC JOURNAL
GEOGRAPHICA PANNONICA
Volume 28, Issue 3, 205–220 (September 2024)
Journal homepage: http://www.dgt.uns.ac.rs/en/homepage/pannonica/

Particulate Air Pollution in Central Serbia and some Proposed Measures for the Restoration of Degraded and Disturbed Mining Areas

Ivana Mihalj[A*], Stamenko Šušak[B,C], Tamara Palanački Malešević[A], Tamara Važić[A], Tamara Jurca[A], Dragoslav Pavić[D], Jelica Simeunović[A], Aleksandra Vulin[B,C], Jussi Meriluoto[A,E], Zorica Svirčev[A,E]

[A] *University of Novi Sad, Faculty of Sciences, Department of Biology and Ecology, UNS, Trg Dositeja Obradovića 2, 21000 Novi Sad, Serbia; ORCID TJ: 0000-0001-5565-5838; JS: 0000-0002-4049-0724*

[B] *University of Novi Sad, Faculty of Medicine, UNS, Hajduk Veljkova 3, 21000 Novi Sad, Serbia; ORCID AV: 0000-0002-4279-6452*

[C] *Institute of Cardiovascular Diseases of Vojvodina, Sremska Kamenica, Serbia*

[D] *University of Novi Sad, Faculty of Sciences, Department of Geography, Tourism and Hotel Management, UNS, Trg Dositeja Obradovića 3, 21000 Novi Sad, Serbia; ORCID DP: 0000-0002-7113-0887*

[E] *Åbo Akademi University, Faculty of Science and Engineering, Biochemistry and Cell Biology, Tykistökatu 6A, 20520 Turku, Finland; JM: 0000-0002-6300-301X; ZS: 0000-0001-8355-7661*

KEYWORDS

mining regions
environmental pollution
particulate matter
recultivation
biocrusts
cyanobacteria

ABSTRACT

Mining causes soil degradation, particle emission, and air and water quality deterioration. This study estimates some health risks in districts of Central Serbia affected by surface mining activities, and proposes measures for land restoration. The epidemiological risk assessment was based on data for seven cancers and three cardiovascular diseases during 2010 - 2020. Results showed a statistically significant increase in the incidence of lung and bronchial cancer in critical districts. Borski district stood out with the highest incidence rates for cardiovascular diseases. The suspected role of particulate air pollution from the mining industry in health deterioration calls for intensified air quality monitoring and development of mitigation technologies. A restoration strategy called the Pan-Life-Carpet technology is proposed for the restoration of mining areas and for air and water pollution control.

Introduction

Land is a vital resource for human social and economic wellbeing. However, many parts of land ecosystems are under climatic and anthropogenic pressure. Anthropogenic climate changes accelerate natural and induce anthropogenic land degradation (Talukder et al., 2021). Land degradation leads to the deterioration of terrestrial and aquatic ecosystems and decrease of biodiversity. It presents one of the most severe ecological challenges of today (Perović et al., 2021) that leads to the reduction or loss of the biological or economic productivity and complexity of the land (UNCCD, 1994). Besides natural processes, main causes of land degradation are improper soil and vegetation management, overgrazing, industrial activities, waste deposition and mining, urbanization and infrastructure development, release of airborne pollutants, disturbance of the water cycle (UNDP, 2022), while climate

* Corresponding author: Ivana Mihalj, e-mail: ivana.mihalj@dbe.uns.ac.rs

doi: 10.5937/gp28-50537

Received: April 19, 2024| Revised: September 18, 2024| Accepted: September 19, 2024

change further amplifies the impact of drivers of land degradation (IPBES, 2018).

One of the most visible processes of soil degradation is soil erosion (UNDP, 2022). Soil erosion is a major environmental problem, threatening human safety and global socio-economic development (Sun et al., 2013; Jiang et al., 2019). Soil erosion can affect water and air quality. Erosive and unprotected soil presents a source of particulate pollution, while soil particles can contain other pollutants such as metals and organic pollutants (Goudie, 2014; Giltrap et al., 2021). The global emission of dust from the soil to the atmosphere has been estimated to be 3000 million tons annually (Katra, 2020).

Mining modifies, degrades and pollutes land (Padro et al., 2022). Surface mining induces immediate loss of soil, formation of waste (ash, slag, and tailings) and wastewater resulting from tailing processing (Pavlović et al., 2017). A major problem of mining is the mining waste, i.e. deposits of ash, slag and tailing that are usually disposed of without further utilization (Pavlović et al., 2017). Serbia produces about 40 million tons of mining waste every year (Official Gazette of the Republic of Serbia, No 12/2022). Mining is one of the main processes connected with soil loss and degradation in Serbia (Ličina et al., 2011; Pavlović et al., 2017). Emission of the soil particles to the atmosphere deteriorates air quality of the surroundings and remote areas (Goudie, 2014; Giltrap et al., 2021). Tian et al. (2019) showed that more than half of road dust sieved to 10 μm, collected at different distances to the mine and tailings, originate from the mine.

The primary pollutant produced by surface mining is particulate matter (PM) (Kumar Patra et al., 2016). PM consists of heterogeneous components, formed due to chemical reactions between inorganic and organic substances (soot, dust, soil components, vehicle exhaust gases, combustion products, etc.) (Manisalidis et al., 2020; Matić Savićević, 2020). According to the size PM are divided into three groups: PM10 (coarse particles, between 2.5-10 μm), PM2.5 (fine particles, < 2.5 μm) and PM0.1 (ultrafine particles, < 100 nm) (Franck et al., 2011; USEPA, 2016). The carbon core of PM can adsorb various chemicals such as aromatic and aliphatic compounds, biological allergens, endotoxins, heavy metals (e.g. Pb, As, Cd, Ni) etc. (Matić Savićević, 2020; Knežević et al., 2021) (Figure 1).

PM are associated with various health issues (Kelly & Fussel, 2015), and according to the International Agency for Research on Cancer (IARC) of the WHO, they belong to the Group 1 carcinogens, together with outdoor pollution (Loomis et al., 2013; IARC, 2016). It is estimated that exposure to air pollution, especially PM, results in millions of deaths annually (Kelly & Fussel, 2015; WHO, 2019; 2021). The effect of PM on the human body is determined by size (Valavanidis et al., 2008). Particles larger than 10 μm are generally trapped in the mucous membrane of the nose and throat and can be swallowed (Giltrap et al., 2021). Most PM10 are deposited in the upper airways (Brown et al., 2002) and can get deposited in the lungs where they cause inflammatory processes (Knežević et al., 2021). PM2.5 penetrate deep lung tissue (Giltrap et al., 2021) (Figure 1). Particle shape (International Commission on Radiological Protection, 1995; Sankaran et al., 2023), adsorbed substances (Valavanidis et al., 2008), origin, chemical compositions (Valavanidis et al., 2008; Xing et al., 2016), exposure time (Yang et al., 2019; Orellano et al., 2020), mechanisms of toxicity (Valavanidis et al., 2008) medical condition (e.g. preexisting heart and lung disease, diabetes) and stage of life (elderly and children) (Sacks et al., 2011; Manisalidis et al., 2020) determine the effects of PM on the human body, also.

PM is an important pollution in open mine areas, especially PM10 (Bui et al., 2019). In recent years, the concentration of PM10 in Serbia has been higher than the allowed 50 μg/m^3 (WHO, 2019). Mining has a long-standing tradition in the Republic of Serbia with potential to expand (Popović et al., 2015). Kumar Patra et al. (2016) summarized medical evidence of health deterioration due to inhalation of PM pollution from surface mines. Mining impacts cardiovascular and respiratory systems, contributes to the neurological disorders and kidney damages (Ku-

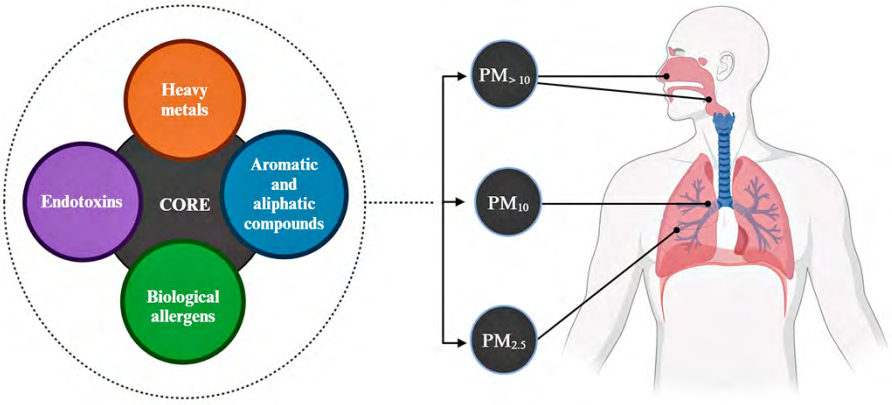

Figure 1. Description of heterogeneity of PM in the air and their impact on the respiratory system depending on the size of the PM (made with https://www.biorender.com/)

mar Patra et al., 2016; da Silva-Rego et al., 2022). One of the Sustainable Development Goals (SDGs) in the Agenda 2030 is to "substantially reduce the number of deaths and illnesses from hazardous chemicals and air, water and soil pollution and contamination" by 2030 (UN, 2015). Therefore, this work aims to estimate the health risk in the districts of Central Serbia that are affected by surface mining and mining waste disposal, as well as to propose measures for simultaneous mining land restoration, air pollution reduction and health risk decrease.

Data and methods

Databases for epidemiological analyses

The epidemiological risk assessment was based on the incidences of cancers and cardiovascular diseases. According to the Batut definition, standardized incidence and mortality rates represent theoretical values obtained through a specific technical process involving the introduction of a standard population. Typically, this standard population can be the world population (ASR-W), the European population (ASR-E), or a truncated population (ASR-TRUNC). These standardized rates overcome differences (most commonly by sex and age) that exist in different populations, making them suitable for comparisons (Batut, 2023c). The possible relation between PM pollution in degraded/disturbed areas and incidence of cancers and cardiovascular diseases in Central Serbia was based on data published by the Institute of Public Health of Serbia, 'Dr Milan Jovanović Batut' (Batut, 2023, 2023b, 2023c).

The seven examined cancers and three cardiovascular diseases are listed in Table 1, including corresponding abbreviations, as well as their codes from the 10th revision of the International Statistical Classification of Diseases and Related Health Problems (ICD), a medical classification list by the World Health Organization (WHO). The collected data concerning the mentioned diseases covered the period 2010 - 2020. The data included information concerning cancers in both males and females, except for the cancers of pharynx, oral cavity, and larynx, for which data on females was not available.

Table 1. Examined cancers and cardiovascular diseases with abbreviations

Abbr.	ICD - 10 codes	Cancer and cardiovascular diseases
C1	C00 - C14	Malignant neoplasm of lip, oral cavity and pharynx
C2	C32	Malignant neoplasm of larynx
C3	C34	Malignant neoplasm of bronchus and lung
C4	C67	Malignant neoplasm of bladder
C5	C71	Malignant neoplasm of brain
C6	C91 - C95	Leukemia
C7	C00 - C97	Malignant neoplasms
CV1	I21	Acute myocardial infarction
CV2	I20.0	Unstable angina pectoris
CV3	I24.9	Acute coronary syndrome

Source: https://icd.who.int/browse10/2019/en#/C06.9 (Internet 1).

Regional division of Central Serbia

According to the administrative division, Central Serbia has 18 districts. The investigated districts and corresponding abbreviations are presented in Table 2. The incidence of investigated types of cancers and cardiovascular diseases are documented by districts. Thus, it is possible to estimate the occurrence of diseases in degraded mining areas.

Table 2. Investigated districts of Central Serbia and the total number of inhabitants for the period 2010 – 2020 per district

№	District	Average number of inhabitants per district 2010 - 2020
1	Kolubarski	168612
2	Mačvanski	289074
3	Raški	305209
4	Moravički	205360
5	Zlatiborski	276884
6	Rasinski	231362
7	Šumadijski	286174
8	Pomoravski	205571
9	Braničevski	174794
10	Podunavski	192521
11	Zaječarski	113092
12	Borski	118762
13	Nišavski	367036
14	Pčinjski	204323
15	Jablanički	208448
16	Toplički	87473
17	Pirotski	88156
18	Beograd	1541347

Statistical analysis

A division was made into critical and non-critical districts. For critical districts were considered those which are affected by soil degradation and dust pollution from main mining sites of Central Serbia. The minings in Bor, Majdanpek, Kostolac and Kolubara as well as mining waste

disposals 'Nikola Tesla A' and 'Nikola Tesla B' were considered as main degraded mining sites (Figure 2, circled). The influence of dominant winds was also considered in districts categorisation. Among the 18 examined districts, ten were critical and represented the first group in the statistical comparison (Beograd city, Podunavski, Borski, Moravički, Kolubarski, Šumadijski, Mačvanski, Braničevski, Zaječarski and Pomoravski). The rest of the districts of Central Serbia were considered as non-critical districts (Pčinjski, Rasinski, Jablanički, Nišavski, Raški, Toplički, Pirotski and Zlatiborski).

The values of the incidences of selected cancers and cardiovascular diseases were statistically analyzed using Student's t-test. Survey results were obtained using statistically significant differences between critical and non-critical districts in Serbia with a reliability of 95% ($p = 0.000 < 0.05$). The normality of the distribution was determined using the Shapiro-Wilk test. Derived values are presented in diagrams in order to visualize possible relationships between the incidences of seven types of cancers and three types of cardiovascular diseases with degraded mining areas which are a source of PM air pollution.

Results

Degraded mining areas in Serbia as particulate matter air pollution source

According to the analysis of the map showing damaged and degraded areas in Serbia with prominent main mining areas (Figure 2), following districts could be considered as most exposed to the PM air pollution from mining areas: Beograd city district, Mačvanski district, Kolubarski district, Moravički district, Šumadijski district, Podunavski district, Pomoravski district, Braničevski district, Borski district and Zaječarski district.

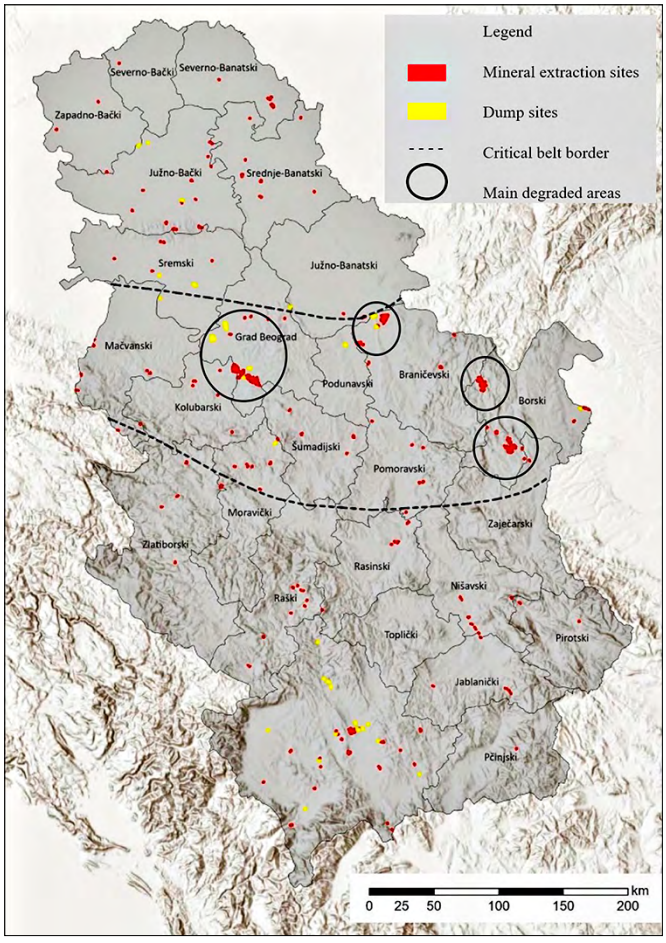

Figure 2. Map of damaged and degraded areas as a source of particulate air pollution in Serbia with ten affected districts in Central Serbia (based on Corine Land Cover 2018 (V2020_20u1), European Environment Agency (EEA))

Epidemiological analyses

The ratio of the incidence of cancer and cardiovascular diseases was determined by district in Central Serbia for the period 2010 - 2020. Critical districts showed a statistically significant association with an increased incidence of lung and bronchial cancer compared to the non-critical districts ($p = 0.027$, $p < 0.05$) (Figure 3a). The highest mean incidence of lung and bronchial cancer was determined in the following critical districts: the Beograd city (75.86) and Podunavski (70.15) districts. Statistical analyses showed the association of critical districts with an increased incidence of cancer of the oral cavity and pharynx (cavitas and pharynx) was marginally significant ($p = 0.086$, $0.05 \leq p < 0{,}1$) (Figure 3b). However, incidence analysis for other investigated cancers (C2, C4, C5, C6, C7) showed that there is

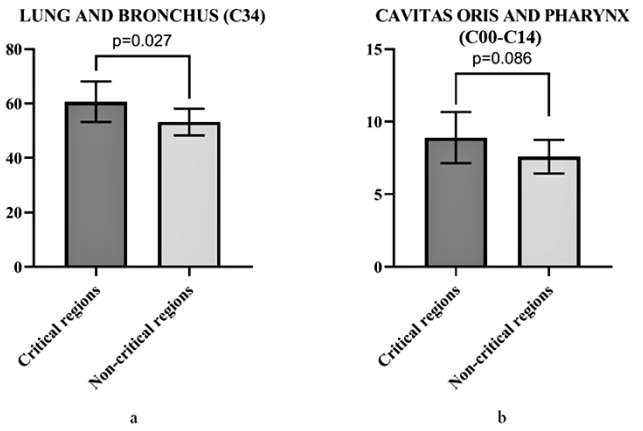

Figure 3. Incidence of lung and bronchial cancer (a), oral cavity and pharynx cancers (b) in Central Serbia for the period 2010 – 2020

no statistically significant difference between the critical and non-critical districts.

The incidence analysis for the examined cardiovascular diseases (CV1, CV2, CV3) showed that there is no statistically significant difference between the selected critical and non-critical districts. Due to the fact that cardiovascular diseases are the most common cause of death in Serbia in 2019 (Vasić et al., 2022), the incidence values among all districts in Central Serbia were compared, whereby the Borski district stood out in particular. Based on the incidence values, this district took the first place in the case of acute coronary syndrome, the second place in the case of unstable angina pectoris, and the third place in the case of acute myocardial infarction. Owing to the fact that this district is the most affected by soil (surface) degradation, the incidence values of the Borski district in the period from 2010 - 2020. years were compared with each district individually as well. Analyses proved that there is no statistically significant difference between the Borski district on one side and the districts with the highest incidence values.

Acute coronary syndrome disease in Borski district, with a standardized incidence rate of 200.768 per 100,000 inhabitants, ranks this district with the highest incidence compared to other districts (Figure 4). Statistical processing of the data did not show statistical significance difference in comparison with Zaječarski district that belongs to the group of critical districts as well (p = 0.466).

In the case of unstable angina pectoris, the Borski district, with standardized incidence rate values of 64.077 per 100,000 inhabitants in the observed period, ranked second in terms of the incidence, after the Nišavski district (incidence value = 76.064) and ahead with the Zaječarski district (incidence value = 58.732) (Figure 5). Statistical analyses show no significant difference between the Borski district and Nišavski (p = 0.426), Zaječarski (p = 0.574) and the Beograd city district (p = 0.505) on the other side. Results show that Borski, Zaječarski and the Beograd city districts, belonging to critical districts, are among the leading districts for unstable angina pectoris according to incidence values.

In the case of acute myocardial infarction, the Borski district, with standardized incidence rate values of 135.964 per 100,000 inhabitants in the observed period, ranked third in incidence, after Šumadijski and Raški districts with incidence values of 146.305 and 137.084 respectively (Figure 6). There is no statistically significant difference in the incidence values for the acute myocardial infarction between Borski and some other critical districts: Šumadijski (p = 0.615), Raški (p = 0.327), Rasinski (p = 0.515), Toplički (p = 0.557), Zaječarski (p = 0.484), Pčinjski (p = 0.405), Pirotski (p = 0.420), Mačvanski (p = 0.346) and Kolubarski (p = 0.283). Still, Borski district stood out as the district with the leading high incidence for analyzed cardiovascular disease in the observed period.

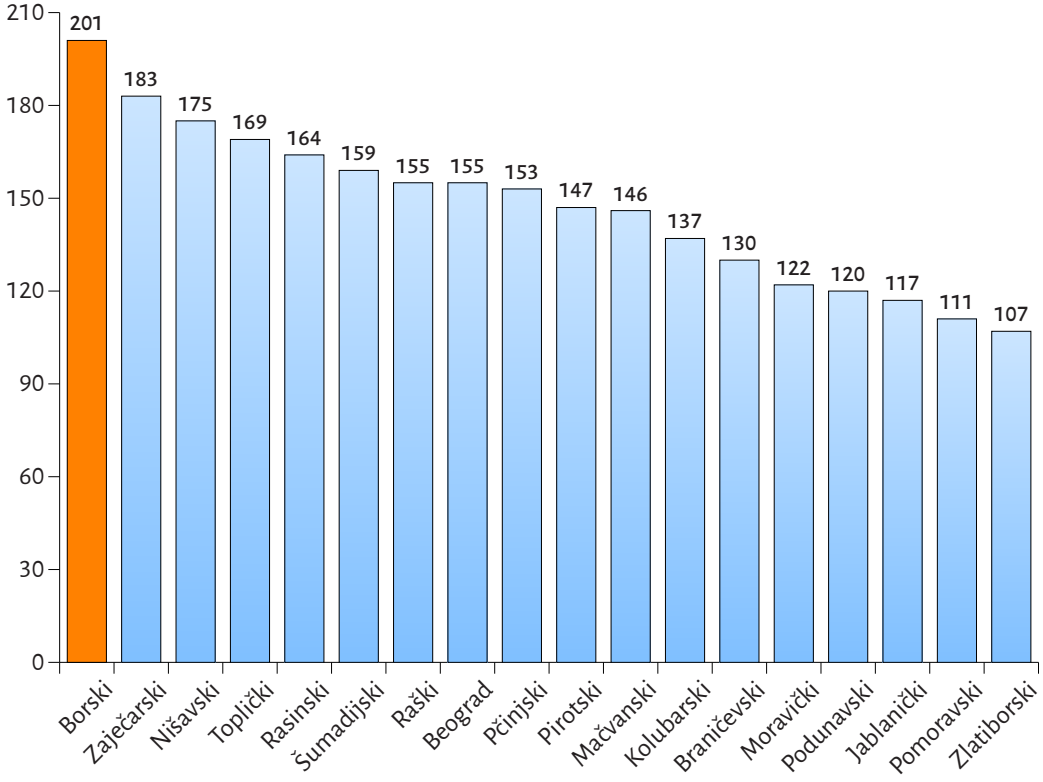

Figure 4. Standardized incidence rates (per 100,000 inhabitants) of acute coronary syndrome disease in Central Serbia for the period 2010 – 2020

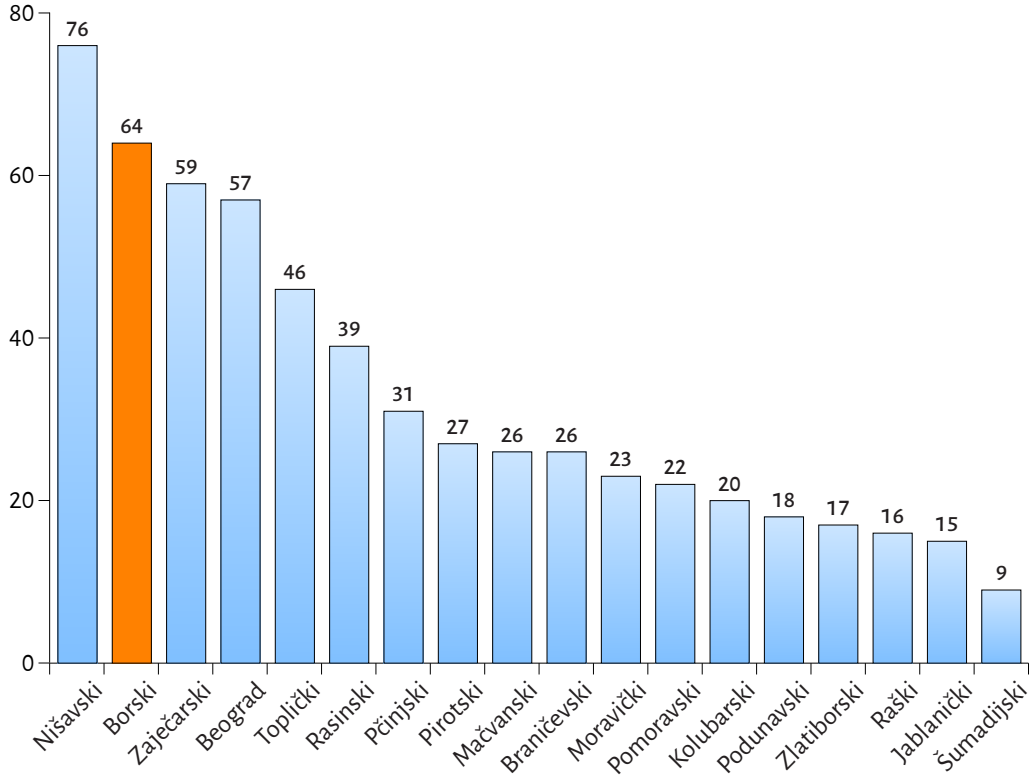

Figure 5. Standardized incidence rates (per 100,000 inhabitants) of unstable angina pectoris in Central Serbia for the period 2010 – 2020

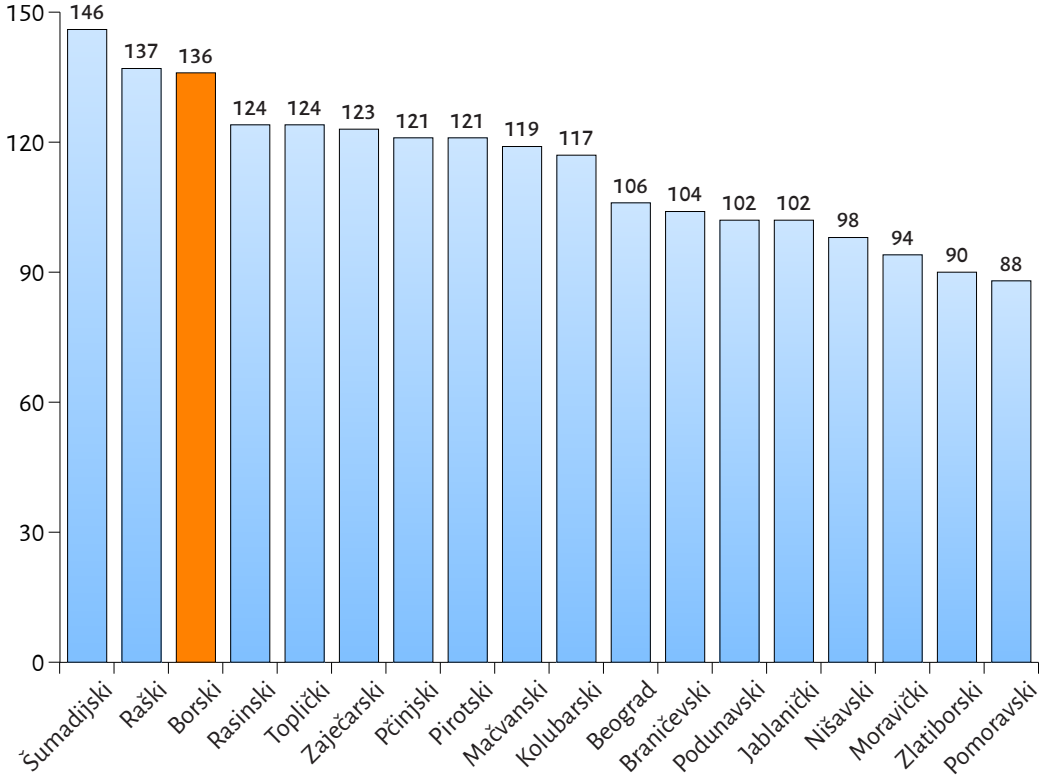

Figure 6. Standardized incidence rates (per 100,000 inhabitants) of acute myocardial infarction in Central Serbia for the period 2010 – 2020

Discussion

Mining activities as a health risk in Central Serbia

Land degradation is a world-wide problem. Serbia is under a high risk of land degradation and associated consequences, with an expected increase in the future (Pavlović et al., 2017; UNDP, 2022). The most pronounced process of soil degradation in Serbia and many other European countries is soil erosion (Pavlović et al., 2017; SEPA, 2018). Degraded soil presents a source of air pollution (Giltrap et al., 2021). Soil degradation by mining activities and tailings and waste disposals plays an important role in the generation of atmospheric dust with respect to the quantity of the particulates generated (Csavina et al., 2012). Based on the map of damaged and degraded areas in Serbia (Figure 2), districts around the main mining areas in Central Serbia could be considered as the most exposed districts suffering from PM air pollution from surface mining activities, and thus they have been regarded as critical districts in this study. Regardless of the presence of the surface mines in Vojvodina, this region was not taken into consideration in this study due to high industrialization and agricultural areas. Agricultural areas in Serbia are mostly located in Vojvodina, where more than 60% of the area is in the category of hazardous sensitivity and 36% in the category of medium sensitive to wind erosion (Baumgertel et al., 2019). Mines in Bor and Majdanpek (Figure 2, circled) are one of the main surface mining areas in Serbia. They are located in the borderline of Borski district with surrounding Zaječarski, Pomoravski and Braničevski districts. Kostolac mine (Figure 2, circuled) is located in Braničevski district, close to Podunavski district. Kolubara mine (Figure 2, circled) and 'Nikola Tesla A' and 'Nikola Tesla B' mine waste disposals (Figure 2, circled) in Beograd city district are surrounded by Mačvanski, Kolubarski, Moravički, Šumadijski and Podunavski districts. The geographical positions of the mentioned districts, in relation to mines and mine waste disposals, indicate their exposure to mine-originating PM air pollution. Therefore, the mentioned districts form a potential critical belt with the increased risk of exposure to PM air pollution from degraded mining lands and mining waste disposal sites.

Statistical analyses indicated a statistically significant association between an increased incidence of lung/bronchial cancer in the critical districts for the period 2010 - 2020 (Figure 3a). Beograd city district showed the highest incidence of lung and bronchial cancer during the observed period of 11 years compared to other districts of Central Serbia. Main mining and degraded areas impacted Beograd city district are Kolubara coal basin with total area of about 600 km^2 (Milanović et al., 2017) and thermal power plant ash disposal sites 'Nikola Tesla A' with an area of 400 ha (Gajić, 2014) and 'Nikola Tesla B' with an area of 600 ha (Nišić et al., 2015). Opencast coal mines in Serbia are mainly located in areas of fertile alluvial soils and occupy about 12,000 ha, with an expected increase of 200 ha each year (Pavlović et al., 2017). The eight thermal power plants in Serbia produce 8 Mt of ash annually (Electric Power Industry of Serbia, Technical Report 2010), while only 2.7% of the ash in Serbia is utilized for other purposes, mainly in the construction industry (Pavlović et al., 2017). Mining waste that is not subjected to further utilization is usually deposited in the open air (Pavlović et al., 2017). Large areas of deposited mining waste and opencast mines are exposed to the environmental erosive forces, e.g. wind erosion. Wind directions reported for the meteorological stations Beograd and Valjevo (Republic Hydrometeorological Service of Serbia) can contribute to the dispersion of particles from ash disposals and the Kolubara mine degraded land (Figure 7). Studies have shown increased lung cancer risk among miners with exposure to coal dust (Une et al., 1995; Hosgood et al., 2012; Tomaskova et al., 2012). Minowa et al. (1988) showed a higher lung cancer mortality in administrative units with coal mines in Japan. Fly coal ash has also been recognised as a health risk factor for lung cancer development (Whiteside & Herndon, 2018). Thus, the results of this study and current knowledge of the role of coal dust and fly ash in lung cancer development indicate that district Beograd city, where Kolubara coal mine and ash disposals ('Nikola Tesla A' and 'Nikola Tesla B') are located as, well as surrounding districts could be considered as risk areas for lung cancer development. Besides cancers, coal mine dust (Ross & Murray, 2004; Laney & Weissman, 2014) and fly ash (Shrivastava et al., 2015) are promoting other respiratory diseases in the affected areas. Tomaskova et al. (2012) showed increased lung cancer risk in coal miners with pneumoconiosis, compared to those without pneumoconiosis. This indicates a greater susceptibility to developing lung cancer in people with an already impaired immune system. Examining the health status of the population in the territory of the municipality of Lazarevac, district affected by Kolubara mining activities, Muratović (2015) pointed out the importance of air pollution of the mining areas in the development of respiratory diseases such as bronchitis, asthma and pneumonia. This study did not include the mentioned diseases due to the lack of official data. Therefore, monitoring and future research should cover a wider spectrum of respiratory diseases in relation to target districts due to the significant contribution of mine activities to air pollution.

This study showed that there is a statistically significant but marginal association between elevated incidence of cancer of the oral cavity and pharynx in the male popu-

lation and critical districts. Due to lack of data, this study did not include the female population in examining the association of cancer of the oral cavity and pharynx in the critical districts. There are studies that showed the association of pharynx cancer with exposure to coal dust (Goldberg et al., 1997; Laforest et al., 2000). Thus, the contribution of PM air pollution from mine sites in development of this cancer should not be underestimated, but deserves more attention in further research.

According to the World Health Organization, particulate air pollution is significantly associated with cardiopulmonary diseases and mortality (WHO, 2021). Cardiovascular diseases are one of the main causes of death in Serbia (Vasić et al., 2022) and world-wide (Gaziano, 2001; Gaidai et al., 2023; Samuel et al., 2023; Woodruff et al., 2024). This study showed that there is no statistically significant difference between the selected critical and non-critical districts in analyzed cardiovascular diseases. One of the reasons could be that the development of cardiovascular diseases is influenced by an array of factors (Dahlöf, 2010), and not only by air pollution originating from surface mining activities. Still, among all districts in Central Serbia, Borski district has the leading high incidence for analyzed cardiovascular disease. Most of the land degraded by surface mining in Serbia is located in Borski district and it is caused by copper mining in Majdanpek and Bor (Pavlović et al., 2017). The mining activity has degraded areas of about 1110 ha in Bor and 12,060 ha in Majdanpek which is about 60% of the total agricultural land (Pavlović et al., 2017). Wind directions measured from the meteorological station Crni Vrh (Republic Hydrometeorological Service of Serbia) in Borski district indicate possible contribution of wind to the emission of particles from mine degraded lands to neighbor and remote sites (Figure 7). Bor is one of the most air polluted regions in Serbia and beyond. Air quality monitoring for Bor showed that annual arsenic concentrations exceeded the proposed limit value at all measuring sites and annual lead and cadmium concentrations frequently exceeded the proposed limit value for the period from 2009 to 2015 (Serbula et al., 2017). Mining activities in Majdanpek also negatively impacted the environment, and consequently air quality (Ilić Krstić et al., 2020). Study conducted by Nkosi et al. (2016) showed that elderly people exposed to pollution arising from mine dumps in South Africa had a significantly higher prevalence of cardiovascular and respiratory diseases and that living close to mine dumps was significantly associated with asthma, hypertension, pneumonia, emphysema, arrhythmia, and myocardial infarction. Higher mortality rates from chronic cardiovascular disease compared to non-mining areas have also been observed in mining areas of Central Appalachian States (Esch & Hendryx, 2011). Based on the known negative impact of air pollution from mining areas on the cardiovascular system (e.g. Esch & Hendryx, 2011; Nkosi et al., 2016.) and results of this study, mining activities and consequent heavy metal pollution should be considered as important risk factors for development of cardiovascular diseases.

Despite the existence of the Kostolac mine in Braničevski district, the low incidence of analyzed diseases can be

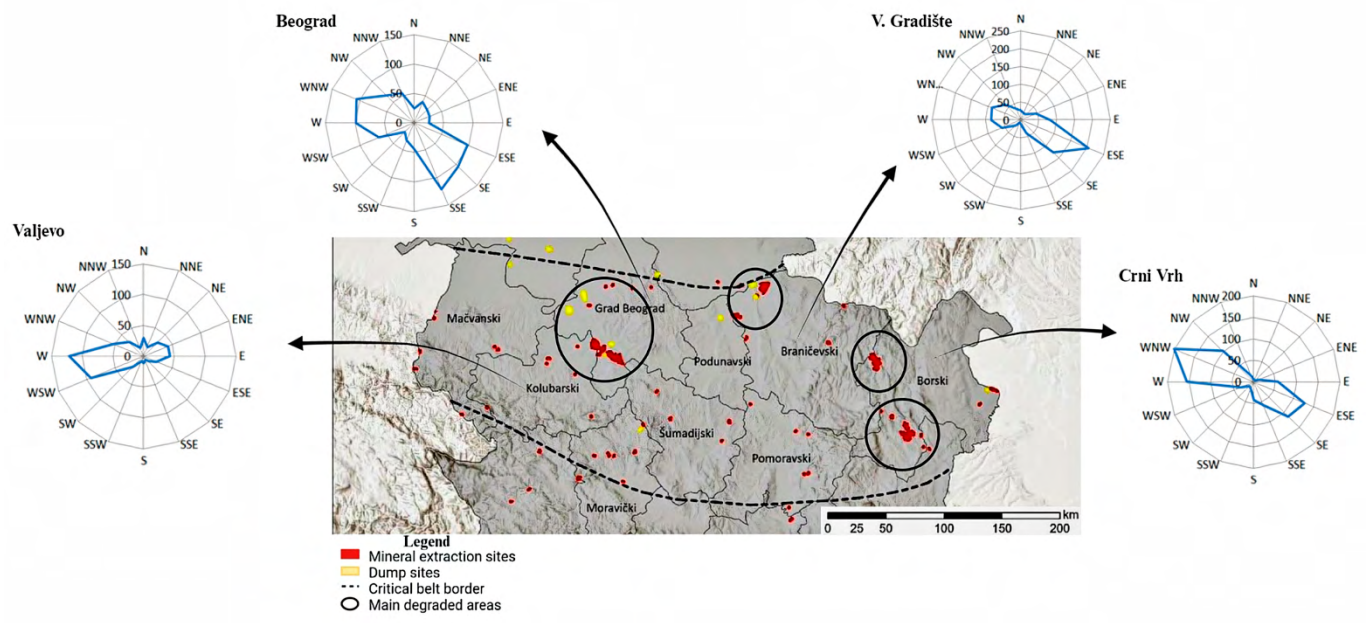

Figure 7. Representative relative frequencies of wind directions in per mille (1981 - 2010) for critical belt: Borski district (meteorological station Crni Vrh), Braničevski district (meteorological station V. Gradište), Begrad city district (meteorological station Beograd) and Kolubara district (meteorological station Valjevo) (based on Corine Land Cover 2018) (V2020_20u1), European Environment Agency (EEA), (Republic Hydrometeorological Service of Serbia)

due to its position in the border zone and the dominant east-southeast wind (ESE wind, Veliko Gradište meteorological station) (Republic Hydrometeorological Service of Serbia) (Figure 7).

Mining activities such as excavation, crushing, grinding, separation, smelting, refining, and tailings are important sources of contaminated dust that can be wind-transported to neighbour places (Serbula et al., 2010; Csavina et al., 2012; Zanetta-Colombo et al., 2022). Local copper mining activities in northern Chile are connected to the increased metal concentrations in dust collected from roofs and windows of indigenous villages (Zanetta-Colombo et al., 2022). However, in Serbia there is an insufficient monitoring of particle pollution (Matić Savićević & Stojanović, 2019), even though air pollution harms the economy of the country through lower labour output (World Bank, 2016), increased health expenses, damage to crops and infrastructure, and costs related to climate change and environmental protection (WHO, 2021). Total treatment costs in 2017 were 30% higher compared to 2010, and amounted to circa €1.7 billion and €1.4 billion, respectively. The modern way of living is considered to have a huge impact on the increase in the cost of treating cardiovascular diseases. According to the WHO, particulate air pollution is significantly associated with cardiopulmonary diseases and mortality, and other health conditions (WHO, 2021).In studies from other countries (Minowa et al., 1988; Une et al., 1995; Goldberg et al., 1997; Laforest et al., 2000; Ross & Murray, 2004; Esch & Hendryx, 2011; Hosgood et al., 2012; Tomaskova et al, 2012; Laney & Weissman, 2014; Shrivastava et al., 2015; Nkosi et al., 2016; Whiteside & Herndon, 2018) and this study from the Republic of Serbia indicate the role of the particulate air pollution from the mine industry in health deterioration. Thus, intensified monitoring of PM air pollution originating from mining activities, assessment of their influence on the health and combating particulate air pollution is of environmental, health, economic and social importance in Serbia and world-wide.

Proposed measures for restoration of degraded and disturbed mining areas to combat particulate air pollution

Even though there have been made certain efforts towards improving restoration practice in Serbia, restoration activities in Serbian mining basins are considered poorly applied in practice (Ranđelović et al., 2017). Natural recovery of the vegetation cover could take a long time and the success of land restoration by higher plants in these environments could be limited. The process of natural recovery of satisfactory vegetation cover on mine wastes could last from 50 to 100 years (Bradshaw, 1997). Restoration of the mine tailings and waste deposits by recultivating higher plants is limited because of adverse environmental factors present in these environments, such as water and nutrient deficiency, high temperatures, adverse chemical properties of the substrates (Pavlović & Mitrović, 2013; Pavlović et al., 2017; Li & Liber, 2018). Li & Liber (2018) study showed that low levels of soil moisture and available nitrogen were the major limiting factors affecting plant community development on the coal gob pile, not metal toxicity.

Dominant biological cover in the environments where development of higher vegetation is hindered is represented by biological soil crusts (biocrusts) (Veste, 2005). Biocrusts are bio-sedimentary complexes of organisms (cyanobacteria, mosses, lichens, fungi and bacteria) and soil particles (Eldridge & Green, 1994; Williams et al., 2012). This community is highly tolerant to desiccation and long-term drought (Veste, 2005). Biocrust characterizes successional development that begins with cyanobacterial colonization of the soil (Lan et al., 2012; Williams et al., 2012). Several cyanobacteria genera are nitrogen fixers within biocrusts (Belnap & Lange, 2003). They produce protective layers of exopolysaccharides that have multiple roles in the biocrust community such as binding the soil particles, retaining water and nutrients (Colica et al., 2014; Rossi & De Philippi, 2015; Mugnai et al., 2017). Cyanobacteria and their exopolysaccharides form a complex protective network with incorporated soil particles over the soil surface (Dulić et al., 2017; Palanački Malešević et al., 2021). They trap (Malam Issa et al., 2001; Williams et al., 2012; Svirčev et al., 2013; 2019; Dulić et al., 2017; Palanački Malešević et al., 2021), metabolize and stabilize the airborne particles (Dulić et al., 2017; Palanački Malešević et al., 2021; Svirčev et al., 2013; 2019). Accordingly, colonization of the surface of the substrate by biocrusts provides essential ecosystem functions. They control water and nutrient availability and soil stability in the environment (Chamizo et al., 2016; 2018; Palanački Malešević et al., 2021).

Artificially induced biocrusts have been proposed to fight land degradation in adverse environmental conditions, and cyanobacterial inoculation have been introduced as a potential solution (e.g. Wang et al., 2009; Rossi et al., 2017; Chamizo et al., 2018; Antoninka et al., 2020; Rossi, 2020). Some of the latest studies employing cyanobacteria for the restoration of degraded land and the mitigation of adverse environmental conditions are reviewed in the study by Palanački Malešević et al. (2024). The importance of biocrusts and cyanobacteria in the land restoration after soil disturbance induced by mining has been recognized (Doudle & Williams, 2010; Doudle et al., 2011; Williams et al., 2019). Cyanobacterial inoculation induces biocrusts development on mine tailings, which further mitigates wind erosion and enhances tailing fertility enabling establishment of vegetation cover (Rezasoltani et al., 2023). However, biocrusts development in the field conditions can be hindered by adverse environmental factors. Water is a primary factor affecting biocrust growth (Bu et

al., 2014) and drought is common in most mine environments (Zhu et al., 2022). Dew enables physiological activity of cyanobacteria and maintenance of biocrust biomass, but for biocrust biomass growth a higher amount of water than dew is needed (Rao et al., 2009). Since the restoration process could take a long time due to the lack of moisture during the initial phase of biocrust development, it is necessary to find strategies for acceleration of the biocrusts establishment and further growth. Assisted development of artificially induced biocrusts through mitigation of key limiting factors could provide promotion of inoculum viability and growth rate. Biocrust carpet engineering could enable quick, sustainable and environmentally friendly solutions to mining land restoration.

The role of biocrust carpet engineering, through assisted development of artificially induced biocrusts, in the restoration of mine tailings and waste deposits of mining to control air pollution should not be neglected. To provide a quick, sustainable, and environmentally friendly solution, some requirements must be met:

- Providing ***interaction of dust particles with cyanobacteria*** would lead to particle capture into the sticky cyanobacterial biofilm and their further entrapment in this community during dry and wet environmental conditions (Svirčev et al., 2013; 2019; Palanački Malešević et al., 2021). Inoculation of cyanobacterial biomass in the affected environments would promote this interaction.
- Providing an ***extended wet period*** would enable longer metabolic activity of cyanobacteria and thus active collection of air particles by sticky biofilm. During wet environmental conditions, metabolically active cyanobacteria trap, metabolize and deposit airborne particles as part of their life strategy in providing minerals for biocrusts growth (Williams et al., 2012; Svirčev et al., 2013; 2019). Polysaccharide support to cyanobacterial inoculum could improve water availability, provide extended wet period, and promote cyanobacterial metabolic activity and biocrusts growth. There are studies that indicate the potential of superabsorbent polymer (Park et al., 2014) and nanocomposite (Chi et al., 2020; Li et al., 2021) as soil fixing and water retention agents in promoting biocrust growth.

Attention should be paid to the technical feasibility of the polysaccharide-supported inoculation of cyanobacteria in the field. A physical support to the polysaccharide-cyanobacterial carpet should be engineered to enable easier carpet applicability at the field. This polysaccharide-cyanobacterial carpet with physical support creates microenvironmental conditions for the accelerated initiation and growth of biocrusts. This technology could be called the Pan-Life-Carpet (PLC) concept, i.e. a carpet for the initiation of life on mining and other degraded land areas.

Degraded land is a source for dust emission and precondition for sediment erosion. Such land directly causes air pollution by dust emission to the atmosphere and water pollution by soil and sediment erosion to neighboring water bodies (Figure 8a). Airborne particles from polluted air are carried by the wind to distant regions and very often end up in water ecosystems. In this way, water bodies are also indirectly polluted by airborne particles from polluted air. Therefore, there is a need for sustainable solutions to the problems of land degradation and consequent air and water pollution in such challenging environments. Cyanobacteria and their sticky exopolysaccharides, that are part of PLC technology, are known to capture, accumulate and stabilize airborne particles (Svirčev et al., 2013; 2019; Palanački Malešević et al., 2021). Implemented PLC technology and consequent accelerated biocrust development stabilize soil surface, prevent dust emission and sediment erosion, providing land restoration and prevention of air and water pollution, respectively (Figure 8b). The sticky structure of PLC provided by cyanobacterial exopolysaccharide

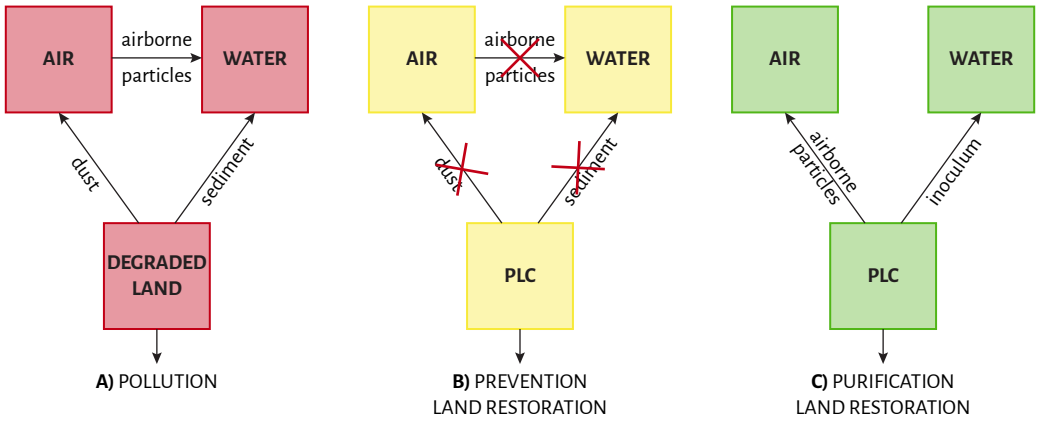

Figure 8. The role of Pan-Life-Carpet (PLC) in land restoration, prevention of air and water pollution as well as air and water purification (made with https://www.biorender.com/)

captures airborne particles from polluted air, decreases their concentration in the air and thus provides air purification (Figure 8c). Cyanobacterial biomass from polluted water bodies can be taken away from water ecosystems and used as inoculum for PLC development, which further contributes to water purification (Figure 8c).

The PLC technology thus exhibits a double impact on air quality: 1) by stabilizing substrate surfaces it prevents dust particle emission to the atmosphere and thus prevents air pollution (Figure 8b); 2) by capturing and further stabilizing airborne particles it purifies already polluted air (Figure 8c). The PLC technology exhibits similar benefits for the water ecosystems: 1) by preventing air pollution and purifying air it prevents indirect pollution of water ecosystems Figure 8b; 2) the use of cyanobacterial biomass from eutrophic lakes for PLC preparation purifies water ecosystems, as well (Figure 8c). Thus, biocrust carpet engineering, i.e. the PLC concept, by providing land restoration, air and water pollution prevention as well as air and water purification addresses global environmental problems of land degradation and air and water pollution.

Conclusion

The present study addressed the health risk assessment in districts of Central Serbia due to exposure to PM pollution originating from degraded mining areas. Epidemiological estimation was based on the incidence of seven types of cancers and three types of cardiovascular diseases in 18 districts of Central Serbia for the period 2010 – 2020. Locations of surface mines, mine disposals and ash disposal sites, as well as frequencies of wind directions, were also observed.

The obtained results showed a statistically significant increase in lung and bronchial cancer incidence in critical districts affected by soil degradation and dust pollution from main mining sites compared to non-critical districts. Among them, Beograd city had the highest incidence due to the proximity and wind impact from thermal power plant ash disposal sites 'Nikola Tesla A', 'Nikola Tesla B', and Kolubara coal basin. Based on the incidence values, the Borski district, where most of the land was degraded by copper mining (Bor and Majdanpek), stood out among the top three districts for examined diseases.

According to the results of the study, intensified monitoring of air pollution originating from mining areas, as well as mitigation technology for restoration of such degraded land, are necessary. Pan-Life-Carpet technology based on artificially induced biocrusts, with the dominance of cyanobacteria, has been proposed as a potential quick, sustainable, and environmentally friendly solution for mining land restoration and air and water pollution control. The PLC concept is becoming ready for field testing and expected to facilitate processing of degraded land surfaces.

Funding

This research was supported by the Science Fund of the Republic of Serbia, [#7726976], Integrated Strategy for Rehabilitation of Disturbed Land Surfaces and Control of Air Pollution–RECAP. The authors gratefully acknowledge the financial support of the Ministry of Science, Technological Development and Innovation of the Republic of Serbia [Grants No. 451-03-66/2024-03/ 200125 & 451-03-65/2024-03/200125]. We gratefully acknowledge Kone Foundation for funding the BIONEER project [Grant No. 202205754].

References

Antoninka, A., Faist, A., Rodríguez-Caballero, E., Young, K. E., Chaudhary, V. B., Condon, L. A., & Pyke, D. A. (2020). Biological soil crusts in ecological restoration: emerging research and perspectives. *Restoration Ecology*, 28(S2), 3-8. https://doi.org/10.1111/rec.13201

Batut (2023). Institute of Public Health of Serbia 'Dr Milan Jovanović Batut' https://www.batut.org.rs/index.php?content=186 (04.10.2023).

Batut (2023b). Institute of Public Health of Serbia 'Dr Milan Jovanović Batut' https://www.batut.org.rs/index.php?content=1413 (10.10.2023).

Batut (2023c). Internet 3: Institute of Public Health of Serbia 'Dr Milan Jovanović Batut' https://www.batut.org.rs/index.php?category_id=109 (23.10.2023).

Baumgertel, A., Lukić, S., Belanović Simić, S., & Kadović, R. (2019). Identifying Areas Sensitive to Wind Erosion—A Case Study of the AP Vojvodina (Serbia). *Applied Sciences*, 9(23), 5106. 10.3390/app9235106

Belnap, J., & Lange, L.O. (2003). Biological soil crusts: Structure, function, and management. In *Ecological studies*. 10.1007/978-3-642-56475-8

BioRender. (2024). https://www.biorender.com/ (01.02.2024).

Bradshaw, A. (1997). Restoration of mined lands—using natural processes. *Ecological Engineering*, 8(4), 255 – 269. https://doi.org/10.1016/s0925-8574(97)00022-0

Brown, J. S., Zeman, K. L., & Bennett, W. D. (2002). Ultrafine particle deposition and clearance in the healthy and obstructed lung. *American Journal of Respiratory and Critical Care Medicine*, 166(9), 1240 – 1247. 10.1164/rccm.200205-399oc

Bu, C., Wu, S., Yang, Y., & Zheng, M. (2014). Identification of factors influencing the restoration of Cyanobacteria - Dominated biological soil crusts. *PloS One*, 9(3), e90049. https://doi.org/10.1371/journal.pone.0090049

Bui, X. N., Lee, C. W., Nguyen, H., Bui, H., Long, N. Q., Le, Q., . . . Moayedi, H. (2019). Estimating PM10 Concentration from Drilling Operations in Open-Pit Mines Using an Assembly of SVR and PSO. *Applied Sciences (Basel)*, 9(14), 2806. 10.3390/app9142806

Chamizo, S., Cantón, Y., Rodríguez-Caballero, E., & Domingo, F. (2016). Biocrusts positively affect the soil water balance in semiarid ecosystems. *Ecohydrology*, 9(7), 1208 - 1221. 10.1002/eco.1719

Chamizo, S., Mugnai, G., Rossi, F., Certini, G., & De Philippis, R. (2018). Cyanobacteria inoculation improves soil stability and fertility on different textured soils: gaining insights for applicability in soil restoration. *Frontiers in Environmental Science*, 6. https://doi.org/10.3389/fenvs.2018.00049

Chi, Y., Li, Z., Zhang, G., Zhao, L., Gao, Y., Wang, D., Wu, Z. (2020). Inhibiting desertification using aquatic cyanobacteria assisted by a nanocomposite. *ACS Sustainable Chemistry & Engineering*, 8(8), 3477 – 3486. https://doi.org/10.1021/acssuschemeng.0c00233

Colica, G., Li, H., Rossi, F., Li, D., Liu, Y., & De Philippis, R. (2014). Microbial secreted exopolysaccharides affect the hydrological behavior of induced biological soil crusts in desert sandy soils. *Soil Biology & Biochemistry*, 68, 62 – 70. 10.1016/j.soilbio.2013.09.017

Csavina, J., Field, J. A., Taylor, M. P., Gao, S., Landázuri, A. C., Betterton, E. A., & Sáez, A. E. (2012). A review on the importance of metals and metalloids in atmospheric dust and aerosol from mining operations. *Science of the Total Environment*, 433, 58 – 73. 10.1016/j.scitotenv.2012.06.013

Da Silva Rêgo, L. L., De Almeida, L. A., & Gasparotto, J. (2022). Toxicological effects of mining hazard elements. *Energy Geoscience*, 3(3), 255 – 262. 10.1016/j.engeos.2022.03.003

Dahlöf, B. (2010). Cardiovascular disease risk factors: Epidemiology and risk assessment. *The American Journal of Cardiology*, 105(1), 3A - 9A. https://doi.org/10.1016/j.amjcard.2009.10.007

Doudle, S., & Williams, W. (2010). Can we kick-start mining rehabilitation with cyanobacterial crusts?. In D.J. Eldridge, & C. Waters (Eds), *Proceedings of the 16th Biennial conference of the Australian rangeland society.* Bourke: Australian Rangeland Society, Perth.

Doudle, S., Williams, W. & Galea, V. (2011). Improving rehabilitation outcomes using biocrusts. *Eight International Heavy Minerals Conference* 2011 (pp.85-97), Perth, WA, Australia, 5-6 October 2011. Carlton South, VIC, Australia: Australasian Institute for Mining and Metallurgy (AusIMM).

Dulić, T., Meriluoto, J., Palanački Malešević, T., Gajić, V., Važić, T., Tokodi, N., . . . Svirčev, Z. (2017). Cyanobacterial diversity and toxicity of biocrusts from the Caspian Lowland loess deposits, North Iran. *Quaternary International*, 429, 74 – 85. https://doi.org/10.1016/j.quaint.2016.02.046

Eldridge, D.J., & Greene, R.S. (1994). Microbiotic soil crusts: A review of their roles in soil and ecological processes in the rangelands of Australia. *Australian Journal of Soil Research*, 32(3), 389 – 415. 10.1071/SR9940389

Electric Power Industry of Serbia - EPS. (2010). Technical Report. https://www.eps.rs/eng/Documents/yearreports/EPS%20Annual%20report%202010.pdf (23.09.2024).

Esch, L., & Hendryx, M. (2011). Chronic cardiovascular disease mortality in mountaintop mining areas of central Appalachian states. *The Journal of Rural Health*, 27(4), 350 – 357. https://doi.org/10.1111/j.1748-0361.2011.00361.x

European Environment Agency - EEA. (2018). Corine Land Cover V2020_20u1.

Franck, U., Odeh, S., Wiedensohler, A., Wehner, B., & Herbarth, O. (2011). The effect of particle size on cardiovascular disorders - The smaller the worse. *Science of the Total Environment*, 409(20), 4217 – 4221. 10.1016/j.scitotenv.2011.05.049

Gaidai, O., Cao, Y., and Laginov, S. (2023). Global Cardiovascular Diseases Death Rate Prediction. *Current Problems in Cardiology*, 48(5), 101622. https://doi.org/10.1016/j.cpcardiol.2023.101622

Gajić, G., (2014). *Ekofiziološke adaptacije odabranih vrsta zeljastih biljaka na deponiji pepela termoelektrane 'Nikola Tesla A' u Obrenovcu*. (Ecophysiological adaptations of selected species of herbaceous plants at the ash dump of the thermal power plant 'Nikola Tesla A' in Obrenovac) Belgrade: University of Belgrade.

Gaziano, J.M. (2001) Global burden of cardiovascular disease. In R. Zorab. (Ed.), Heart Disease. *A textbook of cardiovascular medicine* (pp. 1 - 18). Philadelphia: W.B. Saunders Company.

Giltrap, D., Cavanagh, J., Stevenson, B., & Ausseil, A. (2021). The role of soils in the regulation of air quality. *Philosophical Transactions of the Royal Society B*, 376(1834), 20200172. 10.1098/rstb.2020.0172

Goldberg, P., Leclerc, A., Luce, D., Morcet, J-F., & Brugère, J. (1997). Laryngeal and hypopharyngeal cancer and occupation: results of a case control-study. *Occupational*

and Environmental Medicine, 54(7), 477 – 482. https://doi.org/10.1136/oem.54.7.477

Goudie, A.S. (2014). Desert dust and human health disorders. *Environment International*, 63, 101 – 113. https://doi.org/10.1016/j.envint.2013.10.011

Hosgood, H. D., Chapman, R. S., Wei, H., He, X., Tian, L., Liu, L. Z., ... Lan, Q. (2012). Coal mining is associated with lung cancer risk in Xuanwei, China. *American Journal of Industrial Medicine*, 55(1), 5 – 10. 10.1002/ajim.21014

Ilić Krstić, I., Malenović Nikolić, J., & Janaćković, G. (2020). Ecological security in Majdanpek mining area – a case study. *Facta Universitatis*, 17(1), 65 - 74. https://doi.org/10.22190/fuwlep2001065i

International Agency for Research on Cancer (IARC) (2016). Outdoor Air Pollution: IARC Monographs on the Evaluation of Carcinogenic Risks to Humans. Vol. 109. Lyon, France: IARC.

International Commission on Radiological Protection - ICRP. (1995). *Human Respiratory Tract Model for Radiological Protection*. Elsevier Health Sciences, 66.

Internet 1. International Statistical Classification of Diseases and Related Health Problems https://icd.who.int/browse10/2019/en#/C06.9 (25.09.2023).

The Intergovernmental Science-Policy Platform on Biodiversity and Ecosystem Services (IPBES) (2018). Summary for policymakers of the assessment report on land degradation and restoration of the Intergovernmental Science-Policy Platform on Biodiversity and Ecosystem Services. In R. Scholes, L. Montanarella, A. Brainich, N. Barger, B. ten Brink, & M. Cantele... (eds). IPBES secretariat: Bonn, Germany.

Jiang, C., Zhang, H., Wang, X., Yu, F., & Labzovskii, L. (2019). Challenging the land degradation in China's Loess Plateau: Benefits, limitations, sustainability, and adaptive strategies of soil and water conservation. *Ecological Engineering*, 127, 135 – 150. 10.1016/j.ecoleng.2018.11.018

Katra, I. (2020). Soil erosion by wind and dust emission in Semi-Arid soils due to agricultural activities. *Agronomy (Basel)*, 10(1), 89. https://doi.org/10.3390/agronomy10010089

Kelly, F. J., & Fussell, J. C. (2015). Air pollution and public health: emerging hazards and improved understanding of risk. *Environmental Geochemistry and Health*, 37(4), 631 – 649. 10.1007/s10653-015-9720-1

Knežević, J., Jović, B., Marić Tanasković, L., Mitrović-Josipović, M., Ljubičić, A., Stamenković, D., Dimić, B. (2021). *Annual report on the state of air quality in the Republic of Serbia in 2020.* Serbian Ministry of Environmental Protection.

Kumar Patra, A., Gautam, S., & Kumar, P. (2016). Emissions and human health impact of particulate matter from surface mining operation - A review. *Environmental Technology and Innovation*, 5, 233 – 249. 10.1016/j.eti.2016.04.002

Laforest, L., Luce, D., Goldberg, P., Bégin, D., Gérin, M., Demers, P.A., Brugère, J., Leclerc, A. (2000). Laryngeal and hypopharyngeal cancers and occupational exposure to formaldehyde and various dusts: a case-control study in France. *Occupational and Environmental Medicine*, 57(11), 767 – 773. 10.1136/oem.57.11.767

Lan, S., Wu, L., Zhang, D., & Hu, C. (2012). Successional stages of biological soil crusts and their microstructure variability in Shapotou region (China). *Environmental Earth Sciences*, 65(1), 77 – 88. https://doi.org/10.1007/s12665-011-1066-0

Laney, A.S., & Weissman D.N. (2014). Respiratory Diseases Caused by Coal Mine Dust. *Journal of Occupational and Environmental Medicine*, 56(0 10), S18 - S22. 10.1097/JOM.0000000000000260.

Li, S., & Liber, K. (2018). Influence of different revegetation choices on plant community and soil development nine years after initial planting on a reclaimed coal gob pile in the Shanxi mining area, China. *Science of the Total Environment*, 618, 1314 – 1323. 10.1016/j.scitotenv.2017.09.252

Li, Z., Chen, C., Gao, Y., Wang, B., Wang, D., Du, Y., . . . Cai, D. (2021). Synergistic effect of cyanobacteria and nano-sand-stabilizer on biocrust formation and sand fixation. *Journal of Environmental Chemical Engineering*, 9(1), 104887. https://doi.org/10.1016/j.jece.2020.104887

Ličina, V., Nešić, Lj., Belić, M., Hadžić, V., Sekulić, P., Vasin, J., & Ninkov, J. (2011). The soils of Serbia and their degradation. *Ratarstvo i Povrtarstvo*, 48(2), 285–290.

Loomis, D., Grosse, Y., Lauby-Secretan, B., El Ghissassi, F., Bouvard, V., Benbrahim-Tallaa, L., ... Straif, K. (2013). The carcinogenicity of outdoor air pollution. *The Lancet Oncology*, 14(13), 1262 – 1263. 10.1016/s1470-2045(13)70487-x

Malam Issa, O., Le Bissonnais, Y., Défarge, C., & Trichet, J. (2001). Role of a cyanobacterial cover on structural stability of sandy soils in the Sahelian part of western Niger. *Geoderma*, 101(3–4), 15 – 30. https://doi.org/10.1016/s0016-7061(00)00093-8

Manisalidis, I., Stavropoulou, E., Stavropoulos, A., & Bezirtzoglou, E. (2020). Environmental and Health Impacts of Air Pollution: A review. *Frontiers in Public Health*, 8. 10.3389/fpubh.2020.00014

Matić Savićević B. & Stojanović M. (2019). *Zagađenost urbanog vazduha na teritoriji Republike Srbije merena u mreži institucija javnog zdravlja u 2018. godini* [Urban air pollution in the territory of the Republic of Serbia measured in the network of public health institutions in 2018]. Beograd: Institut za javno zdravlje Srbije 'Dr Milan Jovanović Batut'.

Matić Savićević, B. (2020). *Zagađenost urbanog vazduha na teritoriji Republike Srbije merena u mreži institucija javnog zdravlja u 2020. godini* [Urban air pollution in the territory of the Republic of Serbia measured in the network of

public health institutions in 2020]. Beograd: Institut za javno zdravlje Srbije 'Dr Milan Jovanović Batut'.

Milanović, M., Tomić, M., Perović, V., Radovanović, M., Mukherjee, S., Jakšić, D., Petrović, M., & Radovanović, A. (2017). Land degradation analysis of mine-impacted zone of Kolubara in Serbia. *Environmental Earth Sciences*, 76(16). 10.1007/s12665-017-6896-y

Minowa, M., Stone, B.J., & Blot, W.J. (1988) Geographic pattern of lung cancer in Japan and its environemtal correlation. *Japanese Journal of Cancer Research*, 79, 1017 - 1023.

Mugnai, G., Rossi, F., Felde, V. J.M.N.L., Colesie, C., Büdel, B., Peth, S., . . . De Philippis, R. (2017). Development of the polysaccharidic matrix in biocrusts induced by a cyanobacterium inoculated in sand microcosms. *Biology and Fertility of Soils*, 54(1), 27 – 40. https://doi.org/10.1007/s00374-017-1234-9

Muratović, E. (2015). Životna sredina, zdravstveno stanje stanovništva i teritorijalni razvoj opštine Lazarevac [Environment, population health and teritorial development of the Lazarevac muncipality]. In: *Zbornik radova mladih istraživača, Planska i normativna zaštita prostora i životne sredine*. Palić-Subotica.

Nišić, D. D., Knežević, D.N. & Pantelić, U.R., (2015). Klasifikacija deponije pepela Termoelektrane 'Nikola Tesla B' po stepenu rizičnosti. *Tehnika*, 70(5), 769 - 776. 10.5937/tehnika1505769N

Nkosi, V., Wichmann, J., & Voyi, K. (2016). Comorbidity of respiratory and cardiovascular diseases among the elderly residing close to mine dumps in South Africa: A cross-sectional study. *South African Medical Journal*, 106(3), 290 - 297. https://doi.org/10.7196/samj.2016.v106i3.10243

Orellano, P., Reynoso, J., Quaranta ,N., Bardach, A., & Ciapponi, A. (2020). Short-term exposure to particulate matter (PM10 and PM2.5), nitrogen dioxide (NO2), and ozone (O3) and all-cause and cause-specific mortality: Systematic review and meta-analysis. *Environment International*, 142, 105876. 10.1016/j.envint.2020.105876

Padró, J. C., Cardozo, J., Montero, P., Ruiz-Carulla, R., Alcañiz, J. M., Serra, D., & Carabassa, V. (2022). Drone-Based identification of erosive processes in Open-Pit mining restored areas. *Land*, 11(2), 212. https://doi.org/10.3390/land11020212

Palanački Malešević, T., Dulić, T., Obreht, I., Trivunović, Z., Marković, R., Kostić, B., . . . Svirčev, Z. (2021). Cyanobacterial Potential for Restoration of Loess Surfaces through Artificially Induced Biocrusts. *Applied Sciences (Basel)*, 11(1), 66. https://doi.org/10.3390/app11010066

Palanački Malešević, T., Meriluoto, J., Mihalj, I., Važić, T., Marković, R., Jurca, T., Codd, G.A., Svirčev, Z. (2024). Restoration of damaged drylands through acceleration of biocrust development. *CATENA*, 244, 108265. https://doi.org/10.1016/j.catena.2024.108265

Park, C. H., Li, X., Jia, R.L., & Hur, J. S. (2014). Effects of superabsorbent polymer on cyanobacterial biological soil crust formation in laboratory. *Arid Land Research and Management*, 29(1), 55 – 71. https://doi.org/10.1080/15324982.2014.928835

Pavlović, P., & Mitrović, M, (2013). Thermal power plants in Serbia—the impact of ash on soil and plants. In: Anđelković, M. (ed) *Energy and the environment, scientific meetings, Book 4.* Serbian Academy of Sciences and Arts (SANU), Belgrade, pp 429 – 433 (in Serbian).

Pavlović, P., Kostić, N., Karadžić, B., & Mitrović, M. (2017). The soils of Serbia. In *World soils book series*. 10.1007/978-94-017-8660-7

Perović, V., Kadović, R., Djurdjević, V., Pavlović, D., Pavlović, M., Čakmak, D., … Pavlović, P. (2021). Major drivers of land degradation risk in Western Serbia: Current trends and future scenarios. *Ecological Indicators*, 123, 107377. 10.1016/j.ecolind.2021.107377

Popović, V., Živanović Miljković, J., Subić, J., Jean-Vasile, A., Nedelcu, A., & Nicolăescu, E. (2015). Sustainable land management in mining areas in Serbia and Romania. *Sustainability (Basel)*, 7(9), 11857 – 11877. https://doi.org/10.3390/su70911857

Ranđelović, D. (2017). Reclamation methods and their outcomes in Serbian mining basins. *2nd International and 14th National Congress of Soil Science Society of Serbia-Solutions and Projections for Sustainable Soil Managemen*t.25-28th September 2017, (pp. 40-48). Novi Sad, Serbia.

Rao, B., Liu, Y., Wang, W., Hu, C., Li, D., & Lan, S. (2009). Influence of dew on biomass and photosystem II activity of cyanobacterial crusts in the Hopq Desert, northwest China. *Soil Biology & Biochemistry*, 41(12), 2387 – 2393. https://doi.org/10.1016/j.soilbio.2009.06.005

Rezasoltani, S., Champagne, P., & Mann, V. (2023). Improvement in mine tailings biophysicochemical properties by means of cyanobacterial inoculation. *Waste and Biomass Valorization*, 15, 1689-1699. https://doi.org/10.1007/s12649-023-02195-4

Ross, M. H., & Murray, J. (2004). Occupational respiratory disease in mining. *Occupational Medicine*, 54(5), 304 – 310. https://doi.org/10.1093/occmed/kqh073

Rossi, F. (2020). Beneficial biofilms for land rehabilitation and fertilization. *FEMS Microbiology Letters*, 367(21). https://doi.org/10.1093/femsle/fnaa184

Rossi, F., & De Philippis, R. (2015). Role of cyanobacterial exopolysaccharides in phototrophic biofilms and in complex microbial mats. *Life*, 5(2), 1218 – 1238. https://doi.org/10.3390/life5021218

Rossi, F., Li, H., Liu, Y., & De Philippis, R. (2017). Cyanobacterial inoculation (cyanobacterisation): Perspectives for the development of a standardized multifunctional technology for soil fertilization and desertification reversal. *Earth-Science Reviews*, 171, 28 –43. https://doi.org/10.1016/j.earscirev.2017.05.006

Sacks, J. D., Stanek, L.W., Luben, T.J., Johns, D.O., Buckley, B.J., Brown, J.S., & Ross, M. (2011). Particulate Matter–Induced health effects: Who is susceptible? *Environmental Health Perspectives*, 119(4), 446 – 454. 10.1289/ehp.1002255

Samuel, P.O., Edo, G.I., Emakpor, O.L., Oloni, G.O., Ezekiel, G.O., Essaghah, A.E.A., Endurance Agoh, E., Agbo, J.J. (2023). Lifestyle modifcations for preventing and managing cardiovascular diseases. *Sport Sciences for Health*, 20, 23-36. https://doi.org/10.1007/s11332-023-01118-z

Sankaran, G., Tan, S.T., Yap, R., Chua, M.L., Ng, L.C., & George, S. (2023). Characterization of size-differentiated airborne particulate matter collected from indoor environments of childcare facilities. *Chemosphere*, 340, 139670. 10.1016/j.chemosphere.2023.139670

Serbian Environmental Protection Agency - SEPA. (2018). Report on soil conditions in the Republic of Serbia. Ministry of Environmental Protection, Belgrade.

Serbula, S. M., Antonijević, M. M., Milošević, N., Milić, S., & Ilic, A. A. (2010). Concentrations of particulate matter and arsenic in Bor (Serbia). *Journal of Hazardous Materials (Print)*, 181(1 – 3), 43 – 51. https://doi.org/10.1016/j.jhazmat.2010.04.065

Serbula, S. M., Milosavljević, J., Radojević, A. A., Kalinović, J. V., & Kalinović, T. S. (2017). Extreme air pollution with contaminants originating from the mining–metallurgical processes. *Science of the Total Environment*, 586, 1066 – 1075. https://doi.org/10.1016/j.scitotenv.2017.02.091

Shrivastava, S., Sahu, P., Singh, A., & Shrivastava L. (2015) Fly ash disposal and diseases in nearby villages (A Survey). *International Journal of Current Microbiology and Applied Sciences*, 4(2), 939 - 946.

Sun, W., Shao, Q., & Liu, J. (2013). Soil erosion and its response to the changes of precipitation and vegetation cover on the Loess Plateau. *Journal of Geographical Sciences*, 23(6), 1091 – 1106. 10.1007/s11442-013-1065-z

Svirčev, Z., Dulić, T., Obreht, I., Codd, G. A., Lehmkuhl, F., Marković, S. B., . . . Meriluoto, J. (2019). Cyanobacteria and loess—an underestimated interaction. *Plant and Soil*, 439(1 – 2), 293 – 308. https://doi.org/10.1007/s11104-019-04048-3

Svirčev, Z., Marković, S. B., Stevens, T., Codd, G. A., Smalley, I., Simeunović, J., . . . Hambach, U. (2013). Importance of biological loess crusts for loess formation in semi-arid environments. *Quaternary International*, 296, 206 – 215. https://doi.org/10.1016/j.quaint.2012.10.048

Talukder, B., Ganguli, N., Matthew, R. A., vanLoon, G. W., Hipel, K. W., & Orbinski, J. (2021). Climate change–triggered land degradation and planetary health: A review. *Land Degradation & Development*, 32(16), 4509 – 4522. 10.1002/ldr.4056

Tian, S., Liang, T., & Li, K. (2019). Fine road dust contamination in a mining area presents a likely air pollution hotspot and threat to human health. *Environment International*, 128, 201 – 209. 10.1016/j.envint.2019.04.050

Tomášková, H., Jirák, Z., Šplíchalová, A., & Urban, P. (2012). Cancer incidence in Czech black coal miners in association with coalworkers' pneumoconiosis. International *Journal of Occupational Medicine and Environmental Health*, 25(2). 10.2478/s13382-012-0015-9

U.S. Environmental Protection Agency - USEPA. (2016). Particulate matter (PM) basics. Available at: https://www.epa.gov/pm-pollution/particulate-matter-pm-basics (23.09.2024.)

Une, H., Esaki, H., Osajima, K., Ikui, H., Kodama, K., & Hatada, K. (1995). A Prospective Study on Mortality among Japanese Coal Miners. *Industrial Health*, 33(2), 67 – 76. 10.2486/indhealth.33.67

United Nations (UN). (2015). Transforming Our World: The 2030 Agenda for Sustainable Development. Resolution Adopted by the General Assembly on 25 September 2015. https://sustainabledevelopment.un.org/content/documents/21252030 %20Agenda%20for%20Sustainable%20Development%20web.pdf (13.09.2024).

United Nations Convention to Combat Desertification (UNCCD) (1994). *United Nations Convention to Combat Desertification in Those Countries Experiencing Serious Drought and/or Desertification Particularly in Africa*. United Nations: Paris, France.

United Nations Development Programme - UNDP. (2022). *Soil Degradation and Climate Change in Serbia*. ISBN 978-86-7728-356-8.

Valavanidis, A., Fiotakis, K., & Vlachogianni, T. (2008). Airborne particulate matter and human health: toxicological assessment and importance of size and composition of particles for oxidative damage and carcinogenic mechanisms. *Journal of Environmental Science and Health, Part C*, 26(4), 339 – 362. 10.1080/10590500802494538

Vasić, A., Vasiljević, Z., Mickovski-Katalina, N., Mandić-Rajčević, S., & Soldatović, I. (2022). Temporal Trends in Acute Coronary Syndrome Mortality in Serbia in 2005 – 2019: An Age–Period–Cohort Analysis Using Data from the Serbian Acute Coronary Syndrome Registry (RAACS). *International Journal of Environmental Research and Public Health*, 19, 14457. 10.3390/ijerph192114457

Veste, M. (2005). Importance of biological soil crusts for rehabilitation of degraded arid and semi-arid ecosystems. *Science of Soil and Water Conservation*, 3(4), 42 - 47.

Wang, W., Liu, Y., Li, D., Hu, C., & Rao, B. (2009). Feasibility of cyanobacterial inoculation for biological soil crusts formation in desert area. *Soil Biology & Biochemistry*, 41(5), 926 - 929. https://doi.org/10.1016/j.soilbio.2008.07.001

Waste Management Program of the Republic of Serbia for the period of 2022 - 2031. Official Gazette of the Republic of Serbia, No 12/2022. https://www.ekologija.gov.rs/

Whiteside, M., & Herndon, J. M. (2018). Coal fly ash aerosol: risk factor for lung cancer. *Journal of Advances in Medicine and Medical Research*, 25(4), 1 – 10. 10.9734/jammr/2018/39758

Williams, A. J., Buck, B. J., & Beyene, M. (2012). Biological Soil Crusts in the Mojave Desert, USA: Micromorphology and Pedogenesis. *Soil Science Society of America Journal*, 76(5), 1685 – 1695. https://doi.org/10.2136/sssaj2012.0021

Williams, W., Chilton, A., Schneemilch, M., Williams, S., Neilan, B., & Driscoll, C. (2019). Microbial biobanking – cyanobacteria-rich topsoil facilitates mine rehabilitation. *Biogeosciences*, 16(10), 2189 – 2204. https://doi.org/10.5194/bg-16-2189-2019

Woodruff, R. C., Tong, X., Khan, S. S., Shah, N. S., Jackson, S. L., Loustalot, F., & Vaughan, A. S. (2024). Trends in cardiovascular disease mortality rates and excess deaths, 2010–2022. *American Journal of Preventive Medicine*, 66(4), 582–589. https://doi.org/10.1016/j.amepre.2023.11.009

World Bank, 2016. *The cost of air pollution: strengthening the economic case for action*. World Bank Group. Washington, D.C.

World Health Organization - WHO. (2019). Health Impact of ambient air pollution in Serbia. A call to action. World Health Organization. Regional Office for Europe.

World Health Organization - WHO. (2021). WHO global air quality guidelines. Particulate matter (PM2.5 and PM10), ozone, nitrogen dioxide, sulfur dioxide and carbon monoxide. Geneva.

Xing, Y. F., Xu, Y. H., Shi, M. H., & Lian, Y. X. (2016). The impact of PM2.5 on the human respiratory system. *Journal of Thoracic Disease*, 8(1), E69 – E74. 10.3978/j.issn.2072-1439.2016.01.19

Yang, Y., Ruan, Z., Wang, X., Yang, Y., Mason, T.G., Lin, H., & Tian, L. (2019). Short-term and long-term exposures to fine particulate matter constituents and health: A systematic review and meta-analysis. *Environmental Pollution*, 247, 874 – 882. 10.1016/j.envpol.2018.12.060

Zanetta Colombo, N. C., Fleming, Z. L., Gayó, E. M., Manzano, C., Panagi, M., Valdés, J., & Siegmund, A. (2022). Impact of mining on the metal content of dust in indigenous villages of northern Chile. *Environment International*, 169, 107490. https://doi.org/10.1016/j.envint.2022.107490

Zhu, S. C., Zheng, H. X., Liu, W. S., Liu, C., Guo, M. N., Huot, H., . . . Tang, Y. T. (2022). Plant-Soil Feedbacks for the restoration of degraded mine lands: a review. *Frontiers in Microbiology*, 12. https://doi.org/10.3389/fmicb.2021.751794

INTERNATIONAL SCIENTIFIC JOURNAL
GEOGRAPHICA PANNONICA
Volume 28, Issue 3, 221–237 (September 2024)
Journal homepage: http://www.dgt.uns.ac.rs/en/homepage/pannonica/

Smart Heat-health Action Plans: A Programmatic, Progressive and Dynamic Framework to Address Urban Overheating

Aveek Ghosh[A*]

[A] *Nitte Institute of Architecture, Mangalore, India*

KEYWORDS

- extreme heat
- urban overheating
- smart heat-health action plan
- long-term planning
- collaborative approach
- urban sustainability

ABSTRACT

Cities stand at the focal point of vulnerability to heat waves (HWs) as they threaten urban livability and sustainability. National, regional, and local heat-health action plans (HHAPs) are vital for combating HWs and are increasingly crucial as adaptation measures to extreme heat. The present article highlights the most recent development on the working mechanism of HHAPs, its contemporary challenges, barriers to it and a range of operational heat management and planning strategies. It introduces the concept of 'smartness' to the existing mechanism of HHAPs which holds a significant potential to be intelligent, explicit and dynamic to address the growing and multifaceted impacts of extreme heat. It emphasizes urgent priorities including long-term heat planning, multisectoral heat-early warning systems, building urban heat resilience and recommends the application of eight core elements endorsed by the World Health Organization (WHO) for effective implementation of HHAPs. Collaboration among meteorological, epidemiological, public health, and urban planning experts is essential for addressing the multidimensional challenges of extreme heat.

Introduction

The phenomenon of global warming has substantially escalated climate-related challenges and occurrence of extreme weather events. Global climate change causes a serious increase of the frequency, magnitude and duration of extreme heat events (EHEs) or HWs (Perkins, 2015). HWs are characterized as extended durations of abnormally elevated temperatures and has emerged as the deadliest climate risk contributing to thousands of preventable deaths each year (IPCC, 2018, 2022). Extreme heat is a complex hazard that presents risks both acute and chronic. Recently, climate scientists and experts have dedicated their attention to a greater disconcerting occurrence commonly referred to as 'global boiling' indicating a heightened intensification of temperature extremes (Amnuaylojaroen, 2023; Thomas, 2023). In the context of the shift from global warming to global boiling, an expanding corpus of research efforts have underscored scientific investigations of EHEs in urban areas (Santamouris, 2020; Nazarian et al., 2022, 2024; Feng et al., 2023; Ghosh & Vidyasagar, 2023).

Urban heat island (UHI) is a widely environmental phenomenon where urban areas experience significantly higher temperatures compared to their rural surroundings (Wouters et al., 2017; Kotharkar et al., 2024c). Urban overheating is the combined effect of frequent HWs and growing heat islands associated with anthropogenic climate change and rapid urbanization (Santamouris, 2020;

* Corresponding author: Aveek Ghosh, e-mail: aveek.ghosh@nitte.edu.in

doi:10.5937/gp28-51694

Received: June 18, 2024| Revised: September 20, 2024| Accepted: September 21, 2024

Kotharkar et al., 2024a). Their significant ramifications on environmental, economic, social, and health aspects have also been widely reported (Ebi et al., 2021; Kotharkar et al., 2019, 2021, 2022). In recent years, the frequency, duration, intensity, and seasonality of EHEs have escalated quickly, and are projected to increase in the future (IPCC, 2022). The multifarious impact of HWs is threatening the livelihoods and sustenance of urban dwellers and profoundly affects the livability and sustainability of cities (Kotharkar et al., 2024b). Such a scenario presents an immense threat to swiftly urbanizing areas and burgeoning populations.

In this context, HHAPs and heat action plans (HAPs) were introduced as a guide to minimize the adverse effects of extreme heat and enhancing public health responses to extreme heat through a series of coordinated efforts between specialized agencies (WMO and WHO, 2015; Casanueva et al., 2019; He, 2023; Ulpiani et al., 2024). HHAPs provide a strong framework dedicated to address heat vulnerability and serve as an effective tool for directing heat-related adaptation and mitigation strategies across different spatial scales. In scientific literature, the terms 'HAP' and 'HHAP' have been interchangeably used. While both plans aim to mitigate the effects of extreme heat, HAPs have a broader focus on overall heat management, and HHAPs specifically address health-related concerns and strategies (Guardaro et al., 2020; He, 2024). A HAP is primarily concerned with general strategies for managing and responding to extreme heat which includes measures related to infrastructure, emergency response, public awareness, and logistics. HAPs have a broader scope that includes general preparedness to address a wider range of stakeholders and is particularly evident in Asian and Western Pacific countries. In contrast, HHAPs specifically target the health impacts of extreme heat and is focused on protecting public health and minimizing heat-related morbidity and mortality (Martinez et al., 2019; Li et al., 2022). HHAPs, a characteristic of European and Eastern Mediterranean nations often targets health professionals and protect vulnerable populations (Martinez et al., 2022).

In this regard, the sixth assessment report (AR6) of the Intergovernmental Panel on Climate Change (IPCC) alerts of a faster warming trend across most of the land areas (IPCC, 2022). It confirms that without constructive adaptation solutions, heat extremes will be unbearable for human health. The present study undertakes the following key pointers:

1. The escalation of extreme heat poses growing health hazard, propelled by the rapid urbanization and demographic shifts in nations with aging populations.
2. Globally, the exposure of populations to HWs is poised to amplify alongside further warming, exhibiting pronounced geographical variations in heat-related fatalities unless additional adaptation measures are undertaken.
3. Projections suggest that potent geographical differentials in heat-induced mortality will emerge in the latter part of this century, predominantly steered by population expansion in regions characterized by tropical and sub-tropical climates.
4. Within cities, hot extremes including HWs have intensified, amplifying heat risks, particularly within urban areas, attributable to alterations in regional heat patterns compounded by the 'heat island' phenomenon.
5. Adaptation strategies necessitate action plans integrating early warning systems and responsive protocols to mitigate heat-related risks.
6. Future heat risk adaptation options entail comprehensive arrangements featuring early warning systems and response strategies tailored for both urban and non-urban locales, with a focus on safeguarding vulnerable demographics through iterative enhancements.
7. Addressing short-term heat-health hazards can be complemented by long-term urban development strategies, incorporating nature-based solutions to mitigate UHI effects.
8. Embracing a multi-sectoral approach, involving diverse stakeholders, holds promise in fortifying responses to enduring heat risks, with initiatives encompassing climate-conscious urban planning and design measures.

Aim, objectives and scope

Underscoring these facts, this paper aims to detail the significance and critical functioning of HHAPs apropos of rapid urban growth and rising EHEs and envision a smart version to tackle the multi-dimensional nature of extreme heat. The research is primarily divided for a three-fold purpose with a intent to serve unique objectives, which are to (i) outline contemporary extreme heat-related efforts within the HHAPs including the wide range of extreme heat countermeasures as prescribed by international bodies or organizations; (ii) identify the limitations, barriers, and challenges in operationalizing heat management and heat planning strategies/efforts; and (iii) propose the development of a smart HHAP which is an evidence-based programmatic and progressive pathway to counter the evolving and multi-faceted impacts of extreme heat. The present study does not account for the cultural, political, economic and complex physiological factors related to the operational mechanism of HHAPs.

Methodology

The present research critically examined the current progress in extreme heat management and planning with a focus on identifying the key concerns in the operational mechanism of HHAPs. It adopts a mixed-method approach and go beyond a review of existing literature. It recognizes limitations and barriers in the effective functioning of a HHAP via a critical review and suggests key recommendations to augment the overall efficacy and operation of action plans. In addition to policy documents, the representative sample of peer-reviewed original research was limited to those focused on mitigation or adaptation solutions as a part of broader action plans (HAPs, HHAPs, and heat response plans). The review was restricted to publications available online, excluding those published in physical journals or books and any studies with restricted access. The paper concludes with key recommendations for both researchers and policymakers including the need for a smart HHAP to offer a dynamic stance involving active collaboration among various specialized sectors.

Literature review

This section summarizes the global efforts to counter the threat of HWs including the discussion of international polices and guidelines and their recent developments. Thirdly, it details the core concept or the basic working mechanism of HHAPs which includes a range of contextual and cross-cutting extreme heat countermeasures. Lastly, it discusses the issues, barriers, and challenges in the contemporary extreme heat management and planning efforts which paves the way for the ideation of smart HHAPs.

International efforts and guidelines to address extreme heat

International scientific bodies including the IPCC, WHO, and WMO, concur that the impacts of extreme heat can be mitigated through concerted efforts, necessitating a comprehensive array of actions with active coordination among diverse agencies (IPCC, 2022; WHO, 2008; WMO &WHO, 2015). In response to the rising incidence of EHEs, national governments and international organizations instituted heat-health warning systems (HHWSs) during the 1990s (Ebi, 2007, 2019; Sheridan & Kalkstein, 2004). The inception of the first hot weather health watch/warning system in Philadelphia, USA, in 1995 marked a pivotal moment (Kalkstein et al., 1996), followed by the large-scale public health interventions initiated in the aftermath of the 2003 European HW (Wilhelmi & Hayden, 2010; Keith et al., 2022). These initiatives catalyzed the development of numerous national and sub-national heat-health frameworks worldwide. Subsequently, various countries embarked on heat-health research to formulate implementable action plans. Many communities and states have since established HHAPs to effectively manage the public health consequences of HWs, incorporating early warning and effective response systems (Casanueva et al., 2019; Martinez et al., 2022). In 2008, the WHO Regional Office for Europe played a crucial role in guiding the development of HHAPs, providing comprehensive guidance documents and supplementary materials for the preparation of these plans (WHO, 2015; WMO & WHO, 2015). These resources have been widely adopted by national, regional, and local authorities as a blueprint for the prevention and management of HWs (WHO, 2011; WMO & WHO, 2021; Martinez et al., 2019, 2022; WHO, 2021).

The establishment of the Ahmedabad HAP in 2013 marked a significant milestone, pioneering the approach in the South Asia region (Kotharkar & Ghosh, 2021b). Since then, many countries have adopted similar action plans, wherein the onset of hot weather triggers a range of interventions aimed at minimizing health impacts. However, national HHAPs are currently operational in only 47 countries, with the majority situated in Europe (35), followed by South-East Asia (5), Western Pacific (4), Americas (2), and Eastern Mediterranean (1) (Kotharkar & Ghosh, 2021a). In 2021, the WHO Regional Office for Europe conducted a survey on the status of national/federal heat-health prevention across its member states, revealing significant variations in the implementation of core elements of HAPs (WHO, 2021). Nevertheless, there is strong evidence of progressive improvement in the development and implementation of HHAPs within the WHO European and South-East Asian region (Martinez et al., 2019, 2022; WHO, 2021).

Recent developments on extreme heat-related countermeasures

Extreme heat prevention efforts became more systematic and institutionalized since the aftermath of the 2003 European HW which led to over 70,000 excess deaths (He et al., 2023). HHAPs have surfaced prominently in regions grappling with rapidly escalating urban heat challenges, showcasing promising momentum, particularly in South-East Asia, the Eastern Mediterranean, and the Pacific. Additionally, stakeholders from diverse disciplines and organizations, including the Natural Resources Defense Council (NRDC), Red Cross, and regional partners, are actively collaborating with national governments to deepen understanding of the causes and formulate effective responses to this pressing risk. Concurrently with preventive measures, there has been a surge in research and pub-

lications focusing on HHAPs, both on a global scale and within Europe (Campbell et al., 2018; Casanueva et al., 2019; Santamouris, 2020; Nazarian et al., 2022, 2024; Ulpiani et al., 2024).

Over the past decade, numerous member states within the WHO European Region have instituted HHAPs of diverse scopes and complexities. Major states/cities in India vulnerable to HWs have their own plans, though active participation of local governments is limited (NDMA, 2019). Several states in the US including Kansas, Minnesota, and Wisconsin have developed specific guidelines to increase awareness and readiness among the population while a few others have employed heat officers to ensure priority action for local governments (Keith et al., 2021). Select cities including Arizona and Sydney have collaboratively developed extreme heat planning toolkits with support from local governments. These toolkits harness the latest research, information, and innovative ideas to facilitate the adaptation of urban spaces and enhance resilience against extreme heat (WSROC, 2021; Keith & Meerow, 2022). Additionally, collaborative efforts by the international organizations are underway to enhance guidance on heatwave and heat health early warning systems, through the Global Heat Health Information Network (GHHIN).

Understanding the working mechanism of HHAPs

The beginning of the twenty-first century has witnessed the initiation and development of cross-cutting extreme heat countermeasures. HHAP epitomizes practical and policy action/response to the negative effects of extreme heat to be undertaken at different levels and scales. HHAPs offer a comprehensive guide to minimize the negative impacts of extreme heat and delineate a portfolio of actions for the prevention and management of HWs. It offers a definitive mechanism to influence built environment outcomes, improve public health responses and controls that have the potential to reduce the impacts of urban heat. This includes a wide range of guidelines ranging from the formation of a lead body, meteorological early warning systems, timely public and medical advice, improvements to housing and urban planning and ensuring preparedness of health care and social systems (WHO, 2008; WMO & WHO, 2015, WHO, 2021). Additionally, it outlines a variety of spatio-temporal actions for concerned stakeholders and advocates periodic monitoring and evaluation of processes and outcomes to ensure the effectiveness of intended activities.

HHAPs encompass a comprehensive set of guidelines designed to facilitate various facets of heat risk reduction and preparedness. They serve as a vital tool for identifying and implementing heat-related adaptation and mitigation strategies. In recent years, HHAPs have emerged as indispensable instruments for guiding measures against extreme heat, continually evolving to enhance their effectiveness. Established HHAPs have demonstrated success in mitigating heat-related mortality and its adverse impacts. The WHO's guidance on HHAPs acknowledges that the detrimental effects of HWs are largely preventable, necessitating specific actions at multiple levels for successful implementation (WHO, 2008). These actions are integrated within HHAPs, which comprise robust health preparedness systems, epidemiological evidence, precise meteorological early warning systems, and enhancements in urban management and planning. Further, it acknowledged the need for heat-health systems to strengthen stewardship functions and a proactive, multidisciplinary, and multi-sectoral approach with governments, agencies, and international organizations.

Contemporary issues, barriers, and challenges in extreme heat management efforts

Despite making commendable national and regional initiatives along with international efforts, there remains significant gaps in the HHAP apparatus and its operation. The current mechanism of HHAP remains static in function, rigid in replication, and unprogressive in nature. Most of the heat plans focus on managing the negative consequences of extreme heat rather than long-term climate change adaptation and heat-health planning. It is also evident that response measures to HWs are primarily short-term, reactive in behaviour, and fail to capture and treat pseudo-effects at large. Current heat plans do not account for changing climates and hence do not provide a dynamic solution to the multifarious impacts of HWs. Furthermore, the effectiveness of HHAPs is significantly hampered by the absence of periodic monitoring and evaluation mechanisms. There is a notable deficiency in frameworks designed to assess the efficacy of policies in diminishing heat-related mortality and morbidity. The present study highlights a few shortcomings in contemporary extreme heat management efforts:

1. Lack of consistency in defining HWs and its poor scientific understanding
2. Threshold definition and its limited application in HHWSs
3. Static heat alert systems and action plans
4. Restricted coverage of HHAPs
5. Limited knowledge of intra-urban heat vulnerability and heat hotspots

It is clearly manifested that the widespread impact of HW leads to public health deterioration and increased risk of heat-related morbidity and mortality. In addition to this, the present research identified several ripple effects of extreme heat on urban systems which adds further burden on intended measures:

1. Higher energy consumption coupled with dangerous levels of pollution
2. Damage to urban infrastructure and services
3. Loss of economy and workers' productivity
4. Exacerbated water stress and widespread droughts
5. Power outages and energy crisis

In addition to the above-listed issues, HHAPs also face implementation failures, data-sharing and are not adequately resourced. Most heat plans specify roles and responsibilities at the national level but lack specificity at the sub-national and local levels. In terms of linkages with other policies, HHAPs are less frequently integrated and barely a part of environmental/disaster management policies. The key challenges for HHAPs that hinder their overall functioning are:

1. Lack of trained/skilled manpower to implement heat-related countermeasures
2. Inadequate weather stations to record meteorological data
3. Poor integration of HHAPs with national planning policies & development plans
4. Limited real-time surveillance
5. Inadequate monitoring and evaluation of processes/outcomes

Smart HHAP: A programmatic, progressive and dynamic framework

In view of the growing heat stress in urban areas, it is important to expand extreme heat adaptation and improve heat-related preparedness through a holistic and anticipatory approach. The multifaceted and growing impacts of extreme heat call for an urgent and collaborative mechanism coupled with long-term investment in research and innovation. The global community and policymakers need to look beyond short-term solutions to promote long-term urban heat resilience. The next section outlines a range of constructive recommendations best suited to application in their unique contexts in synchronization with the suggestions given by the IPCC AR6 report.

In this context, we introduce the concept of 'smartness' to the existing working mechanism of HHAPs. A smart HHAP by design refers to a programmatic, progressive and dynamic framework to mitigate urban overheating involving the collaborative intervention of multiple specialized sectors (see Fig. 1). This enables its operation to be intelligent, explicit, and dynamic to address the multifaceted aspects of extreme heat primed for effective reduction of negative heat-health outcomes. It involves a combination of countermeasures to protect public health, infrastructure, and the environment. The present work proposes a

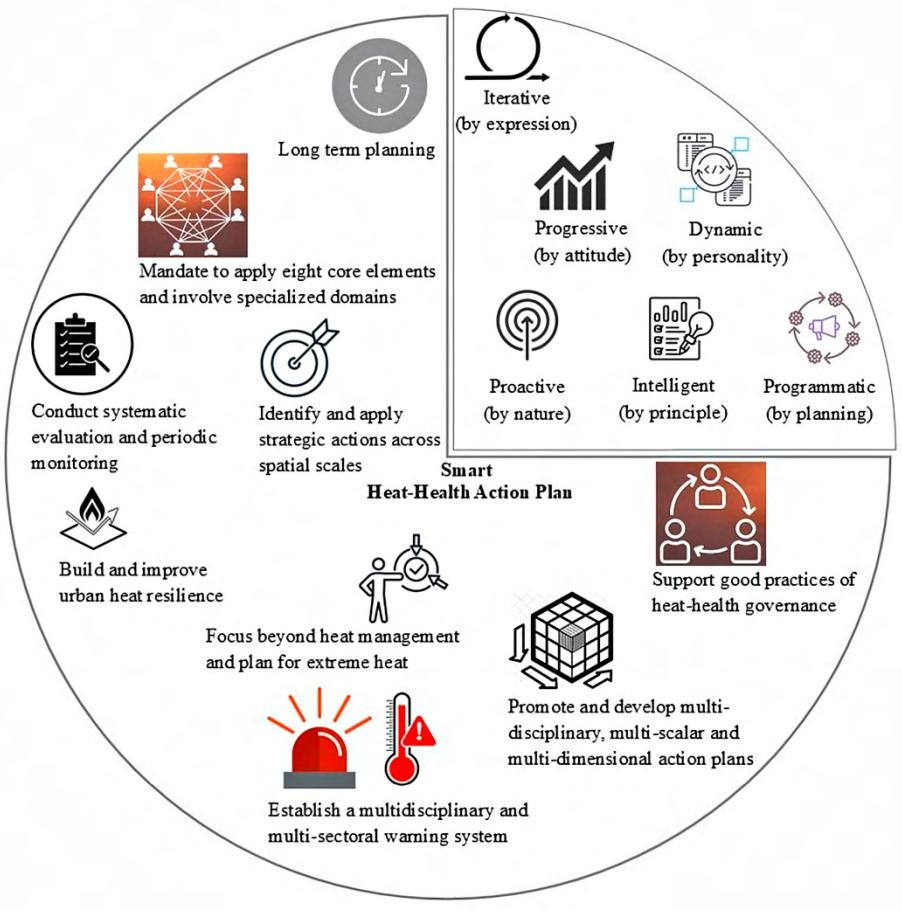

Figure 1. Working framework of a functioning smart HHAP

few directives as a part of smart HHAPs against the setting of changing urban landscape, fluctuating climate, and worrying future weather projections of temperature extremes. It sets an agenda to augment the overall efficacy and operation of HHAPs via condensed multidisciplinary directives which includes:

a) Long-term planning

Extreme heat is a silent killer and poses a huge challenge to sustainable development. The majority of contemporary extreme heat countermeasures and their respective application remain reactive and short-sighted. Urgent attention should be directed towards substantial and targeted adaptive investments, particularly aimed at safeguarding the most vulnerable populations (WHO, 2008; WMO & WHO, 2015; Ebi, 2019; Ebi et al., 2021; WHO, 2021). Comprehensive efforts must encompass year-round planning and the development of threshold-based heat metrics to bolster early warning systems (Li et al., 2022; Brimicombe et al., 2024). Smart HHAP offers a holistic approach encompassing diverse actions such as land-use planning, climate-responsive building design, community resilience, and emergency planning and response to effectively manage long-term heat risks. Furthermore, advancements should entail documenting the contributions and interactions of controllable and non-controllable factors influencing the UHI effect, identifying and addressing sources of heat vulnerability among the population, and enhancing heat risk management through comprehensive emergency response preparation and inter-agency collaboration (WHO, 2021; Keith et al., 2022). These multifaceted approaches hold promise in mitigating the impacts of EHEs, thus fostering greater resilience within communities.

b) Mandate: apply eight core elements and involve specialized domains

Extreme heat countermeasures often remain ineffective and fail to cover a wider audience due to their siloed operation. This creates and calls for the need for an inclusive approach consisting of diverse stakeholders with a set of expertise to join hands and effectively contribute towards a holistic reduction of heat-related impacts. This particularly applies to the formulation of HHWS, which is part of wider HHAP and can be improved by knowledge sharing and active collaboration between stakeholders (WMO & WHO, 2015; WHO, 2021; Brimicombe et al., 2024). Therefore, it is urgent to prioritize the development of a robust plan that integrates meteorological warnings and public health interventions, supported by epidemiological data, coupled with appropriate urban planning strategies. Local conditions will dictate the plan's details, but practice in different parts of the world has demonstrated that core elements are indispensable (Casanueva et al., 2019; WHO, 2021). These have been highlighted by a guidance document for the preparation of HHAPs as published by WHO including (WHO, 2008):

1. Establishing agreement on a lead body tasked with coordinating and facilitating collaboration among relevant stakeholders.
2. Ensuring clear links and effective communication channels between national and community early warning systems, extending to all pertinent stakeholders for achieving last-mile connectivity.
3. Identifying vulnerable groups and areas requiring priority response guided by a comprehensive heat-health information plan.
4. Implementing evidence-based triggers and graduated thresholds for action, tailored to locally appropriate metrics such as temperature, humidity, and the anticipated duration of the heat event.
5. Enacting appropriate early and anticipatory actions to mitigate risks and safeguard both people and livelihoods.
6. Establishing operational preparedness and readiness measures for local first responders for swift and effective response.
7. Developing a robust public communications plan, incorporating nationally harmonized, action-oriented key messages, for disseminating critical information to the public.
8. Implementing real-time monitoring, evaluation, and learning mechanisms for continuously assessing the effectiveness of interventions and fostering iterative improvements.

c) Identify and apply strategic actions across spatial scales

Smart HHAP advocates the application of temporal actions i.e., short-term, medium-term and long-term measures to manage, respond, and plan for extreme heat risks respectively (refer Fig. 2). While short-term actions are aimed at immediate or relatively temporary solutions (0-6 months) and are usually applied after a HW has struck or during a hot weather season, medium-term actions (6-24 months) cover extended efforts to manage/control the adverse effects of HWs. Long-term efforts are largely executed through substantial time and planning involving future considerations for several years. Smart HHAP embraces a nested governance approach which entails working concurrently across various scales, ranging from the design of microclimates at specific sites to broader neighborhood, city, and regional planning scales, and can lead to sustainable extreme heat considerations (Keith et al., 2019; 2022; WHO, 2021). Growing emphasis on regional heat planning recognizes the territorial impact of HWs and the climatic effects of different land use or policy changes (Nazarian et al., 2022; Ulpiani et al., 2024). A robust action plan

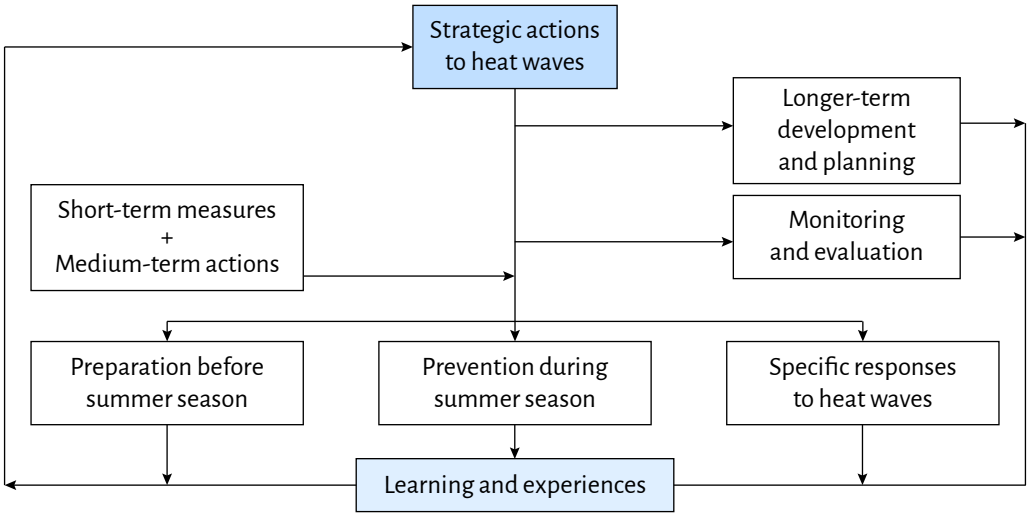

Figure 2. A periodic extreme heat planning and management cycle

should entail these strategies and planning interventions to prevent as well as to prepare. Subsequently, implementation of the plan and its elements depends the periodic monitoring and evaluation of intended measures drawing from past experiences. This forms a circularity in action planning template which can break large plans into smaller implementable actions while providing clarity towards the course of action.

d) Conduct systematic evaluation and periodic monitoring

Evaluation of HHAPs encompasses two primary categories: '*process*' evaluations, which assess whether their implementation aligns with its intended objectives, and '*outcome*' evaluations, which gauge their effectiveness in mitigating the adverse impacts of extreme heat (WHO, 2021; Dwyer et al., 2022). However, the evaluation of processes remains largely underrated and undervalued, impeding the formal assessment of HHAP components, roles, and the potential efficacy of implemented measures. Thorough assessment and evaluation of actions taken before, during, and after HW events are crucial for enhancing the effectiveness and continual improvement of HHAPs. Subsequently they can serve as crucial adaptation solutions, thus underscoring the importance of their evaluation and iterative updating in response to evolving climate dynamics and changes in heat-health associations. The development of progressive methodologies and inclusion of socio-economic factors are critical aspects and can facilitate effective and comprehensive responses. Evaluation involves a multidisciplinary and collaborative effort among various stakeholders to address the diverse aspects and components of the HHAP, including user needs and potential challenges (refer Fig. 3). Formal evaluation of HHAP effectiveness is important to:

- assess whether activities are achieving their intended outcomes;
- evaluate the cost-effectiveness of activities;
- assess whether the implemented measures are ethical and address health inequalities
- determine if activities are acceptable to the target population;
- ensure that evaluation is integrated at every stage of the planning, development, implementation, and review of programs
- track health impacts and changes over time

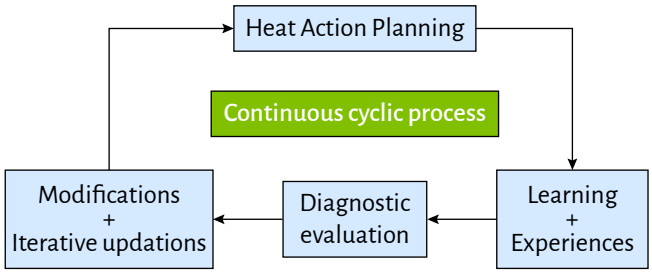

Figure 3. Evaluation and monitoring of HHAPs

e) Establish a multidisciplinary and multi-sectoral warning system

As a wider component of HHAP, HHWSs use forecasts of high-risk weather conditions to trigger public health warnings (Sheridan & Kalkstein, 2004; VanderMolen et al., 2022). Ideally, warning systems should encompass a comprehensive, multi-stakeholder action plan that can be established at various levels, including national, regional, or local. The efficacy of HHWSs should rely on threshold-based assessments rather than absolute weather parameters (Li et al., 2022; Brimicombe et al., 2024). It is imperative to develop thresholds that integrate ther-

mo-physiological considerations and account for seasonal variations (Casanueva et al., 2019; Martinez et al., 2022). Such efforts should be founded on robust scientific principles, drawing upon extensive and long-term data, complemented by relevant health statistics. This approach can significantly enhance the applicability of thresholds and indicators in decision-making contexts. Substantial investments can be directed towards impact-based forecasts, which integrate meteorological data with vulnerability information to offer timely analyses and provide lead time in diverse settings.

f) Promote and develop multi-disciplinary, multi-scalar and multi-dimensional action plans

The existing HW management and planning systems lack the ability to replicate adaptation efforts across different spatial scales. Current efforts primarily focus on physical/engineering and health aspects, with insufficient consideration given to urban climate recommendations. This underscores the imperative to develop robust mechanisms and resilient systems capable of coping with escalating heat stress. Addressing this challenge entails embracing a dynamic array of adaptation and mitigation strategies to address the multifaceted impacts of HWs comprehensively. HHAPs must be meticulously tailored to the specific climate, demographics, geography, infrastructure, and socio-economic dimensions of the communities they aim to safeguard. Integration of state-of-the-art knowledge is indispensable to ensure that HHAPs can effectively deliver on their intended benefits. WHO's guidance to HHAPs also outlines several principles to be adopted for planning and responding to extreme heat which underlines the need to use existing systems and response arrangements, effective communication, a multi-agency and intersectoral approach (WHO, 2008; 2021). Several principles linked with planning for and responding to extreme heat revolves around relying on established local, regional, and national emergency response systems and embracing a long-term vision. Additionally, plans require a multi-agency and intersectoral approach, ascertaining formal evaluation, effective communication to target groups and warrant that countermeasures do not worsen the issue of climate change (refer Fig. 4).

In the present study, we urge practitioners and policymakers to effectively frame a set of objectives (tasks) within each domain (meteorological, epidemiological, public health, and urban/regional planning) as a part of smart HHAPs. A detailed list of actions (short-term, medium-term and long-term) complementary to the objectives is provided in Annexure 1. This provides a clear-cut objectives and temporal actions to be taken (short-term, medium-term and long-term) by individuals/agencies directly linked with different core elements. The proposed working principle of an objective-based execution of tasks within a wider HHAP involves a circular approach which is cost effective, iterative and allows easy implementation on ground. This will provide clarity for concerned stakeholders to understand, assess, and execute intended measures. It should essentially encompass the active involvement of multiple domains (D) which typically includes experts from meteorological (D1), epidemiological (D2), public health (D3) and urban/regional planning (D4) background (see Fig. 5).

In this workflow, task managers are required to formulate explicit objectives (O) under each of their working domains (as formulated in Annexure 1). For a case, the first objective of meteorological agency can be denoted as D1O1, the second one as D2O2 and so on. The respective experts of the four domains are expected to do a similar exercise and carry out an implementation of temporal strategies. Additionally, task managers are expected to pinpoint a set of unique indicators which determines the effectiveness of intended measures as a part of the formal evaluation process. The framework entails periodic monitoring, and a diagnostic evaluation procedure which aims to provide a detailed and precise understanding of the issues at hand, which helps in creating an effective treatment or intervention plan. The cycle is completed by incorporating necessary modifications and fit for purpose updations to feed in to the (revised) guidelines of HHAPs. This results in a stronger and robust version of HHAP, which has evolved from the previous model and is now better equipped to handle new challenges.

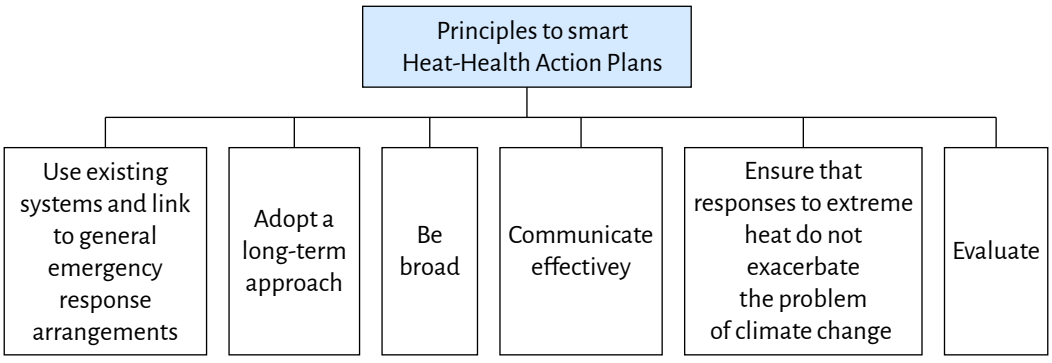

Figure 4. Key principles for effective operationalization of HHAPs

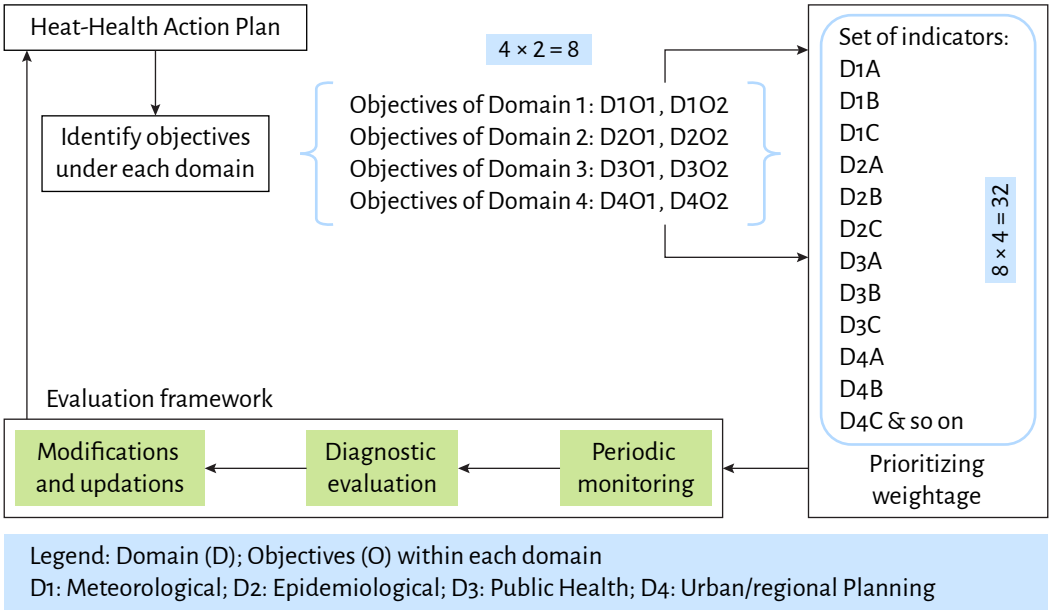

Figure 5. Representative objective-based execution of tasks within a smart HHAP

g) Support good practices of heat-health governance

Solid heat-health governance covers a broad spectrum of public-private networks and stakeholders who deliberate and make decisions regarding heat resilience (Keith et al., 2023; Wan et al., 2023; Ravishankar & Howarth, 2024). While international and national guidelines have outlined good governance principles, their translation into practice remains suboptimal. Current HHAPs often overlook rapidly changing climate and demographic variables, thereby compromising their overall effectiveness. Integrating HHAPs with other climate-sensitive early warning systems, climate-resilient adaptation plans, and disaster management policies could yield synergies and efficiency gains. Moreover, the development of heat governance extends beyond governmental purview; it is crucial to involve non-governmental stakeholders, including private and non-profit organizations, whose decisions significantly impact negating heat vulnerability. Scaling up public heat-health surveillance to inform and target adaptation plan and enhancing public health engagement present opportunities for effective health governance. Mainstreaming heat action planning across global cities, particularly in tropical regions, based on emerging best practices that prioritize closer integration of local health agencies, could enhance heat adaptation outcomes.

h) Build and improve urban heat resilience

Heat resilience, defined as the ability to construct an environment capable of withstanding and enduring extreme heat episodes, is essential (Keith & Meerow, 2022; Lim et al., 2022). Urban heat resilience necessitates an integrated planning approach that harmonizes strategies across community plans and leverages the best available heat risk information to prioritize heat mitigation efforts. Facilitative interventions can empower cities to influence and support actions toward sustainable urban cooling through appropriate policies and programs (Keith et al., 2021). HHAPs must include efforts that should be directed towards embedding urban heat resilience into city policies and plans. Additionally, escalating heat risks attributable to rapid expansion of the built environment and the UHI effect underscore the need to integrate HHAPs with development plans and urban planning policies. HHAPs can benefit from climate-based recommendations, while spatial frameworks such as local climate zone maps can offer critical insights into intra-urban variations in heat vulnerability (Kotharkar et al., 2024). Building resilience to extreme heat, necessitates concerted efforts across sectors and stakeholders to develop inclusive and effective strategies that prioritize equity and social justice.

i) Focus beyond heat management and plan for extreme heat

Historically, response mechanisms to extreme heat have been solely inclined towards managing and minimizing its negative public health outcomes (WHO, 2021; He et al., 2023). These set of countermeasures are often referred to as heat management strategies. 'Heat management' refers to a set of short-term actions intended to minimize the immediate negative consequences of extreme heat. The wide range of contemporary actions and traditional efforts directs a static response and focuses primarily on controlling/reducing the ill effects of extreme heat. Hence, they do not present replicability of actions across spatial scales and offer a poor signature of adaptation efforts. Conversely, smart HHAP is

vocal for 'heat planning' which refers to the portfolio of provisions taken in advance with the potential to reduce the anticipated impacts of extreme heat. These primarily include long-term adaptation and mitigation strategies (design and planning), strengthening heat response systems and associated machinery to proactively translate measures into heat-related prevention efforts. It constitutes periodic monitoring and evaluation (of processes and outcomes) to evaluate practices to deal with the impacts of HWs. Simultaneously, extreme heat planning offers a practical approach to proactively direct extreme heat countermeasures and proposes a predictive method to plan and mitigate urban heat across many systems and sectors it affects.

Discussion

Over the years, heat-health research has examined various aspects of public health, urban planning, and epidemiological evidence to build a thorough and integrated understanding. Matthies & Menne (2009) examined existing HHAPs in Europe and identified best practices for national and local preparedness planning. Another enquiry by Zuo et al. (2015) explored mechanisms to address the impacts of HWs, considering their significant effects on the built environment and community health. Martinez et al. (2019) conducted an updated review of HHAPs in Europe, evaluating future challenges in heat-health governance and stakeholder engagement. In another study, Fragomeni et al. (2020) investigated a collaborative approach to integrate the knowledge of heat vulnerability and urban climatology into the development of heat response plans. Guardaro et al. (2020) focused on bridging the gap between resilience theory and practice, advocating for community-based action plans to promote heat-reducing solutions. Further investigations critically analyzed the need to strengthen connections between research and practical interventions, emphasizing the importance of two-way communication between researchers and implementers in designing effective action plans (Casanueva et al., 2019; Ebi, 2019; Kotharkar & Ghosh, 2021a).

Recent efforts have shifted focus towards practical implementation and effective interventions within urban development policies and action plans (Parsaee et al., 2019; Ulpiani et al., 2024). Efforts have been made to explore collaborative heat response planning, community action plans, and to evaluate the monitoring and effectiveness of HHAPs. The present article provides a critical perspective into contemporary extreme heat-related countermeasures and strategies within the purview of HHAPs. The primary focus of this contribution has been on understanding and responding to overheating challenges, depicting cities as the central point of the emerging issue. It deep dived into the construction of a smart HHAP which provides multidisciplinary solutions while exploring pathways to address urban overheating. The different components of a smart HHAP provides explicit recommendations for heat-health researchers and a portfolio of actions for policymakers. This includes focusing beyond heat management and converging on proactive and long-term planning, building governance structures and supporting urban resilience routes to extreme heat. Investing in multi-disciplinary, multi-scalar and multi-dimensional early warning systems can go a long way in constructing a robust and dynamic HHAP with inputs from collaborative efforts.

Conclusion

Urban overheating, driven by global climate change and rapid urban development poses a major environmental problem that adversely impacts urban systems. The present article underscored the complexity and challenges inherent in contemporary extreme heat management and planning efforts as a part of wider HHAPs. The present work describes a multidisciplinary outlook on countermeasures to urban overheating, which remains yet to be addressed in the context of anthropogenic climate change and rapid urban expansion. The barriers to addressing extreme heat risk include a lack of evidence-based guidance for planning processes, siloed research, and underdeveloped regulatory structures. Additionally, HHAPs are poorly integrated with national policies which further hamper the overall potential and effectiveness of adaptation measures. It is also important to note that HHAPs primarily adopt a public health approach and are oriented toward reducing human mortality and morbidity.

The time is now for a smart version of HHAP. It is necessary to counter the borderless nature of heat hazards and severity of heat extremes in a changing climate. A programmatic and progressive framework backed by strategic long-term investments can support HHAPs to be a game-changing apparatus. Incorporating spatial assessment of intra-urban heat risk mapping at a granular level within HHAPs is a valuable approach for addressing heat vulnerability which accounts for local climatology and urban meteorology. This helps in the knowledge of hyper-local distribution of heat, thus providing climate-based rec-

ommendations for urban planners and policy-makers to devise apposite mitigation measures. Our recommendations include the need for a dynamic stance with a mandate to apply core elements recommended by WHO, embracing a long-term approach, backed by a multidisciplinary and multi-sectoral warning system. Additionally, it promotes to develop multi-disciplinary, multi-scalar and multi-dimensional action plans aided by strong heat-health governance structures to focus proactively on early extreme heat planning. Future empirical research is crucial to examine whether institutional and policy approaches effectively enhance heat resilience in cities.

Acknowledgement

The author thank the Nitte Institute of Architecture, Mangalore for providing the necessary infrastructure and facilities. Special thanks to Dr. Rajashree Kotharkar, Professor for providing constructive inputs during the visualization of the article.

References

Amnuaylojaroen, T. (2023). Perspective on the Era of Global Boiling: A Future beyond Global Warming. *Advances in Meteorology*, 2023(1), 5580606. https://doi.org/10.1155/2023/5580606

Brimicombe, C., Runkle, J. D., Tuholske, C., Domeisen, D. I. V., Gao, C., Toftum, J., & Otto, I. M. (2024). Preventing heat-related deaths: The urgent need for a global early warning system for heat. *PLOS Climate*, 3(7), e0000437. https://doi.org/10.1371/journal.pclm.0000437

Campbell, S., Remenyi, T. A., White, C. J., & Johnston, F. H. (2018). Heatwave and health impact research: a global review. *Health & Place*, 53, 210–218. https://doi.org/10.1016/j.healthplace.2018.08.017

Casanueva, A., Burgstall, A., Kotlarski, S., Messeri, A., Morabito, M., Flouris, A. D., ... & Schwierz, C. (2019). Overview of existing heat-health warning systems in Europe. *International Journal of Environmental Research and Public Health*, 16(15), 2657. https://doi.org/10.3390/ijerph16152657

Dwyer, I. J., Barry, S., Megiddo, I., & White, C. J. (2022). Evaluations of heat action plans for reducing the health impacts of extreme heat: methodological developments (2012-2021) and remaining challenges. *International Journal of biometeorology*, 66(9), 1915–1927. https://doi.org/10.1007/s00484-022-02326-x

Ebi, K. L. (2007). Towards an early warning system for heat events. *Journal of Risk Research*, 10(5), 729–744. https://doi.org/10.1080/13669870701447972

Ebi, K. L. (2019). Effective heat action plans: Research to interventions. *Environmental Research Letters*, 14(12), 122001. 10.1088/1748-9326/ab5ab0

Ebi, K. L., Capon, A., Berry, P., Broderick, C., de Dear, R., Havenith, G., ... & Jay, O. (2021). Hot weather and heat extremes: health risks. *The Lancet*, 398(10301), 698–708. https://doi.org/10.1016/S0140-6736(21)01208-3

Feng, J., Gao, K., Khan, H., Ulpiani, G., Vasilakopoulou, K., Yun, G. Y., & Santamouris, M. (2023). Overheating of Cities: Magnitude, Characteristics, Impact, Mitigation and Adaptation, and Future Challenges. *Annual Review of Environment and Resources*, 48(1). 651–679. https://doi.org/10.1146/annurev-environ-112321-093021

Fragomeni, M. B. A., Bernardes, S., Shepherd, J. M., & Rivero, R. (2020). A collaborative approach to heat response planning: A case study to understand the integration of urban climatology and land-use planning. *Urban Climate*, 33, 100653. https://doi.org/10.1016/j.uclim.2020.100653

Ghosh, A., & Vidyasagar, A. (2023, December). Heat Vulnerability Index for Urban Heat wave Risk Adaptation for Indian Cities: A Case Study of Akola. In *P. Rajagopalan, V. Soebarto, & H. Akbari (Eds.)*, 6th International Conference on Countermeasures to Urban Heat Islands 2019, Proceedings of the 6th International Conference on Countermeasures to Urban Heat Islands (pp. 57-66), Melbourne, Australia.

Guardaro, M., Messerschmidt, M., Hondula, D. M., Grimm, N. B., & Redman, C. L. (2020). Building community heat action plans story by story: A three neighborhood case study. *Cities*, 107, 102886. https://doi.org/10.1016/j.cities.2020.102886

He, B. J. (2023). Cause-related injustice, process-related injustice, effect-related injustice and regional heat action planning priorities: An empirical study in Yangtze River Delta and Chengdu-Chongqing urban agglomerations. *Landscape and Urban Planning*, 237, 104800. https://doi.org/10.1016/j.landurbplan.2023.104800

He, B. J. (2024). Spatial and socioeconomic heterogeneity of heat-related perception, awareness, knowledge and impacts for unbiased heat action plans. *Journal of Cleaner Production*, 469, 143164. https://doi.org/10.1016/j.jclepro.2024.143164

Intergovernmental Panel on Climate Change (IPCC). (2018). *Global warming of 1.5°C: An IPCC special report on the impacts of global warming of 1.5°C above pre-industrial levels and related global greenhouse gas emission pathways, in the context of strengthening the global response to the*

threat of climate change, sustainable development, and efforts to eradicate poverty (V. Masson-Delmotte, P. Zhai, H.-O. Pörtner, D. Roberts, J. Skea, P. R. Shukla, A. Pirani, W. Moufouma-Okia, C. Péan, R. Pidcock, S. Connors, J. B. R. Matthews, Y. Chen, X. Zhou, M. I. Gomis, E. Lonnoy, T. Maycock, M. Tignor, & T. Waterfield, Eds.). In Press.

Intergovernmental Panel on Climate Change (IPCC). (2022). *Climate change 2022: Impacts, adaptation, and vulnerability. Contribution of Working Group II to the Sixth Assessment Report of the Intergovernmental Panel on Climate Change* (H.-O. Pörtner, D. C. Roberts, M. Tignor, E. S. Poloczanska, K. Mintenbeck, A. Alegría, M. Craig, S. Langsdorf, S. Löschke, V. Möller, A. Okem, & B. Rama, Eds.). Cambridge University Press. (In press).

Kalkstein, L. S., Jamason, P. F., Greene, J. S., Libby, J., & Robinson, L. (1996). The Philadelphia hot weather-health watch/warning system: Development and application, summer 1995. *Bulletin of the American Meteorological Society,* 77(7), 1519–1528. 10.1175/1520-0477(1996)077<1519:tphwhw>2.0.co;2

Keith, L., Gabbe, C. J., & Schmidt, E. (2023). Urban heat governance: examining the role of urban planning. *Journal of Environmental Policy & Planning,* 25(5), 642-662. https://doi.org/10.1080/1523908X.2023.2244446

Keith, L., Meerow, S., Hondula, D. M., Turner, V. K., & Arnott, J. C. (2021). Deploy heat officers, policies and metrics. *Nature,* 598(7879), 29–31. https://doi.org/10.1038/d41586-021-02677-2

Keith, L., Meerow, S., & Wagner, T. (2019). Planning for extreme heat: A review. *Journal of Extreme Events,* 6(03n04), 2050003. https://doi.org/10.1142/S2345737620500037

Keith, L., & Meerow, S. (2022). *Planning for urban heat resilience. (PAS Report) 600.* American Planning Association.

Keith, L., Meerow, S., Berke, P., DeAngelis, J., Jensen, L., Trego, S., Schmidt, E., Smith, S. (2022). *Plan Integration for Resilience Scorecard™ (PIRS™) for Heat: Spatially evaluating networks of plans to mitigate heat (Version 1.0).* American Planning Assocation.

Kotharkar, R., Aneja, S., & Ghosh, A. (2019). Heat Vulnerability Index for Urban Heat wave Risk Adaptation for Indian Cities: A Case Study of Akola. In H. Akbari, V. Garg, J. Mathur & V. R. Khare (Eds.), *5th International Conference on Countermeasures to Urban Heat Islands 2019,* Proceedings of the 5th International Conference on Countermeasures to Urban Heat Islands (pp. 109-130), Hyderabad, India. https://doi.org/10.37285/bsp.ic2uhi.10

Kotharkar, R., Dongarsane, P., & Ghosh, A. (2024a). Quantification of summertime thermal stress and PET range in a tropical Indian city. *Urban Climate,* 53, 101758. https://doi.org/10.1016/j.uclim.2023.101758

Kotharkar, R., Dongarsane, P., Ghosh, A. & Kotharkar, V. (2024b). Numerical analysis of extreme heat in Nagpur city using heat stress indices, all-cause mortality and local climate zone classification. *Sustainable Cities and Society,* 101, 105099. https://doi.org/10.1016/j.scs.2023.105099

Kotharkar, R., & Ghosh, A. (2021a). Progress in extreme heat management and warning systems: A systematic review of heat-health action plans (1995–2020). *Sustainable Cities and Society,* 76, 103487. https://doi.org/10.1016/j.scs.2021.103487

Kotharkar, R., & Ghosh, A. (2021b). Review of heat wave studies and related urban policies in South Asia. *Urban Climate,* 36, 100777. https://doi.org/10.1016/j.uclim.2021.100777

Kotharkar, R., Ghosh, A., & Kotharkar V. (2021). Estimating summertime heat stress in a tropical Indian city using Local Climate Zone (LCZ) framework. *Urban Climate,* 36, 100784. https://doi.org/10.1016/j.uclim.2021.100784

Kotharkar, R., Ghosh, A., Kapoor, S., & Reddy, D. G. K. (2022). Approach to local climate zone based energy consumption assessment in an Indian city. *Energy and Buildings,* 259, 11835. https://doi.org/10.1016/j.enbuild.2022.111835

Kotharkar, R., Vidyasagar, A., & Ghosh, A. (2024c). Application of LCZ to Urban Heat Island Studies. In R. Wang, M. Cai, C. Ren & Y. Shi. (Eds.). *Local Climate Zone Application in Sustainable Urban Development: Experience from East and Southeast Asian High-Density Cities* (pp. 79-103). Switzerland: Springer Nature AG.

Lim, T. C., Wilson, B., Grohs, J. R., & Pingel, T. J. (2023). Community-engaged heat resilience planning: Lessons from a youth smart city STEM program. *Landscape and Urban Planning,* 226, 104497. https://doi.org/10.1016/j.landurbplan.2022.104497

Li, T., Chen, C & Cai, W. (2022). The global need for smart heat–health warning systems. *The Lancet,* 400(10362), 1511-1512. https://doi.org/10.1016/S0140-6736(22)01974-2

Martinez, G. S., Kendrovski, V., Salazar, M. A., de'Donato, F., & Boeckmann, M. (2022). Heat-health action planning in the WHO European Region: Status and policy implications. *Environmental Research,* 214, 113709. https://doi.org/10.1016/j.envres.2022.113709

Matthies, F., & Menne, B. (2009). Prevention and management of health hazards related to heatwaves. *International Journal of Circumpolar Health,* 68(1), 8–12. https://doi.org/10.3402/ijch.v68i1.18293

Martinez, G. S., Linares, C., Ayuso, A., Kendrovski, V., Boeckmann, M., & Diaz, J. (2019). Heat-health action plans in Europe: Challenges ahead and how to tackle them. *Environmental Research,* 176, 108548. https://doi.org/10.1016/j.envres.2019.108548

Nazarian, N., Bechtel, B., Mills, G., Hart, M. A., Middel, A., Krayenhoff, E. S., … & Chow, W. (2024). Integration of urban climate research within the global climate change discourse. *Plos Climate,* 3(8), e0000473. https://doi.org/10.1371/journal.pclm.0000473

Nazarian, N., Krayenhoff, E. S., Bechtel, B., Hondula, D. M., Paolini, R., Vanos, J., … & Santamouris, M. (2022). Integrated assessment of urban overheating impacts on human life. *Earth's Future,* 10(8), e2022EF002682. https://doi.org/10.1029/2022EF002682

National Disaster Management Authority - NDMA. (2019). *National guidelines for preparation of action plan-prevention and management of heat wave, 2019.*

Parsaee, M., Joybari, M. M., Mirzaei, P. A., & Haghighat, F. (2019). Urban heat island, urban climate maps and urban development policies and action plans. *Environmental Technology & Innovation,* 14, 100341. https://doi.org/10.1016/j.eti.2019.100341

Perkins, S. E. (2015). A review on the scientific understanding of heatwaves—Their measurement, driving mechanisms, and changes at the global scale. *Atmospheric Research,* 164, 242–267. https://doi.org/10.1016/j.atmosres.2015.05.014

Ravishankar, S., & Howarth, S. (2024). Exploring heat risk adaptation governance: A case study of the UK. *Environmental Science & Policy,* 157, 103761. https://doi.org/10.1016/j.envsci.2024.103761

Santamouris, M. (2020). Recent progress on urban overheating and heat island research. Integrated assessment of the energy, environmental, vulnerability and health impact. Synergies with the global climate change. *Energy & Buildings*, 207, 109482. https://doi.org/10.1016/j.enbuild.2019.109482

Sheridan, S. C., & Kalkstein, L. S (2004). Progress in heat watch–warning system technology. *Bulletin of the American Meteorological Society,* 85(12), 1931–1942. https://doi.org/10.1175/bams-85-12-1931

Thomas, S. P. (2023). Global Boiling: Implications for Mental Health. *Issues in Mental Health Nursing*, 44(9), 797–798. https://doi.org/10.1080/01612840.2023.2244338

Ulpiani, G., Treville, A., Bertoldi, P., Vetters, N., Barbosa, P., Feyen, L., Naumann, G., & Santamouris, M. (2024). Are cities taking action against urban overheating? Insights from over 7,500 local climate actions. *One Earth*, 7(5), 848-866. https://doi.org/10.1016/j.oneear.2024.04.010

VanderMolen, K., Kimutis, N., & Hatchett, B. J. (2022). Recommendations for increasing the reach and effectiveness of heat risk education and warning messaging. *International Journal of Disaster Risk Reduction, 82,* 103288. https://doi.org/10.1016/j.ijdrr.2022.103288

Wan, K., Lane, M., & Feng, Z. (2023). Heat-health governance in a cool nation: A case study of Scotland. *Environmental Science & Policy,* 147, 57-66. https://doi.org/10.1016/j.envsci.2023.05.019

Western Sydney Regional Organisation of Councils – WSROC. (2021). *Urban Heat Planning Toolkit.* Blacktown, NSW.

Wilhelmi, O. V., & Hayden, M. H (2010). Connecting people and place: a new framework for reducing urban vulnerability to extreme heat. *Environmental Research Letters,* 5(1), 014021. https://doi.org/10.1088/1748-9326/5/1/014021

World Health Organisation – WHO. (2004). *Heat waves: Risks and responses.* Health and Global Environmental Change, Series, No. 2. Copenhagen, Denmark.

World Health Organisation – WHO. (2008). Europe. *Heat-health action plans; Guidance.* In F. Mathies, G. Bickler, N. C. Marín, & S. Hales. (Eds.), Copenhagen, Denmark.

World Health Organisation – WHO. (2021). *Heat and health in the WHO European Region: updated evidence for effective prevention.* Copenhagen, Denmark.

World Meteorological Organization and World Health Organization – WMO & WHO (2015). *Heatwaves and Health: Guidance on Warning-System Development.* In G.R. McGregor, P. Bessemoulin, K. Ebi & Menne, B. (Eds.), Geneva, Switzerland

Wouters, H., De Ridder, K., Poelmans, L., Willems, P., Brouwers, J., Hosseinzadehtalaei, P., … & Demuzere, M. (2017). Heat stress increase under climate change twice as large in cities as in rural areas: A study for a densely populated midlatitude maritime region. *Geophysical Research Letters*, 44(17), 8997–9007. https://doi.org/10.1002/2017GL074889

Zuo, J., Pullen, S., Palmer, J., Bennetts, H., Chileshe, N., & Ma, T. (2015). Impacts of heat waves and corresponding measures: A review. *Journal of Cleaner Production,* 92, 1–12. https://doi.org/10.1016/j.jclepro.2014.12

Annexure 1. Specific actions to meet objectives for core elements in a HAP

Core element (CE)	Description	Objectives	Actions		
			Short-term (up to 3-year time span)	Medium-term (3-5 year time span)	Long-term (more than 5-year time span)
CE 1: Agreement on a lead body	to coordinate a multipurpose collaborative mechanism between bodies and institutions and to direct the response if an emergency occurs	1. To form a lead body and coordinate a multi-purpose collaboration mechanism between identified agencies/ stakeholders. 2. Set up objectives related to the management and planning of heat waves. 3. To manage the response, if an emergency occurs. 4. To set up an action plan/steering committee to drive, organize, and govern heat-related efforts.	i. Form a committee/team to oversee the progress and functioning of various preparedness measures ii. Define specific roles and responsibilities for each player iii. Establish inter-agency coordination iv. Identify a lead agency and steering committee (members of different groups) v. Formally define roles and responsibilities across spatial scales. vi. Identification of experts/ stakeholders across various domains	i. Ensure involvement of different agencies/ stakeholders in decision-making processes ii. Ensure adequate funding for sustainability and continuity of activities with support from key decision-makers iii. Conduct a cost-benefit analysis of interventions to estimate the strengths and weaknesses of decisions/intended measures.	i. Integrate HAPs with development planning processes and municipal plans. ii. Apply multi-level governance and include national, regional, and local authorities. iii. Set up protocols for emergencies. iv. Allocate part of research and development in the financial budget for heat wave action planning. v. Make provision for funding. vi. Identify potential avenues of interdisciplinary collaboration between academia and industry.
CE 2: Accurate and timely alert systems	Install heat–health warning systems to trigger warnings, determine the threshold for action, and communicate the risks	1. To provide accurate and timely warnings/forecasts of temperature and weather parameters. 2. To issue graded levels of alert/ warning as per threshold (timely communication). 3. To calculate the city-level threshold (temperature-health association) and periodic monitoring of the threshold.	i. Develop a warning system based on a local threshold or T_{max}, T_{min}, or heat indices. ii. Decide on what should be the threshold. iii. Understand and communicate warnings. iv. Track the occurrence of HWs and issue timely warnings/alerts. v. Forecast heat waves in advance. vi. Identify health conditions based on scientifically sound threshold levels. vii. Provide an effective set of response measures associated with the warning level.	i. Calculate and monitor the threshold. ii. Understand the concept of heat risk and create awareness about it. iii. Evolving communication systems, evaluating them, and communicating the warning.	i. Understanding and evolving the concept of threshold and risk. ii. Forecasting climate patterns (city/regional level model) for preparation of future hazards. iii. Establish multi-hazard warning systems and integrate them with HW action planning. iv. Include climate variability and urban warming projections in HAPs. v. Improve forecasts with advanced lead times. vi. Upgradation of forecast/early warning systems and associated equipment.

Core element (CE)	Description	Objectives	Actions		
			Short-term (up to 3-year time span)	Medium-term (3-5 year time span)	Long-term (more than 5-year time span)
CE 3: A heat-related health information plan	about what is communicated, to whom, and when & communicating the risks of hot weather and HWs and giving behavioral advice	1. To identify the mechanism, timing/issuance, language, and content of information, education, and communication (IEC) materials and activities. 2. To work out mechanisms for the involvement of non-governmental and other related organizations. 3. To establish a systematic information network for the dissemination of alerts and issue heat risk communications through public-friendly content and language.	i. Conduct public awareness and community outreach programs ii. Expand knowledge about different ways to minimize the impacts of extreme heat through precautionary measures. iii. Behavioural advice on staying indoors, avoiding strenuous work, drinking fluids, etc.	i. Prepare an operational heat response plan (including guidance and standards) linked with the warnings. ii. Build awareness, perception, and adaptive capacity to extreme heat. iii. Identify the mechanism of issuing a clear plan of communication for different sectors.	i. Collaborate with non-government organizations and engage civil society groups. ii. Engage and collate research on the detrimental impact of hot weather episodes on public health. iii. Explore the possibility of a dynamic system to show real-time data portals using information and communication technology (ICT).
CE 4: A reduction in indoor heat exposure (in vulnerable areas and public buildings)	epidemiological information to reduce indoor heat, indoor cooling strategies	1. To improve knowledge of indoor overheating and its impact on health. 2. To provide behavioral advice on ways to cool indoor spaces. 3. To bring awareness about continuous exposure to indoor heat risk and strategies to reduce nocturnal discomfort in indoor spaces. 4. To promote green building concept.	i. Identify vulnerable areas and public buildings (typology) for intervention. ii. Conduct diagnostic studies to identify issues in buildings and direct possible countermeasures. iii. Improve wall/roof insulation and ventilation in existing building structures. iv. Reduce internal heat load. v. Reduce heat stress and increase ventilation for indoor spaces. vi. Increase albedo using light-colored materials for cool roofs/ pavements, etc. vii. Allow necessary retrofitting in building envelopes. viii. Incorporate standards to provide thermal comfort in buildings	i. Reduce indoor heat exposure and achieve sustainable thermal comfort in buildings. ii. Allow modifications in housing and introduce appropriate urban landscape measures. iii. Introduce passive cooling and efficient active cooling technologies. iv. Employ measures to reduce local heat islands.	i. Conduct research efforts on understanding the relationship between indoor temperatures and indoor thermal comfort. ii. Adopt a nuanced approach toward air-conditioning to check greenhouse gas emissions. iii. Evaluate the effectiveness of cooling strategies e.g., cool/ green roof, wall insulation, and their potential to reduce heat vulnerability.

Core element (CE)	Description	Objectives	Actions		
			Short-term (up to 3-year time span)	Medium-term (3-5 year time span)	Long-term (more than 5-year time span)
CE 5: Particular care for vulnerable population groups	identification and localization of the most vulnerable population groups, active surveillance programme & preparatory measures to strengthen active outreach activities	1. To identify and make arrangements for vulnerable population groups. 2. To identify heat-prone areas and direct extreme heat countermeasures spatially. 3. To identify determinants of heat vulnerability/risk.	i. Prepare targeted plans to reduce immediate heat-health risks. ii. Mobilize human resources to provide relief material. iii. Establish cooling centers and shaded spaces in public areas and arrange distribution of water, medicines, etc. iv. Setting up temporary outreach clinics in remote areas. v. Ensure occupational safety, rest hours, and shelters for the outdoor working population.	i. Improve housing conditions. ii. Hotspot mapping for vulnerable areas and communities. iii. Conduct heat vulnerability/risk studies. iv. Involve participation of local NGOs or volunteer-based organizations for outreach to vulnerable groups.	i. Undertake heat risk perception and epidemiological studies to understand the impact of extreme heat on various population groups.
CE 6: Preparedness of the health and social care system	an operational plan on the specific procedures hospitals, clinics, retirement, and nursing homes should adopt before and during the summer period and during HWs needs to be defined; these actions need to be linked to heat-health warnings issued	1. To conduct appropriate staff training and planning, and guidance to health professionals on heat illness risk factors, diagnosis, and management. 2. To improve basic health infrastructure. 3. To allow building modifications and interventions to reduce indoor overheating in health care facilities. 4. To build climate-resilient health systems. 5. To improve emergency planning, preparedness, management, planning, and response in health care settings through national/ international initiatives.	i. Establish Standard Operating Procedures (SOPs), preparedness and anticipatory measures. ii. Train healthcare professionals and staff on specific clinical care and health. iii. Establish treatment protocol for high-risk patients. iv. Establish emergency planning and procedures. v. Enhance the preparedness of healthcare providers and facilities. vi. Maintain adequate stock of life-saving drugs and medicines vii. Establish a heat hotline emergency number. viii. Conduct mass awareness campaigns on improving heat-health outcomes.	i. Conduct studies to understand the relation between various vector-borne diseases and extreme events. ii. Develop surge strategies to manage increased demand iii. Develop contingency plans for staff. iv. Develop and modify curricula for training health professionals.	i. Augment health infrastructure and undertake building modifications and interventions to reduce indoor overheating ii. Allow modifications for reduction of carbon footprint in health care facilities.

Core element (CE)	Description	Objectives	Actions		
			Short-term (up to 3-year time span)	Medium-term (3-5 year time span)	Long-term (more than 5-year time span)
CE 7: Long-term urban planning	adaptation measures in built environment to focus on heat resilient cities, reducing urban heat islands and outdoor heat stress with energy efficiency measures	1. To promote actions to design climate-resilient cities. 2. To evaluate the changing dynamics of built environment. 3. To develop and implement climate-sensitive urban planning policies/guidelines.	i. Install canopies and roof structures to provide external shading. ii. Encourage water harvesting. iii. Introduce green roofs and vertical gardens.	i. Urban greening and improve overall green cover in cities. ii. Urban landscape management and other interventions in the built environment to reduce heat islands. iii. Promote walkability and cycle-friendly cities. iv. Enhance & protect existing urban forestry. v. Plan and implement activities to make cool communities. vi. Make provisions for water planning and management in cities. vii. Invest and explore available cooling technologies for existing buildings. viii. Conduct programmes that include housing, environmental, infrastructure improvements, and resource conservation. ix. Implement green building rating systems across spatial scales.	i. Introduce appropriate provisions in development control regulations. ii. Integrate HAPs with development plans and urban/regional planning, energy, transport, and climate change adaptation policies. iii. Support blue-green infrastructure interventions and water-sensitive urban design. iv. Modulate floor space index (FSI) and urban morphological parameters and heat resilient infrastructure development. v. Invest in sustainable and non-motorized transport options to minimize GHG emissions. vi. Generate heat wave vulnerability/risk map for developing strategic adaptation/ mitigation solutions. vii. Conduct diagnostic studies on built environment including UHI/ heat stress/heat risk/pollution.
CE 8: Real-time surveillance and evaluation	communication and collaboration between several institutions, groups, and actors; periodically monitoring the health impacts of HWs and the effectiveness of the interventions; regular evaluation of heat-health action plans	1. To conduct periodic evaluation and monitoring of measures in HAPs 2. To define elements that need improvement (cost-effectiveness of interventions, reducing practical barriers) 3. Set up real-time surveillance systems so that prevention and response measures can be adjusted	i. Establish communication and collaboration between related institutions/groups to monitor changing climatic conditions ii. Conduct process evaluation of measures applied to reduce the impacts of extreme heat. iii. Conduct cyclic evaluation of various measures applied to reduce heat vulnerability/risk.	i. Evaluate whether the measures introduced are ethical and reduce inequalities. ii. Monitor health impacts and changes over time	i. Periodically monitor, review, and evaluate the performance of action plans ii. Evaluate the effectiveness of warning systems and allow modifications iii. Conduct outcome evaluation of intended measures to assess whether policies are valid in reducing heat-health outcomes.